Bromate removal by chemical reduction using iron (II)

Optimizing AOP-MAR process

Vanida A. Salgado Ismodes

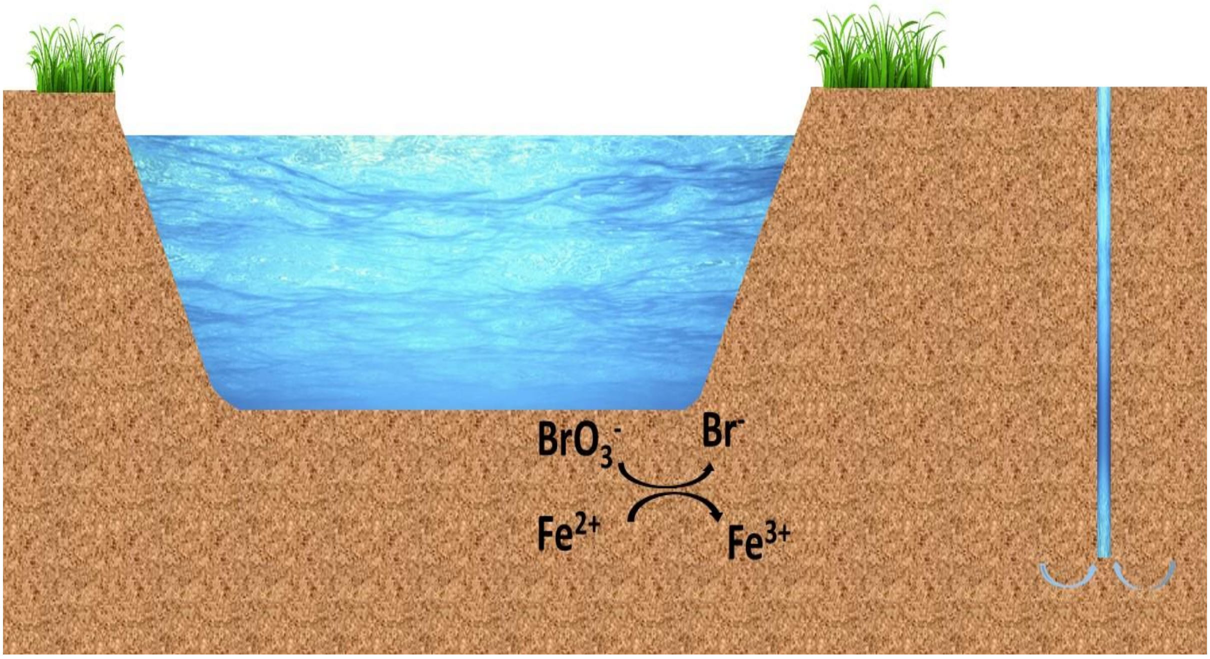

TU Delft Delft University of Technology

BROMATE REMOVAL BY CHEMICAL REDUCTION USING IRON (II)

OPTIMIZING AOP-MAR PROCESS

by

Vanida Salgado Ismodes

in partial fulfillment of the requirements for the degree of

Master of Science
in Civil Engineering

at the Delft University of Technology,
to be defended publicly on Thursday November 17, 2016 at 10:00 AM.

Student number:	4419227	
Thesis committee:	Prof. dr. J. P. van der Hoek,	TU Delft
	MSc. F. Wang,	TU Delft
	Dr. D. van Halem,	TU Delft
	Dr. K. Lekkerkerker-Teunissen,	Dunea
	Prof. P. J. Stuyfzand,	TU Delft

ACKNOWLEDGEMENTS

After 2 years and 3 months the ending of my MSc. studies has come. It has been an nice experience full of hard work and studies but the most important thing I have met wonderful people.

The last 9 months I have been working on my thesis and it has been a continuous learning process. This research has been finished and succeeded, thanks to the technical support, supervision and guidance of Feifei Wang, Doris van Halem and Prof. Jan Peter van der Hoek. Thanks for all your ideas, suggestions and at the same time, the space and freedom that you gave me to conduct this study in the best way.

I would also like to thanks Becas Chile, because my studies were funded by CONICYT PAI/INDUSTRIA 79090016.

People from the Waterlab (Armand and Mohammed) and Het Waterlaboratorium (Luc) thanks for replying my doubts, helping and providing me with the equipment and materials needed for my thesis.

Devina, Nessia, Timon, Max, Alex, Victor, Frans, Agni and the spanish interns, thanks for our conversations, your company and to make my days funnier and easier I enjoyed the time that we spent together.

David de Ridder thanks for helping me and lending me your things in the laboratory and for your interesting chemical conversations, I enjoyed them.

Last but not least, my family and Juan, I could not be able to do this without you. Thanks for your help, support, patience and confidence in me during this years, from the very beginning (since my application to TU Delft). Papi and mami thanks for always believe in me and make me believe that I can achieve my dreams. Kelly after all the things that you have passed through, you have showed me that nothing is impossible and everything can be achieved with perseverance, effort, love and good mood. Juan thanks for being patient and have waited for me.

SUMMARY

This study investigated the removal of bromate, as a by-product of AOP, by chemical reduction using iron (II), and the possibility of using this technology as a water treatment or during the managed aquifer recharge (MAR). Five experiments were carried out under anoxic conditions at 12°C and pH 9.5 to evaluate the bromate reduction at high (5 mg/L) and low (60 $\mu g/L$) concentrations with different iron (II) doses (13 and 52 mg/L for high bromate concentration and 0.15 and 1.5 mg/L for low bromate concentration), in the presence and absence of nitrate (5 and 10 mg/L). The low iron doses are similar to the concentrations found in the dunes. In addition 0.15 mg/L was selected according to the stoichiometry relation necessary to reduce 60 $\mu g/L$ bromate. For the high iron concentrations, 13 mg/L was chosen based on the stoichiometry relation needed for 5mg/L. In addition, nitrate reduction by iron in absence of bromate was evaluated with and without catalyst.

For the high bromate concentration, 90% of bromate was reduced by 13 mg/L iron (II) after the 5th the day in presence and absence of nitrate, while with 52 mg/L iron dose all the bromate was reduced within the first 30 min in absence of nitrate and 2 hours in the presence of nitrate. Bromate was favored by iron over nitrate in the presence of equal and different concentrations.

The reduction of low concentrations of bromate was slow. After 5 days 12% of bromate was reduced with 0.15 mg/L iron dose in the presence of nitrate, while 7% of bromate was reduced with the same iron dose in the absence of nitrate. The 1.5 mg/L iron dose reduced 58 and 75% of bromate in the presence and absence of nitrate, respectively.
Moreover, the experiments of nitrate in absence of bromate showed that nitrate was not reduced by iron (II).

The reduction of bromate by iron (II) strongly depends on the iron dose and the reaction time, therefore this technology could be used as a water treatment technology increasing the iron dose to reduce the reaction time or taking the characteristics of MAR (anoxic environment with iron (II) content and long residence time) as an advantage which would be propitious for bromate reduction.

CONTENTS

1

INTRODUCTION

1.1. ADVANCED OXIDATION PROCESS AOP

Disinfection is used in drinking water treatment to prevent waterborne disease and kill or inactivate pathogens microorganism in water supplies. Chlorine is the most widely used disinfectant since 1900. However, in 1974, researchers in Netherlands and United States demonstrated that water chlorination cause formation of trihalomethanes through a reaction between chlorine or bromide with organic matter [1]. In The Netherlands, the Association of Dutch Water Companies (Vewin) set threshold values for trihalomethanes, and in 2008 the standard values became stricter while if chlorination was used it was not possible to fulfill them. In addition, it was found that Cryptosporidium, Giardia and Legionella were resistant to chlorination.

Moreover, organic micropollutants OMPs include diverse chemical compounds, such as pesticides, pharmaceutical, personal care products among others which enter into the environment through discharges from wastewater treatment plants, industries and hospitals, agricultural run-off and landfill leachates [2, 3]. OMPs have been found in surface waters around the world. OMPs are not new but the development of more accurate techniques with low detection limits allows that more OMPs can be detected, emerging questions about their effects on human health. Although, there is no evidence that most pharmaceuticals have a human health risk, the mixture of them and the presence of carcinogens OMPs even at low concentrations is a concern for human health [4], especially because these compounds do not belong to drinking water.

The need of disinfect water and remove OMPs triggered the development of alternative treatments as oxidation techniques defined as advanced oxidation processes (AOP) which are capable of exploit the high reactivity of hydroxyl radicals (OH°) in oxidation process to achieve complete abatement of pollutants [5]. The most common AOP and suitable for water treatment are UV/H_2O_2 , H_2O_2/O_3, UV/O_3, $UV/H_2O_2/O_3$ or UV/TiO_2 [6, 7]. Moreover, it has been proven that advanced oxidation process can inactivate a wider range of microorganisms such as protozoa and viruses than conventional disinfectants (chlorine, dioxide chlorine) [8]. In addition, AOP will oxidize parent compounds into carbon dioxide and water or into smaller molecules that are more easily biodegradable [3]. Furthermore, water suppliers treat drinking water to protect public health and provide water without taste or odour.

Ozonation fulfills these requirements because it can control taste and odour, remove the colour caused by humic substances, disinfect the water through inactivating bacteria, cysts,viruses and transform OMPs into simpler molecules [4]. However, it has been reported that in bromide-containing waters, the formation of many by-products occurs during ozonation, such as bromate [8, 9]. According to the International Agency for Research on Cancer-IARC, bromate has been classified in Group 2B as a possible carcinogenic to humans. Furthermore, the World Health Organization-WHO has indicated that bromate is mutagenic both in vitro and in vivo [10]. Therefore the formation of by-products, in this case, bromate, needs to be evaluated carefully. Due to the harmful effects of bromate, the WHO and Environmental Protection Agency-EPA have set a drinking water standard of 10 $\mu g/L$ for bromate. However, the Dutch Drinking Water guideline indicates for oxidation 1 $\mu g/L$ or 5 $\mu g/L$ for disinfection [11]. Therefore, the interest of developing new technologies to achieve these low limits in drinking water has increased in the last years.

1.2. BROMATE FORMATION

In order to find an adequate technology for bromate removal, first, it is necessary to understand the mechanism of bromate formation during ozonation.
Ozone (O_3) and OH° are two of the strongest chemical oxidants. Ozone can react with compounds following different reaction pathways. Bromate can be formed from reactions with ozone or reactions with ozone and OH radicals. Bromate formation includes up to six oxidation states of bromine shown in Table 1.1. Due to the fact that both oxidants (O_3 and OH°) can act simultaneously or in sequence on various oxidation states, the whole reaction system is extremely complicated [8].

Table 1.1: Bromine species formed during bromate formation[1]

Species	Chemical formula	Oxidation state (Br)	Controlling oxidizing species
Bromide	Br^-	-1	O_3 OH°
Bromide radical	Br°	0	O_3
Hypobromous acid	HOBr	+1	OH°
Hypobromite	OBr^-	+1	O_3 OH° $CO\check{r}_3^-$
Bromine oxide radical	BrO°	2+	
Bromite	BrO_2^-	+3	O_3
Bromate	BrO_3^-	+5	

Ozone oxidises Br^- to form hypobromous acid HOBr. HOBr reacts with ozone, but only in its ionized form OBr^-. OBr^- is oxidized to BrO_3^- through bromite BrO_2^- as the reaction in Figure 1.1 shows in green.

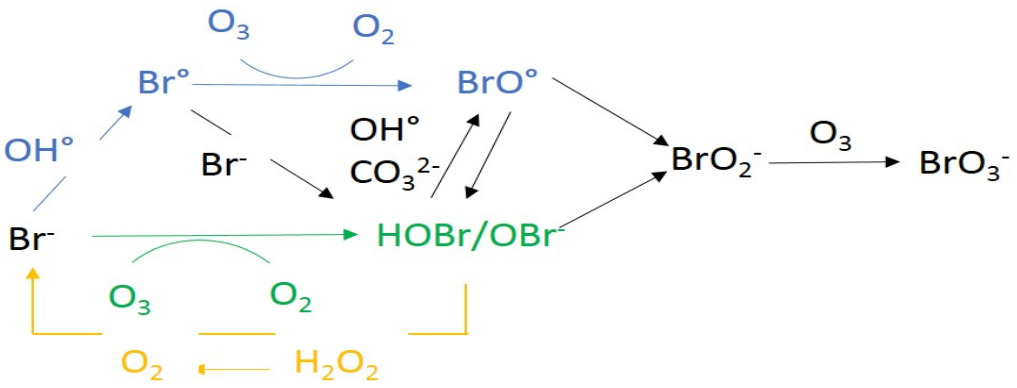

Figure 1.1: Bromate formation by bromide reaction with ozone (green) and with ozone and hydroxyl radical (blue)[2]

.

The second route in blue in Figure 1.1, takes place when the hydroxyl radical OH° reacts with bromide Br- forming bromine radical Br°. Ozone oxidizes bromine radical forming bromine oxide radical BrO°. Accelerated decay of the ozone by hydrogen peroxide will limit the formation of the BrO° radical and therefore it will limit the bromate formation. BrO° radical is unstable and will react further to form bromite BrO_2^- or hypobromite OBr^- [12] as it follows:

$$BrO^\circ + BrO^\circ + H_2O \rightarrow BrO_2^- + OBr^- + H^+ \tag{1.1}$$

After this reaction BrO_2^- will oxidize forming bromate BrO_3^-.

Commonly ozone is added in combination with hydrogen peroxide to control the bromate formation. When hydrogen peroxide is added in excess this can react with hypobromite or hypobromous acid back to bromide as it can be seen on the yellow line of Figure 1.1.

---

[1] Retrieved from von Gunten (2003) [8]

[2] Adapted from [6, 8]

1.3. BROMATE REMOVAL

There are two approaches to control bromate contamination in drinking water. The first one is the inhibition (minimization) of bromate formation during ozonation and the second is the removal of bromate after ozonation. The first approach involves the addition of NH_3, H_2O_2 or organic hydroxyl radical scavengers or by adjusting the pH [12, 13]. However, this brings extra chemicals and can affect the water quality. Moreover, there is a risk that the bromide formed from bromate reduction can be oxidized again to bromate [14]. For the second approach, different methods are available to remove bromate such as adsorption, electrochemical or biological technologies.

The most common bromate removal methods are activated carbon (AC) [15], ion exchange [16], reverse osmosis membrane [17] and ultraviolet UV irradiation [18]. Some of these methods have high operational and maintenance costs, secondary pollution or complicated process in the treatment. On the other hand, adsorption seems to be the most promising due to its economy and easy accessibility. Several adsorbents have been studied for bromate removal including AC [19–21], modified AC [22–24], granular ferric hydroxide [25], iron modified materials [26], graphene [27, 28], layered double hydroxides and zeolites as a material support in catalytic hydrogenation [29, 30].

The modifications of activated carbon can improve the performance of the removal of target pollutants. The surface of activated carbon is modified in order to enhance the affinity for the pollutant making the surface sites more accessible for the pollutant [22–24].
Iron components as ferric hydroxide or ferric hydroxide coated sand which contain chloride in their structure have been also studied, where the chloride is exchanged by bromate for its removal [25].
In addition, layered double hydroxides exposed to thermal activation (300°C-500°C) have been investigated for bromate and bromide removal, in this case the anions and water are removed by calcination, therefore when LDH is in contact with water and anions (e.g. bromate or bromide) the reformation of the structure will happen with the uptake of bromate or bromide. Moreover, zeolites in combination with one or two metals have been used to remove bromate, as well.

Graphene, graphene oxide and hydroxyapatite are materials which could remove bromate or bromide. Graphene and graphene oxide are promising nanomaterials due to their characteristics (high surface area).The use pf graphene membranes could remove anions using their negative surface charge to repulse bromate or bromide. Graphene oxide could also be used in combination with zero valent iron where graphene oxide offers more stability and high surface to reduce bromate into bromide. Furthermore, hydroxyapatite has been used for fluoride removal due to its affinity, and due to the the fact that bromide and fluoride are halogens and have similar characteristics, bromate or bromide removal could be feasible. The materials mentioned above are described in detail in Appendix A.

However, some of these materials are not applicable in practice as drinking water treatment technology, due to their difficult regeneration (high temperatures for LDH), complicated big scale production (graphene) and secondary pollution (ferric hydroxide) which is formed by conventional processes such as coagulation/ flocculation, sedimentation and filtration, among others.

1.4. CHEMICAL REDUCTION WITH IRON (II)

The reduction of bromate by iron occurs as the reaction 1.2 shows. The reaction indicates that bromate requires a sixfold molar excess of iron (II) to be reduced to bromide. It can be seen that in order to bromate reacts with iron, H^+ needs to be present.

$$BrO_3^- + 6Fe^{2+} + 6H^+ \rightarrow Br^- + 6Fe^{2+} + 3H_2O \tag{1.2}$$

In addition redox reactions using ferrous and zero valent iron have been also investigated in the reduction of bromate to bromide in the presence of oxygen [31–35].

The authors which have studied bromate reduction with iron (II) used low concentrations of bromate (25 and 50 $\mu g/L$). Siddiqui et al. (1994) investigated the reduction of 50 $\mu g/L$ BrO_3^- with an iron dose of 15 mg/L, 7 mg/L of dissolved oxygen at pH 7.5, obtaining reduction of 80% after 30 min while Dong et al. (2009) studied the reduction of 25 $\mu g/L\ BrO_3^-$ with an iron dose of 30 mg/L, 2.3 mg/L of dissolved oxygen at pH 7.2 and 25°C reaching 65% reduction after 20 min.

The studies of zero valent iron used iron doses of 5 mg/L and 1.28 g/L. Xie & Shang, (2005) studied the role of humic acid and quinone compounds on bromate reduction, showing that the complexation of humic acid with iron species and its adsorption passivated the iron surface and decreased the rate of bromate reduction by Fe(0), while the quinone model compound did not cause significant effect on the bromate reduction. For this study Xie & Shang (2005) used 5 mg/L of bromate with 1 g/L of Fe (0) reaching almost 90% reduction after 40 min. Westerhoff (2003) investigated the reduction of 1.28 g/L BrO_3^- with 20 g/L of Fe(0) at pH 7 and with two temperatures (28°C and 8°C). Almost a complete reduction of bromate occurred after 120 and 900 min at 28 and 8°C respectively, showing that the reaction happened more rapidly at 28°C.

1.5. SCOPE OF THIS THESIS

Dunea water company uses the multiple barrier approach for surface water treatment. One of the barriers is the managed aquifer recharge (MAR), which is the intended recharge of the aquifer with water followed by recovery after certain period of time, in order to treat, store and level the water quality. There are different types of MAR, such as infiltration ponds which are the case of Dunea. Water from Meuse river is collected and pre-treated, then transported and infiltrated through the dunes with an average residence time of 120 days [3]. Then water is abstracted from the wells to continue with the post-treatment. During the soil passage water flows from an oxic to an anoxic environment, where the spatial distribution of chemical species varies from oxidised to reduced form of ions (e.g. iron (III) in oxic to iron (II) in anoxic water), along the soil passage.

Unfortunately water from river Meuse contains OMPs and the current treatment is not adequate. Therefore, Dunea has been investigating the extension of the multiple barriers, adding AOP before MAR. The reasons to implement AOP before MAR are that the chemical oxidation of the compounds present in water (NOM, OMPs, halogens, etc.) during AOP, with short residence time, allows the formation of smaller and simpler molecules such as assimilable organic carbon or transformation products from OMPs and by-products. These products can be biological and chemically removed during the dune passage with a long residence time.

The scope is the literature research of materials, mostly adsorptive, for bromate removal which is included in Appendix A and the experimental research of chemical reduction of bromate by iron (II). The reduction of bromate, as a by-product of AOP, using iron (II) and zero valent iron in excess has been studied before in presence of oxygen. However, the reduction of bromate to its harmless species bromide using iron (II) as a reductant agent under anoxic conditions has not been studied. The investigation of bromate reduction by iron (II) in the presence and absence of nitrate, could be an important reference to develop a drinking water treatment technology or even translated to the possibility of using the presence of iron (II) in anoxic conditions in the dunes with a long residence time during managed aquifer recharge (MAR) as Figure 1.2 shows.

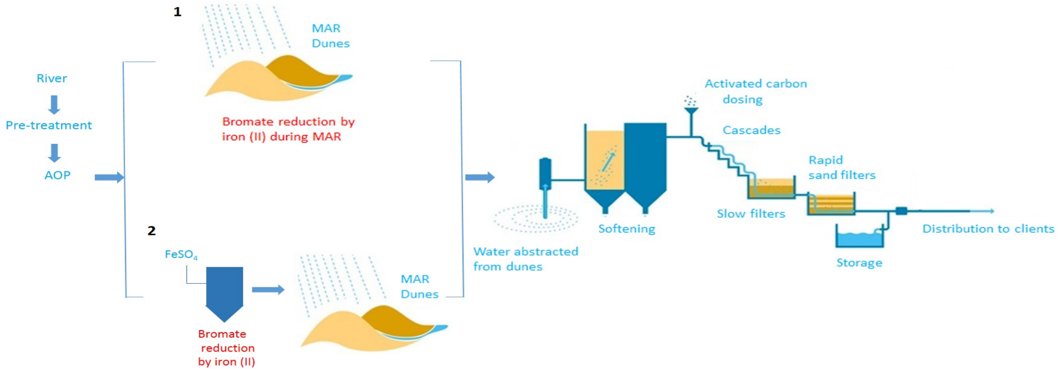

Figure 1.2: Location of bromate reduction step during drinking water treatment process at Dunea [3]

---

[3] Retrieved and adapted from https://www.dunea.nl/drinkwater/drinkwater-maken

For this purpose five experiments were done to evaluate the bromate reduction at high (5 mg/L) and low (60 $\mu g/L$) concentrations with different iron (II) doses (13 mg/L and 52 mg/L for high bromate concentration and 0.15 mg/L and 1.5 mg/L for low bromate concentration), in the presence and absence of nitrate (5 mg/L and 10 mg/L). In addition, nitrate reduction by iron in absence of bromate was evaluated with and without catalyst.

1.6. RESEARCH QUESTIONS

1. What is the state-of- art in adsorption materials for bromate removal (in Annex)?

   How could these technologies be applied at an AOP-MAR treatment plant?

   What typical AOP-MAR water quality aspects can be utilized to improve bromate removal?

2. Is chemical reduction of bromate by iron (II) a promising drinking water treatment technology?

   How does stoichiometry ratio between iron and bromate affect the reaction at high and low concentrations of bromate?

   Do iron dose, pH and reaction time interact in bromate reduction with iron (II)?

   What is the effect of the presence of nitrate at equal concentration with bromate in bromate reduction?

3. Can bromate be reduced by iron (II) during managed aquifer recharge?

   Is low iron concentration a limiting factor?

   What is the effect of the presence of nitrate at different concentrations in bromate reduction?

2

MATERIALS AND METHODS

2.1. EXPERIMENTAL CONDITIONS

All experiments were done at Climate room - Waterlab from the Water Management Department of Civil Engineering Faculty of TU Delft.

Bromate reduction by ferrous iron was studied under anoxic conditions (DO= 0.01 mg/L) at 12°C in jar-test experiments and agitated at 120 RPM with the VWR Orbital shaker, 5000. In order to reach the anoxic conditions each bottle solutions (with bromate, nitrate or bromate and nitrate together and the control) were sparged with nitrogen gas to take out dissolved oxygen until a DO concentration of 0.01 mg/L. All experiments were carried out in duplicate. The used set up for all the batch experiments is shown in Figure 2.1. Glass bottles were sealed with rubber stoppers and caps to guarantee the anoxic conditions. Two needles with their corresponding valves were used as a sampling or dose addition point and the other for nitrogen gas injection.

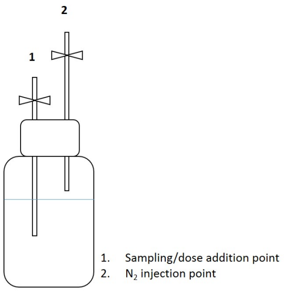

Figure 2.1: Batch test reactor.

2.2. PREPARATION OF SOLUTIONS

Deionized (DI) water (18 $M\Omega$) and reagent grade chemicals (sodium bromate, sodium nitrate, ferrous sulphate heptahydrate, cooper sulphate, sodium bicarbonate and ethylene diamine) were used to prepare all the solutions.

In all experiments, 2 mM $NaHCO_3$ was used as buffer and pH was adjusted with 0.2 M NaOH.

For iron (II) solution, $FeSO_4 * 7H_2O$ was used. In order to prevent iron oxidation, the solution was acidified with concentrated nitric acid (65%) [36]. $FeSO_4 * 7H_2O$ was added to about 50 mL of DI water containing 24 μL of concentrated nitric acid in a 100 mL volumetric flask (final pH ≈ 2).

It should be noted that iron (II) dose added extra NO_3^- (approximately 2.16 mg/L) to the batch experiments due to the use of concentrated nitric acid. This should be considered especially for experiments that include

NO_3^-.

For preservation of samples, that contained bromate, and to stop the conversion of residual hypobromite to bromate, ethylene diamine (EDA) was used [36]. The EDA solution was prepared diluting 5.6 mL of ethylene diamine (99%) with 50 mL DI water. To preserve the sample 1 μL of the EDA solution was added to 1 mL of sample.
Appendix B shows calculations for the preparation of different solutions used in all Batch experiments.

2.3. Redox Batch experiments

Figure 2.2 shows the experiments that were done to evaluate bromate reduction using iron (II) in presence and absence of nitrate.

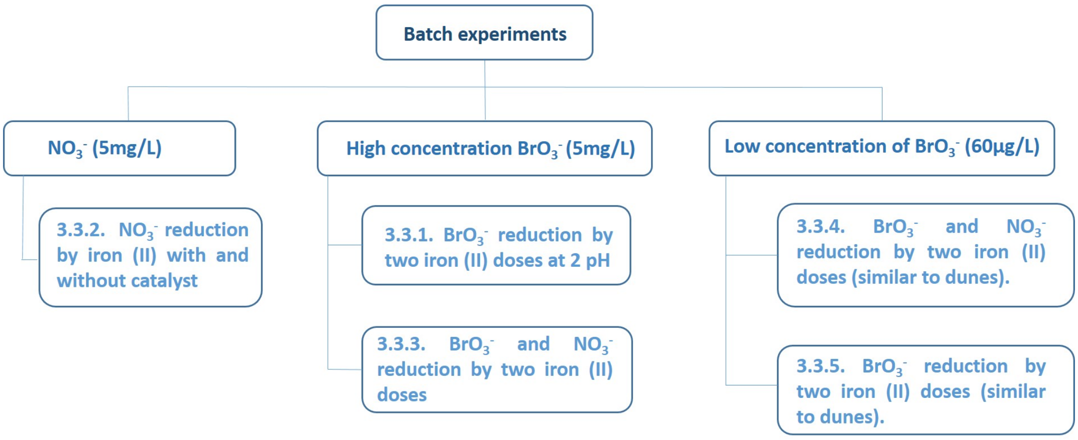

Figure 2.2: Diagram with experiments done in this test.

First, the reduction of high concentrations of bromate (5 mg/L) was tested with two different pH in order to find the pH where the reduction was higher. Second, the reduction of bromate in presence of equal concentrations of nitrate was tested in order to see the effect of the presence of nitrate during bromate reduction. The third experiment was the reduction of 5mg/L nitrate alone using iron (II) in order to see if nitrate can be reduced by iron.

After these experiments, the reduction of low concentrations of bromate (60 $\mu g/L$) in presence of high concentration of nitrate (10 mg/L) using iron (II) was tested to investigate if the difference in concentration has an effect in bromate reduction. Finally, the reduction of (60 $\mu g/L$) bromate in absence of nitrate was tested in order to compare the rate of bromate reduction in absence and presence of nitrate.

2.3.1. Bromate reduction by two iron (II) doses at two different pH

For these experiments, 5 mg/L of BrO_3^- were dosed into 250 mL bottles. Two doses of iron (II) were chosen for bromate reduction. 5.89 mg of $NaBrO_3$ were added per litre of solution to obtain 5 mg/L of BrO_3^-.The first Fe^{2+} dose, 13 mg/L Fe^{2+}, was selected according to the stoichiometry of the reaction 1.2, where reduction of bromate by Fe^{2+} requires a sixfold molar excess of Fe^{2+} to yield Fe^{3+} and Br^-.

$$BrO_3^- + 6Fe^{2+} + 6H^+ \rightarrow Br^- + 6Fe^{2+} + 3H_2O \tag{2.1}$$

The second dose was 52.5 mg/L (4 times higher than the stoichiometric requirement) which was chosen in order to guarantee BrO_3^- reduction. 2.5 mL of Fe2+ stock solution of 1.31g/L and 5.25g/L (for each dose) was added into bottles.

Control bottles for BrO_3^-, without iron doses and also controls for Fe^{2+} without BrO_3^- were used.
Experiments were carried out at two different pH. The pH of the BrO_3^- solution was 7.4 and 9.5 and immediately after the addition of the Fe^{2+} dose the pH dropped to 5.2 and 7 respectively.

Samples of 15mL for BrO_3^-, 2 and 0.5mL for the lowest and highest dose of Fe^{2+} were taken at time 0, 0.25, 0.5, 1, 1.5, 2, 24, 48 and 120 h. Samples for BrO_3^-. were filtered with 0.45 μm syringe filters and preserved with 15 μL of EDA.

2.3.2. NITRATE REDUCTION BY IRON (II) WITH AND WITHOUT CATALYST

These experiments were carried out using 250 mL bottles with 7.17 mg/L NO_3^- solution at pH 7.5. 0.0069 g of $NaNO_3$ were added per litre of solution and after the iron dose addition, nitrate concentration increased to 7.17mg/L. In control groups, iron was not added.
The selected iron dose was 36.13 mg/L, according to stoichiometry of the reaction. Ottley et al. (1997) mentioned several possible reactions where reduction of NO_3^- by Fe^{2+} can occur as can be seen in the Table 2.1. The first equation of the referred Table was selected for these experiments.

Table 2.1: Possible nitrate reduction reactions and resultant ratios of reactants and products

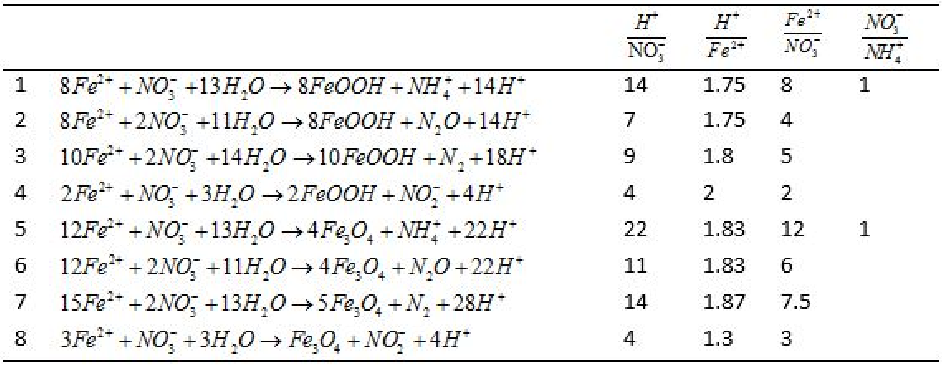

		$\frac{H^+}{NO_3^-}$	$\frac{H^+}{Fe^{2+}}$	$\frac{Fe^{2+}}{NO_3^-}$	$\frac{NO_3^-}{NH_4^+}$
1	$8Fe^{2+} + NO_3^- + 13H_2O \rightarrow 8FeOOH + NH_4^+ + 14H^+$	14	1.75	8	1
2	$8Fe^{2+} + 2NO_3^- + 11H_2O \rightarrow 8FeOOH + N_2O + 14H^+$	7	1.75	4	
3	$10Fe^{2+} + 2NO_3^- + 14H_2O \rightarrow 10FeOOH + N_2 + 18H^+$	9	1.8	5	
4	$2Fe^{2+} + NO_3^- + 3H_2O \rightarrow 2FeOOH + NO_2^- + 4H^+$	4	2	2	
5	$12Fe^{2+} + NO_3^- + 13H_2O \rightarrow 4Fe_3O_4 + NH_4^+ + 22H^+$	22	1.83	12	1
6	$12Fe^{2+} + 2NO_3^- + 11H_2O \rightarrow 4Fe_3O_4 + N_2O + 22H^+$	11	1.83	6	
7	$15Fe^{2+} + 2NO_3^- + 13H_2O \rightarrow 5Fe_3O_4 + N_2 + 28H^+$	14	1.87	7.5	
8	$3Fe^{2+} + NO_3^- + 3H_2O \rightarrow Fe_3O_4 + NO_2^- + 4H^+$	4	1.3	3	

For the experiments with catalyst, copper (II) was used as a catalyst. According to the experiments of Ottley et al. (1997) for nitrate reduction by iron with copper as a catalyst, 1.28 mg/L of copper (II) is necessary to reduce 5 mg/L of nitrate. $CuSO_4$ was used to provide copper (II).

2.5 mL of Fe^{2+} stock solution (3.6 g/L) were added to bottles and for the experiments with catalyst 2.5 mL of Cu^{2+} stock solution (128 mg/L) were added.

The pH of the NO_3^- solution was 7.4 and immediately after the addition of the acidified Fe^{2+} dose the pH dropped to 5.2 approximately.

Samples of 6mL for NO_3^- and NH_4^+ and 2 mL for Fe^{2+} were taken at 0, 0.25, 0.5, 1, 2, 17 24, 44, 67 and 120 h. The samples for NO_3^- were filtered with 0.45 μm.

2.3.3. BROMATE REDUCTION BY HIGH IRON (II) CONCENTRATIONS, IN THE PRESENCE OF NITRATE

For this experiment, 250 mL bottles with 5mg/L of BrO_3^- and 2.84 mg/L of NO_3^- were used. 5.89 mg of $NaBrO_3$ and 0.004 g of $NaNO_3$ were added per litre of solution and after iron dose addition, the nitrate concentration reached 5 mg/L.

Two doses of Fe^{2+} were chosen for bromate reduction. Doses were the same as used in previous experiment. Therefore the first dose only considered the amount of Fe^{2+} to reduce only bromate according to the equation 1.2 and the second dose took into account the amount of Fe^{2+} necessary to reduce 5 mg/L of BrO_3^- and 5 mg/L of NO_3^- together according to stoichiometry of reaction 1.2 and the first equation from the Table 2.1. 2.5 mL of Fe^{2+} stock solution of 1.31 g/L and 5.25 g/L (for each dose) were added to bottles. After the addition of doses, the concentration of NO_3^- was approximately 5 mg/L.

Control bottles for BrO3- with NO_3^- without iron doses and also controls for only Fe^{2+} were used.

The experiments were carried out at pH 9.5. It should be noted that after addition of Fe^{2+} dose, pH dropped to approximately 7 at the beginning of the experiment.

Samples of 15mL for BrO_3^- and NO_3^-, 2mL and 0.5mL for the lowest and highest dose of Fe^{2+} were taken at 0, 0.25, 0.5, 1, 1.5, 2, 72 and 120 h. Samples for BrO_3^- and NO_3^-were filtered with 0.45 μm syringe filters and preserved with 15 μL of EDA.

2.3.4. Bromate reduction by low iron (II) concentrations, in the presence of nitrate

Different concentrations of nitrate and bromate were chosen taking into account the real concentrations in dunes which are approximately 10 mg/L for NO_3^- and 60 $\mu g/L$ for bromate in case AOP is applied.

Two concentrations of iron were chosen for the experiments. The first dose was calculated according stoichiometry from the equation 1.2 taking into account only the presence of BrO_3^- which is 0.16 mg/L of Fe^{2+} to reduce 60 $\mu g/L$ of BrO_3^-.

The second Fe^{2+} dose (1.5 mg/L) was chosen based on information of iron from dunes effluent at two locations of Dunea Water Company during 2015. Figure 2.3 shows the frequency of values of total iron. Due to anoxic/anaerobic conditions of the well, it was considered that the total iron corresponds to Fe^{2+}. As the histogram shows the majority of the values are between 0.083 and 0.4 mg/L with a maximum value of 1.625 mg/L Therefore the chosen doses (0.16 and 1.5 mg/L) are between the values shown in the histogram.

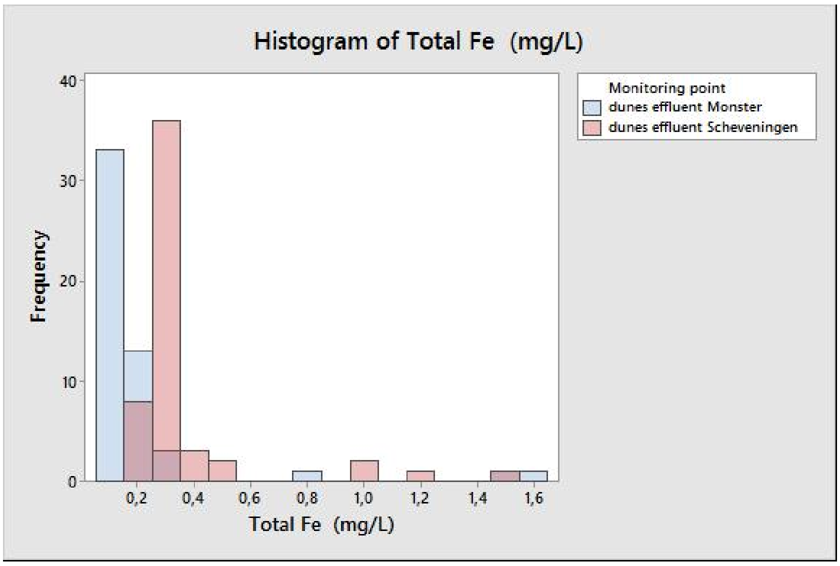

Figure 2.3: Histogram with Iron results from dunes effluent of Monster and Scheveningen during 2015

For this experiment, bottles with 1 L solution of 60 $\mu g/L$ of BrO_3^- and 7.84 mg/L of NO_3^- were used. 1 mL of 60 mg/L BrO_3^- stock solution was added per litre of solution in order to obtain 60 $\mu g/L$ BrO_3^-.

10 mL of Fe2+ stock solution of 15.7 mg/L and 150 mg/L (for each dose) was added to bottles. After addition of doses, the concentration of NO_3^- was approximately 10 mg/L.

Control bottles for BrO_3^- with NO_3^- without iron dose and controls for only Fe^{2+} were used.

The experiments were carried out at pH 9.5 and the pH dropped to approximately 7 after the addition of Fe^{2+} dose at the beginning of the experiment.

Samples of 60 mL for BrO_3^- and NO_3^- and 8 mL for Fe^{2+} were taken at 0, 0.25, 0.5, 1, 1.5, 2, 24 and 120 h. Samples for BrO_3^- with NO_3^- were filtered with 0.45 μm syringe filters and preserved with 60 μL of EDA.

2.3.5. BROMATE REDUCTION BY TWO IRON (II) DOSES (SIMILAR TO DUNES)

For this experiment bottles with 1 L solution of 60 $\mu g/L$ of BrO_3^- were used. For this, 1 mL of 60 mg/L BrO_3^- stock solution was added per litre of solution.

The same two iron doses from the previous experiment were used (0.16 mg/L and 1.5 mg/L). 10 mL of Fe^{2+} stock solution of 15.7 mg/L and 150 mg/L (for each dose) was added to bottles.

Control bottles for only BrO_3^- and only Fe^{2+} were used.

The experiments were carried out at pH 9.5 and the pH dropped to approximately 7 after the addition of Fe^{2+} dose at the beginning of the experiment.

Samples of 60 mL for BrO_3^- and 8 mL for Fe^{2+} were taken at 0, 0.25, 0.5, 1, 1.5, 2, 24 and 120 h. The samples for BrO_3^- were filtered with 0.45 μm syringe filters and preserved with 60 μL of EDA.

2.3.6. MEASUREMENTS

Fe^{2+} was measured by photometry using the Spectroquant ®Iron test (Merck). A dilution factor of 0.25 and 0.0625 was needed to measure the iron (II) in the experiments with dose of 13 and 52.5 mg/L respectively. For the doses 0.16 and 1.5 mg/L of iron, no dilution was needed.
Dissolved oxygen was measured with FDO® 925-optical oxygen sensor (WTW) and pH was measured analysed with electrode SenTix ® 940 (WTW), both using the WTW Multi 3420 multiparameter meter.

For the experiment of nitrate reduction by iron (II), from time 0 to 24 hours ammonium and nitrate were measured with the HACH ® Ammonium and Nitrate cuvette test LCK 303 and 339 respectively.

Bromate, Bromide and Nitrate were measured by ion chromatography(IC). For experiments with a concentration of 5 mg/L a Metrosep A Supp 16 - 150/4.0 column (150 mm x 4 mm) with a Metrohm 881 Compact IC pro-Anion was used. For experiments with concentrations of 60 $\mu g/L$ BrO_3^-, samples were analysed at HET Waterlaboratorium. An IonPac AS9SC column (250 mm x 4 mm ID) Dionex ICS-3000 was used for BrO_3^- and for Br^- two columns were used an IonPac AG22 column (4 x 50 mm) and an IonPac AS22SC column (4 x 250 mm) with the Dionex ICS-1100. The limit of detection of these three last columns is 10 $\mu g/L$ for Br^- and 0.5 $\mu g/L$ for BrO_3^-.

2.3.7. STATISTICAL ANALYSIS

For bromate reduction by two iron (II) doses at two different pH (section 2.3.1) a factorial analysis was designed. Interaction and main (independence) effects were analysed. Design configuration can be seen in Table 2.2.

Same factorial analysis was applied for equal concentrations of bromate and nitrate reduced by two iron (II) doses (section 2.3.3), different concentrations of bromate and nitrate with 2 different doses (similar to dunes) (section 2.3.4) and for bromate reduction by two iron doses (similar to dunes) (section 2.3.5).

Table 2.2: Design configuration of factorial analysis

FACTORS	LEVELS (High concentration BrO_3^-)	LEVELS (Low concentration BrO_3^-)
Iron (II) doses (mM)	0.27	0.007
	1.0	0.03
pH	7.4	9.5
	9.5	
Reduction time (hours)	0	0
	0.25	0.25
	0.5	0.5
	1	1
	2	2
	24	24
	48	120
	120	

One-way ANOVA was used for all tests to find out variability at certain specific reaction time. All statistical calculations were supported by Minitab software, 17 version.

3

Results

3.1. Bromate reduction by two iron (II) doses at two different pH

3.1.1. The two Iron (II) doses: individual behaviour details

Iron dose: 13 mg/L (0.27 mM)

Bromate reduction and consequently bromide formation at two different pH (7.4 and 9.5) in presence of 0.27 mM Fe^{2+} and initial concentration of 5 mg/L BrO_3^- are shown in Figure 3.1. All concentrations are expressed in miliMolar (mM).

Figure 3.1 shows the time dependency of the redox reaction. In addition, a steep curve at the beginning (up to 30 min) indicates a rapid bromide formation/bromate reduction at both pH levels. From 30 min to 24 hours, bromide formation decelerates, followed by a slower conversion that gradually reached the equilibrium when the curve becomes asymptotic.

10 and 11% of bromate was reduced during the first 15 min at pH 7.4 and 9.5. At 2 hours, 23 and 25% of bromate was reduced at pH 7.4 and 9.5 respectively. After 24 hours acceleration can be observed where between the 60 and 80% of bromate was reduced, reaching above 90% reduction after the 5th day. The values of bromate at each time were analysed through ANOVA, showing values of $p>0.05$ which indicates that there was not a significant difference in bromate reduction between both pH. On the contrary, in case of bromide formation, there is a clear difference between the two pH levels ($p<0.01$) showing that bromide formation is faster at pH 9.5 than at 7.4.

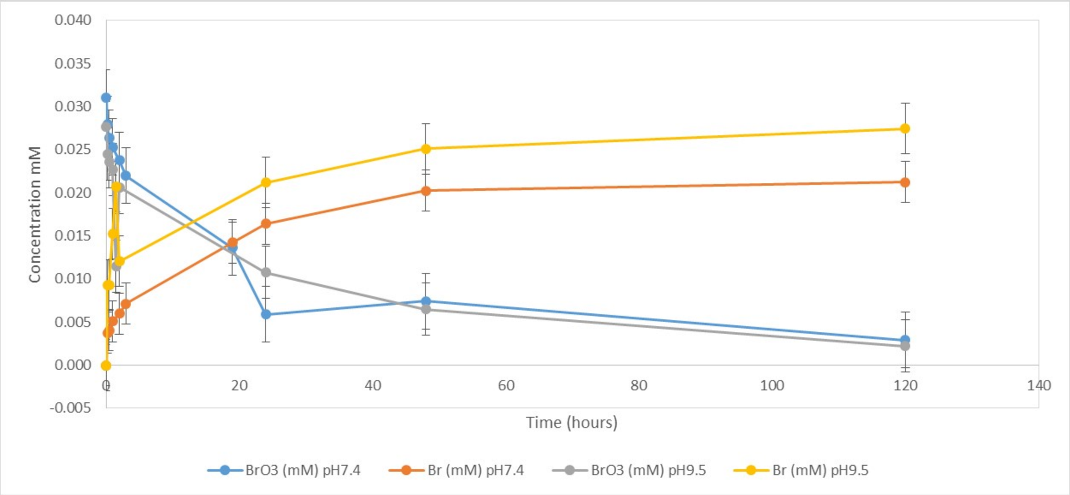

Figure 3.1: Bromate reduction and bromide formation with iron dose 0.27 mM (13 mg/L) at pH 7.4 and 9.5.

A mass balance of Br- and BrO_3^- at pH 9.5 showed that almost all BrO_3^- was reduced to Br^-, while at pH 7.4 this does not occur after 24 hours.

Complementary with bromate reduction and bromide formation, Fe^{2+} concentration decreased along the time as can be seen in Figure 3.2. In addition, Fe^{2+} concentration in the control group did not decrease along time, which confirmed the absence of oxygen in the bottles.

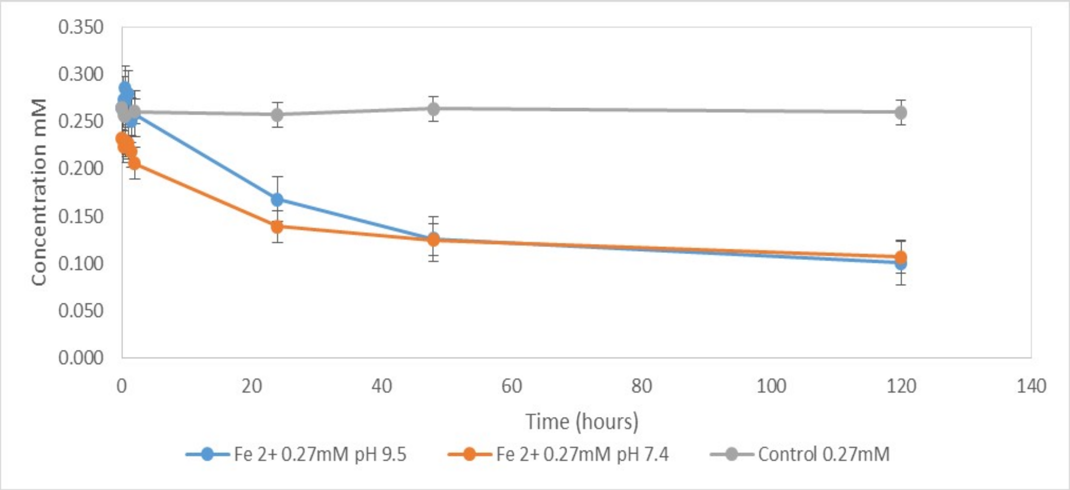

Figure 3.2: Consumption of Fe^{2+} with initial concentration of 0.27mM during bromate reduction at pH 7.4 and 9.5.

IRON DOSE: 52.5 mg/L (1 mM)

Figure 3.3 shows a faster bromate reduction and consequently bromide formation with Fe^{2+} dose of 1 mM (compared with the Fe^{2+} dose of 0.27 mM).There was no significant difference of BrO_3- reduction between two pH levels ($p>0.05$). However, significant difference of Br- formation between the two pH levels was observed ($p<0.05$).

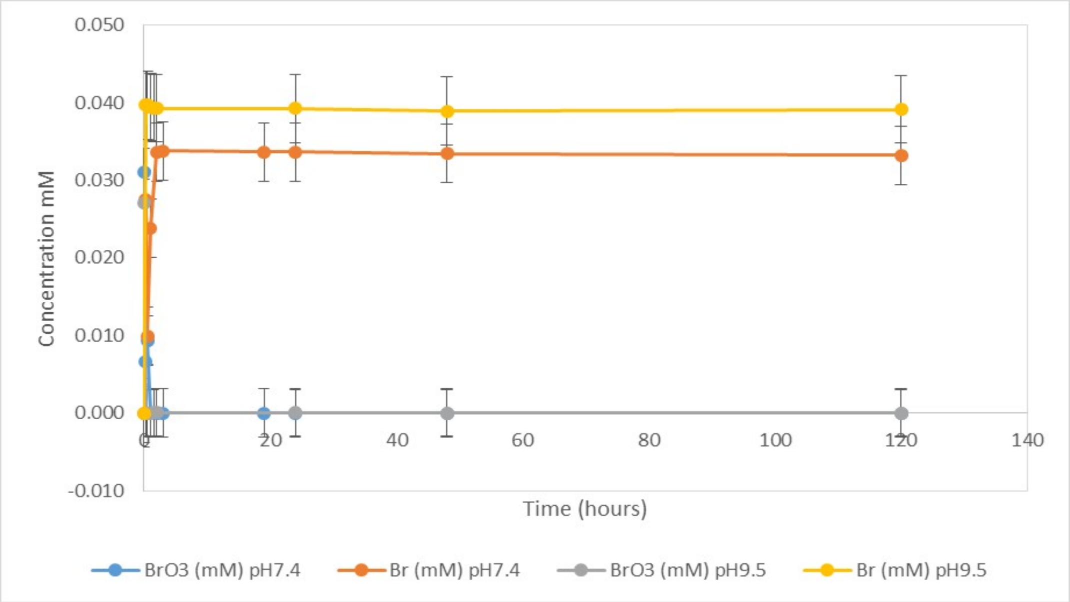

Figure 3.3: Bromate reduction and Bromide formation with 1mM (52.5 mg/L) Fe2+ dose at pH 7.4 and 9.5.

In relation with Fe^{2+} consumption, Figure 3.4 shows that iron concentrations decreased very fast during the first 2 hours. From this time on, a clear difference can be observed between both pH levels. The figure also shows no iron (II) variation for the control bottle which confirms the absence of oxygen.

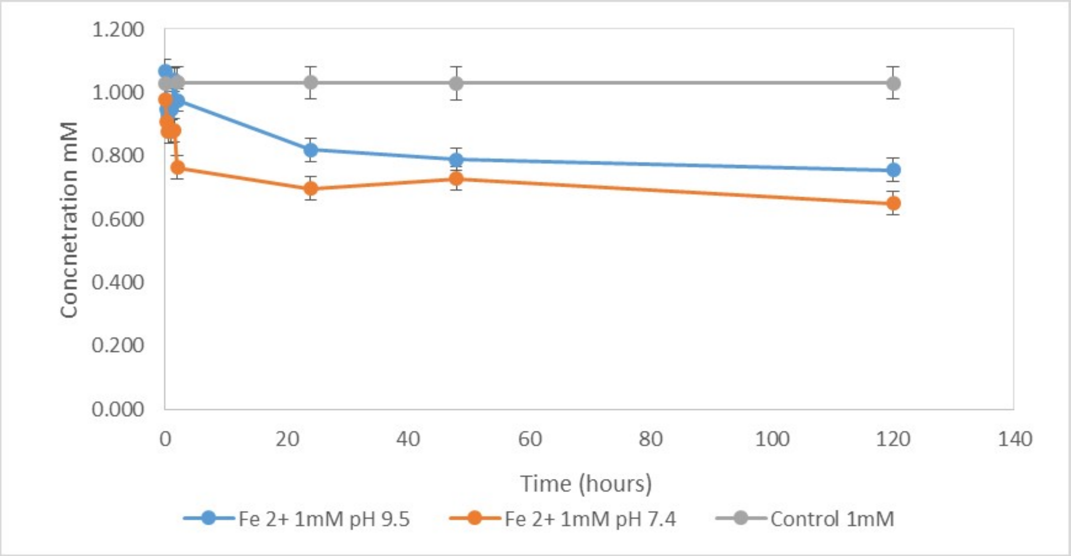

Figure 3.4: Consumption of Fe^{2+} with an initial concentration of 1 mM dose during bromate reduction at pH 7.4 and 9.5.

Regarding the stoichiometry for the 0.27 mM Fe^{2+} dose, it was observed that experimental ratios Fe^{2+}/BrO_3^- at pH 7.4 and 9.5 were 5.3 and 6.5 respectively while the theoretical ratio is 6. For 1 mM Fe^{2+} dose, it was not possible to calculate the ratio of consumed reactants due to lack of data of bromate which was consumed really fast.

For both doses, oxidation of Fe^{2+} into Fe^{3+} was evidenced by colour change in the bottles from transparent at the beginning to yellowish and in case of 1 mM with formation of small flocs. For the high Fe^{2+} dose a light change of colour occurred after 15 min, while for the low Fe^{2+} dose, it occurred after 1 hour. This change in colour can be observed in Figure 3.5 for pH 7.4 and in Figure 3.6 for pH 9.5, where the higher Fe^{2+} dose shows an intense shade of colour for both pH levels. Colour variation over time can be observed in Appendix C.

Figure 3.5: Different shade of colours due to iron oxidation at different iron doses at pH 7.4 after 24 hours (the transparent bottles are the controls for bromate).

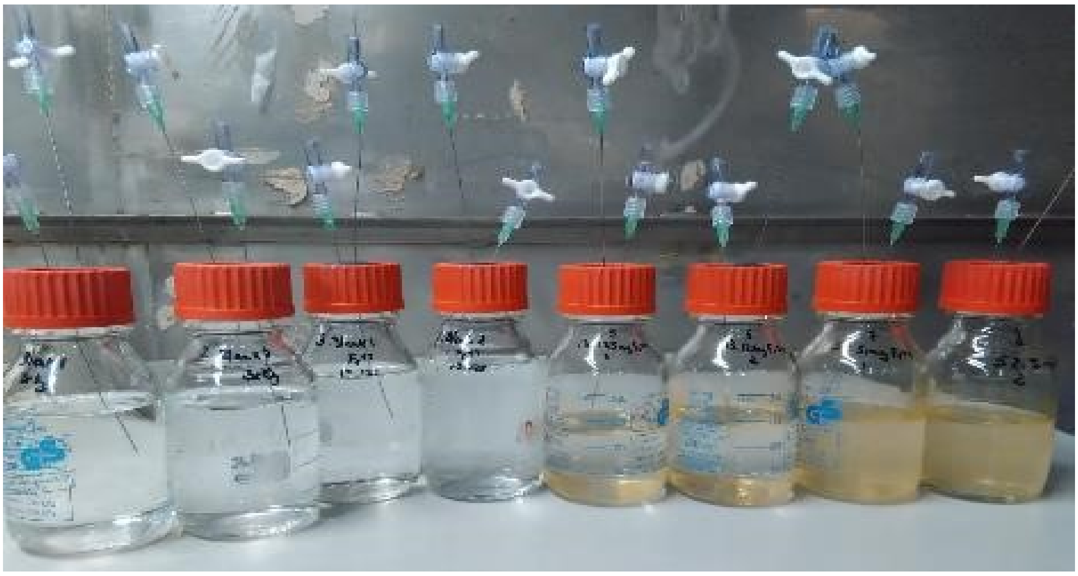

Figure 3.6: Different shade of colours due to iron oxidation at different iron doses at pH 9.5 after 48 hours. The first two bottles are the controls without iron and the third and fourth bottles are the controls without bromate.

3.1.2. INTERACTION EFFECTS BETWEEN IRON DOSES, pH AND REACTION TIME

The factorial analysis shows that there is no significant interaction among the three factors join together ($p>0.05$). However, when two factor interactions are evaluated, only interaction between iron dose and time is highly significant ($p<0.001$) in bromide formation as shown in Figure 3.7. It can be seen that the highest iron dose (1mM) has the highest bromide formation. pH factor does not interact neither with iron doses nor time.

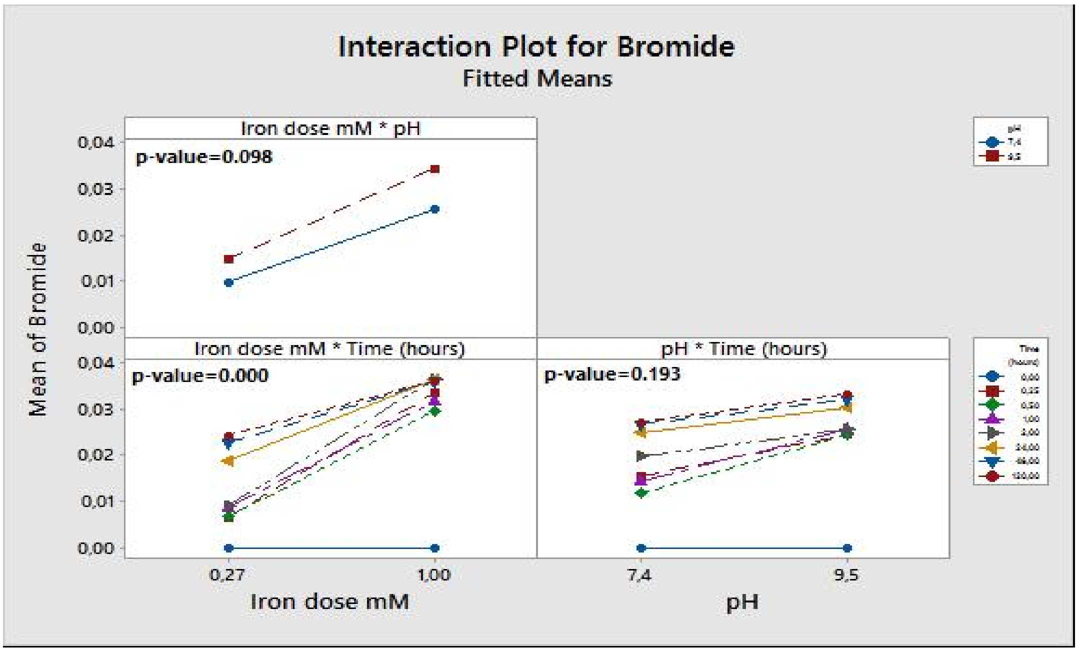

Figure 3.7: 2-way Interaction between iron dose, reaction time and pH for bromide formation.

3.1.3. MAIN EFFECTS OF IRON DOSES, pH AND REACTION TIME

Due to the fact that only interaction between iron dosage and reaction time was highly significant, the main effect of each factor was evaluated as shown in Figure 3.8. The analysis indicates that the independent effect of each factor is very highly significant in the formation of bromide (p<0.001 for each effect). Bromide formation was faster in the presence of highest iron dose (1 mM) and at the highest pH (9.5). The bromate formation at the highest iron dose and highest pH are located above the mean of all treatments. With respect to time, within 2 hours more than 66% of bromide has been formed.

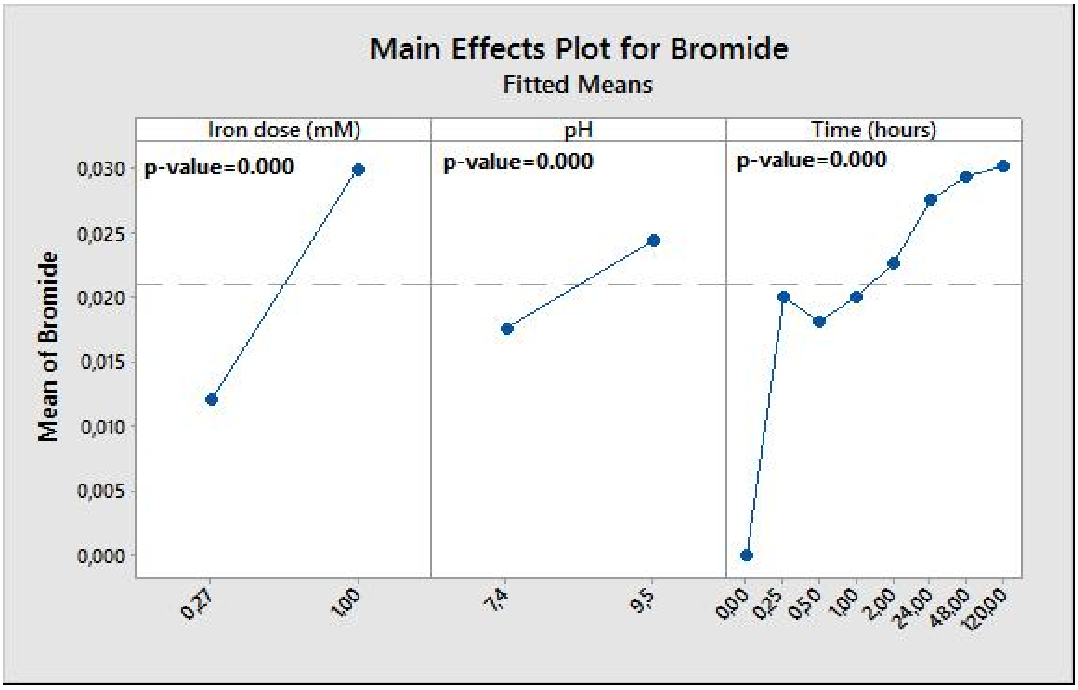

Figure 3.8: Main effects of each factor (iron dose, pH and reaction time) for Bromide formation.

3.2. NITRATE REDUCTION BY IRON (II)

Figure 3.9 and 3.10 show that there was no reduction of nitrate by iron (II) in absence of a catalyst. From time 0 to 24 hours, it was analysed with cuvette test and then by ion chromatography (IC) as described in the methodology. The same trend can be observed in iron concentration along time in Figure 3.11.
In addition, ammonium was measured. However it could not be detected because it was under limit of detection. Therefore the ammonium formation was neglected.

Reduction of nitrate with catalyst can be found in the Appendix C.

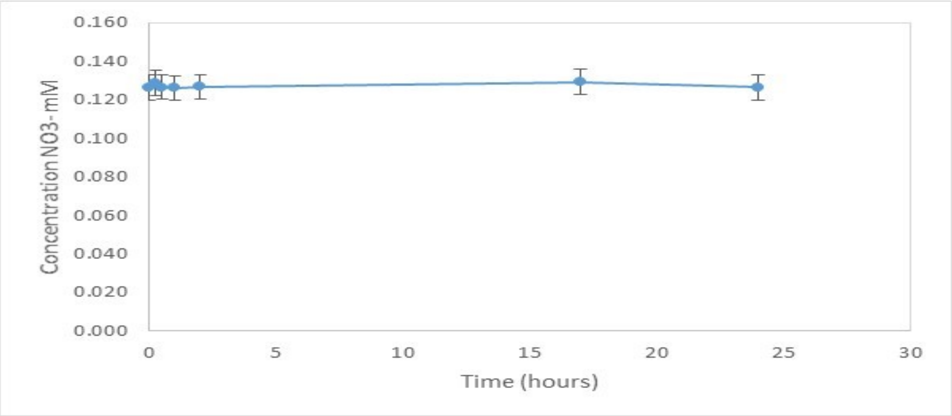

Figure 3.9: Nitrate reduction by iron, measured with cuvette test.

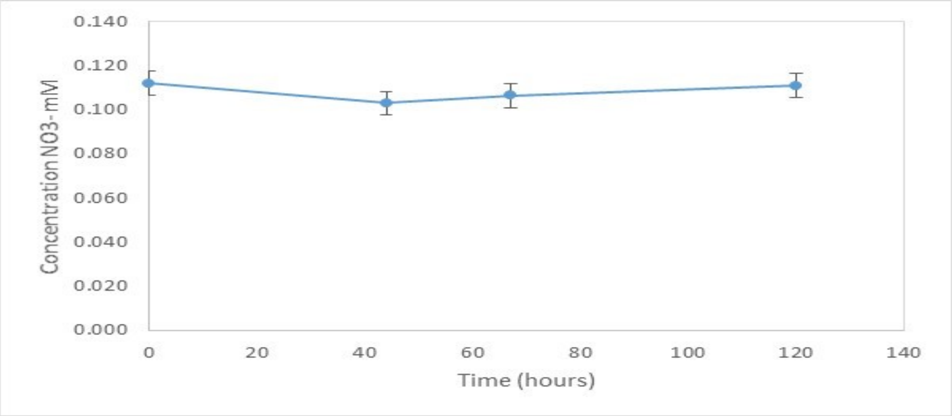

Figure 3.10: Nitrate reduction by iron, measured with ion chromatography.

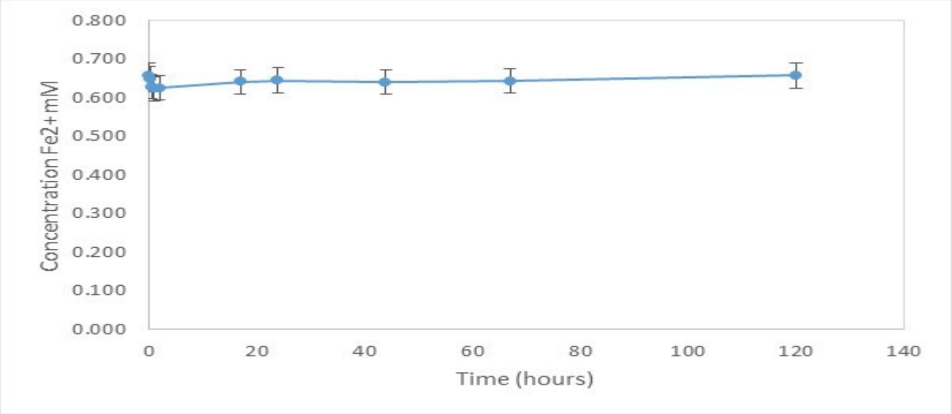

Figure 3.11: Iron concentrations in the nitrate reduction experiments without catalyst.

3.3. BROMATE REDUCTION BY HIGH IRON (II) CONCENTRATIONS, IN THE PRESENCE OF NITRATE

Due to the fact that there was no reduction of nitrate using iron (II) and to confirm that nitrate is not a competitor of bromate for iron in this chemical reduction process, it was decided to evaluate the reduction of bromate and nitrate at equal concentrations using two iron (II) doses at pH 9.5. Bromate reduction and bromide formation with 0.27 mM and 1 mM of Fe^{2+} doses are shown in the Figures 3.12 and 3.13. Nitrate concentration did not vary significantly, behaviour which was observed at both iron doses.

From Figure 3.12 it can be observed that bromate decreased with reaction time. During the first 30 min there is a fast bromate reduction and complementary bromide formation, which tends to decelerate reaching the equilibrium within 5 days.

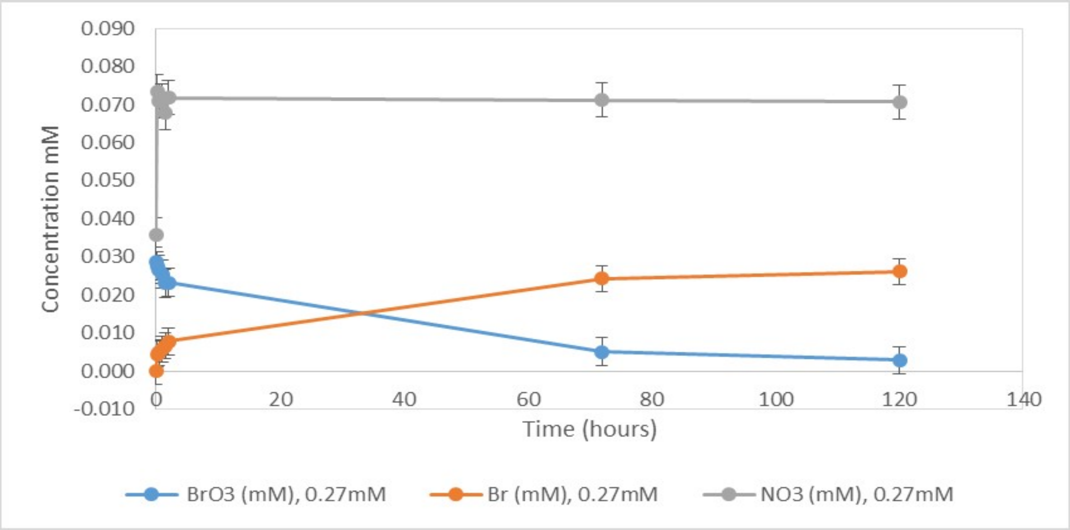

Figure 3.12: Bromate reduction and bromide formation in presence of nitrate with iron dose 0.27 mM.

Figure 3.13 shows bromate reduction and bromide formation with 1 mM of Fe^{2+}. Bromate reduction was achieved during the first 1.5 hours, which differs from the reduction of bromate in absence of nitrate where the reduction was reached within 30 min. A small fluctuation of bromate can also be observed from Figure 3.13, where the concentration increased at time of 2 hours, then decreased with time and finally it rose again at 120 hours.

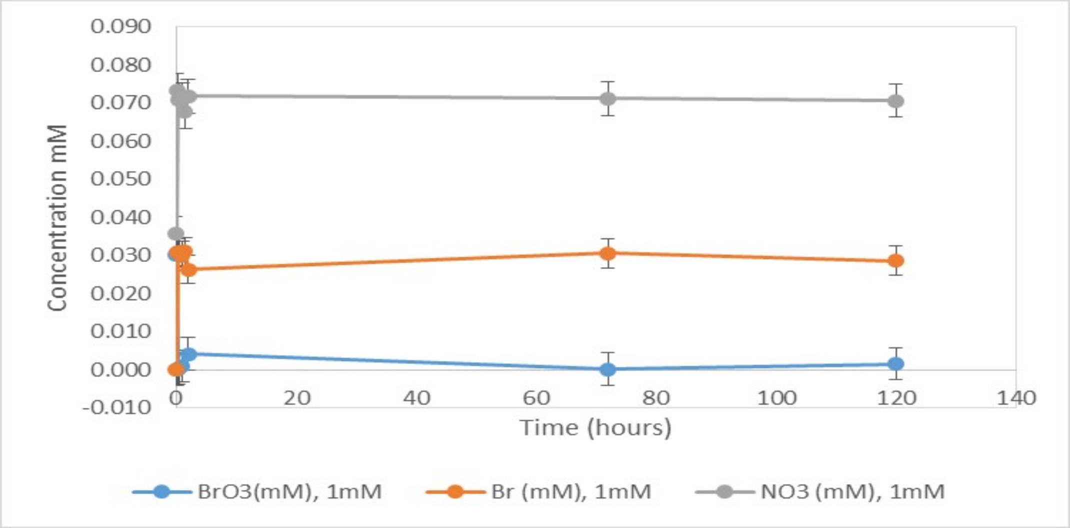

Figure 3.13: Bromate reduction and bromide formation in presence of nitrate with iron dose 1 mM.

The iron consumption is shown in Figure 3.14. The concentration of iron decreased over time for both dosages. The graph indicates that iron consumption during the first hours was fast, matching with the bromate reduction. The decrease of iron concentration after 72 hours for the iron dose is significant ($p<0.05$), while for the dose 0.27 mM is not significant ($p>0.05$).

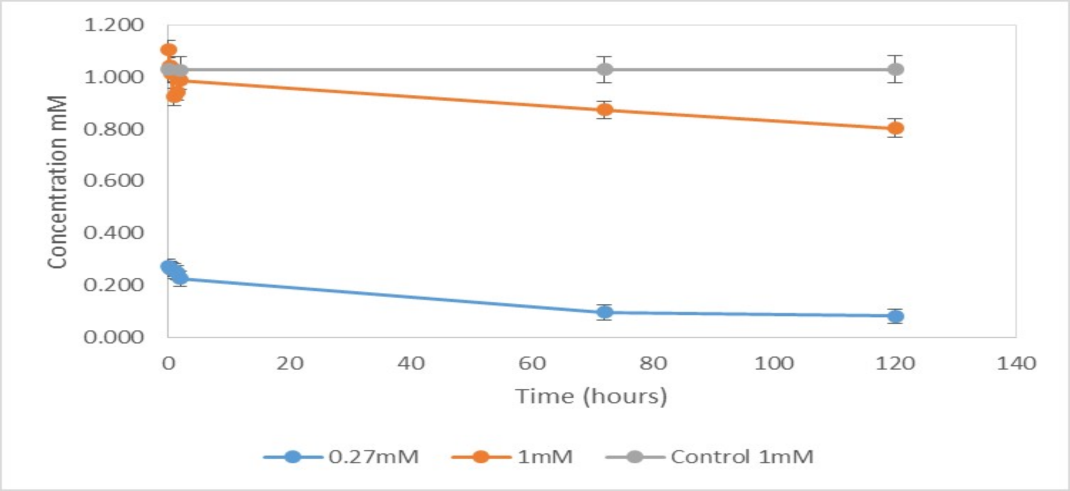

Figure 3.14: Fe^{2+} consumption of two doses during bromate reduction in presence of nitrate.

In relation to the stoichiometry for 0.27 mM Fe^{2+} dose, it was observed that the experimental ratios of the reactants Fe^{2+}/BrO_3^- was 7.4, while for 1 mM Fe^{2+} dose it was 10.5.

The iron oxidation was checked through visual inspection of colour change in bottles. The change of colours of the solution after 72 hours can be observed in Figure 3.15.

Figure 3.15: Coloured solution due to the iron oxidation/bromate reduction in presence of nitrate at 72 hours.

3.3.1. INTERACTION EFFECT BETWEEN IRON DOSES AND REACTION TIME

Factorial analysis showed that there is a very highly significant interaction between iron dose with time ($p<0.001$) at equal concentration of bromate and nitrate (Figure 3.16). A strong influence of higher dose (1 mM) on bromide formation during all times can be observed. In contrast, a low dose (0.27 mM) transformed very few bromate into bromide up to two hours. Just at more than 72 hours, bromide formation almost reached the same level as at the high doses (1 mM). Nitrate was not analysed because the values kept constant along the reaction time.

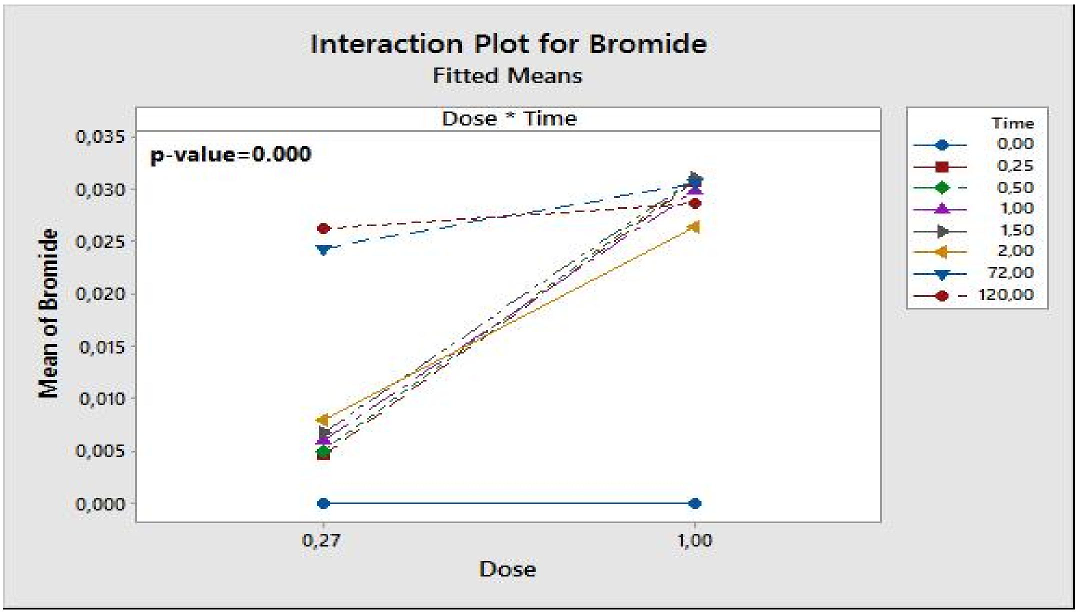

Figure 3.16: 2-Way interaction plot between iron dose and reaction time for Bromide formation.

3.4. BROMATE REDUCTION BY LOW IRON (II) CONCENTRATIONS, IN THE PRESENCE OF NITRATE

The effect of presence of 10 mg/L of nitrate during the reduction of 60 $\mu g/L$ of bromate using similar concentrations of iron (II) found in the dunes was evaluated.

3.4.1. IRON DOSE 0.007 mM

Bromate reduction and bromide formation with 0.007 mM iron (II) (which is the stoichiometric amount needed to reduce 60 $\mu g/L$ BrO_3^- and at the same time it is close to the lowest value found in the dunes) can be observed in Figure 3.17. Even when the bromate and iron concentration are low, it can be noticed that bromate decreased fast the first 2 hours. After that, it can be seen that the rate decreases, reducing 5% of bromate after 24 hours reaching 12% of bromate reduction after 5 days. It should be noted that the bromate and bromide curves neither intersect each other nor reach equilibrium after 5 days.

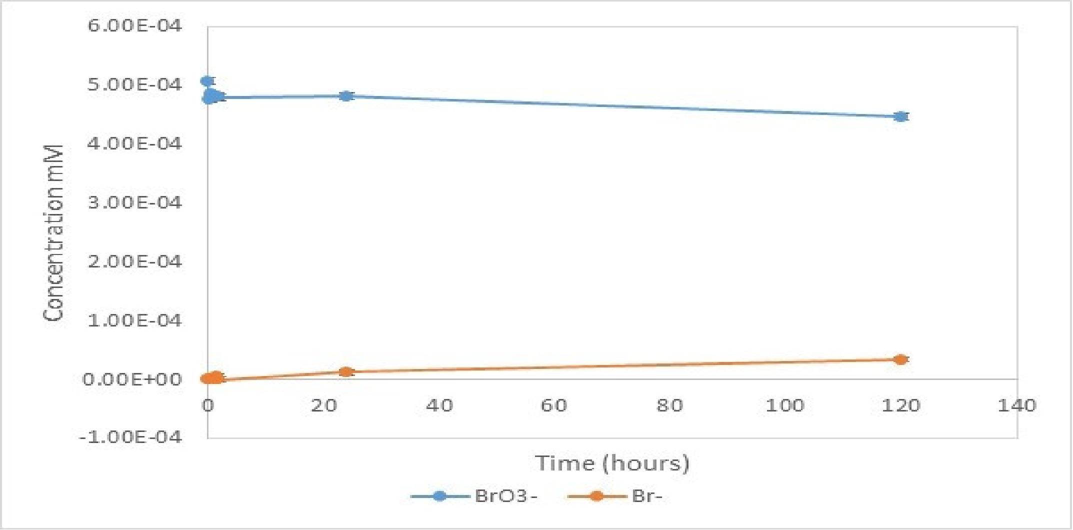

Figure 3.17: Bromate reduction and Bromide formation in presence of nitrate with iron dose 0.007 mM with their respective models

3.4.2. IRON DOSE 0.03 mM

Bromate reduction and bromide formation with 0.03 mM iron (II) (which belongs to the high concentrations found in the dunes) can be observed in Figure 3.18. Fast bromate reduction is performed into the first 2 hours (5% of bromate was reduced). After that it can be seen that the rate decreases, where 20% of bromate is reduced after 24 hours, reaching 58% at the 5th day.

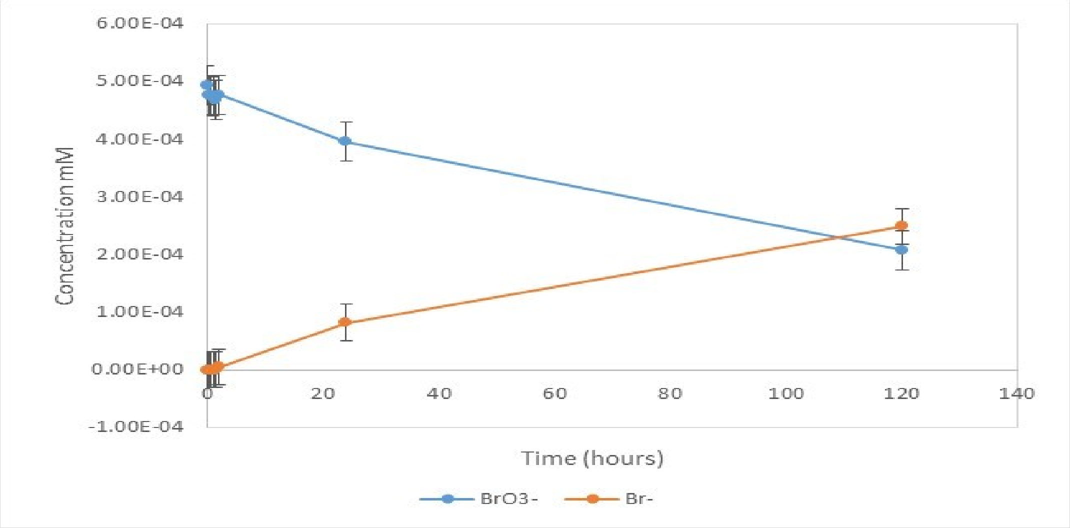

Figure 3.18: Bromate reduction and Bromide formation in presence of nitrate with iron dose 0.03 mM with their respective models.

Nitrate concentration was not reduced during the reduction of bromate with two doses of iron 0.007 and 0.03 mM as it can be seen in Figure 3.19. The increase of nitrate concentration after time 0 is due to the nitrate contained in the iron dose, where after the dose addition, the amount of nitrate reached the desired concentration 0.16 mM (10 mg/L).

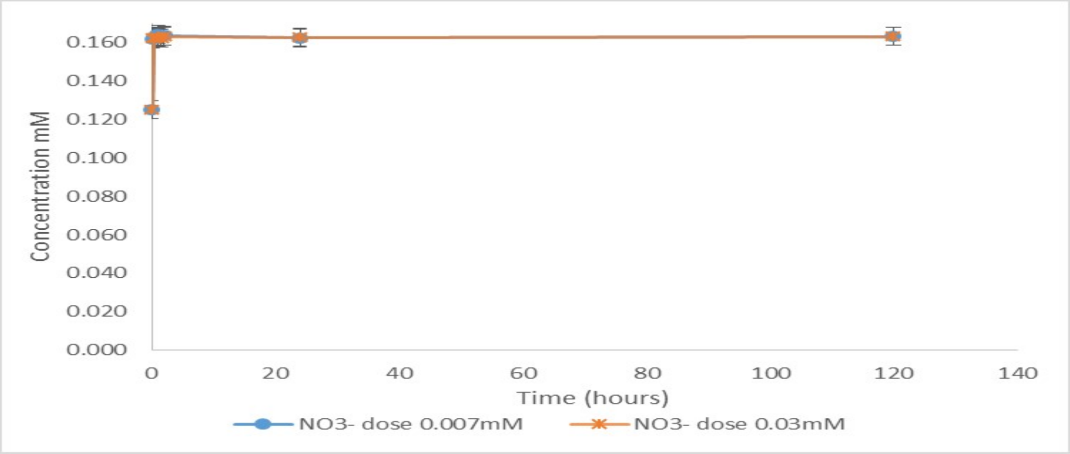

Figure 3.19: Variation of nitrate concentration with time.

Iron concentrations can be seen in Figure 3.20.The concentration in the two controls remained constant over time which confirmed the absence of oxygen in the bottles.

In addition, it can be seen a reduction in the iron concentration for higher dose (0.03 mM) which indicates oxidation of iron and consequently reduction of bromate as it could be seen in Figure 3.18. For lower Fe^{2+} dose, it can be observed a slight reduction in iron concentration which is almost imperceptible due to the low concentrations of bromate and iron that were reacting.

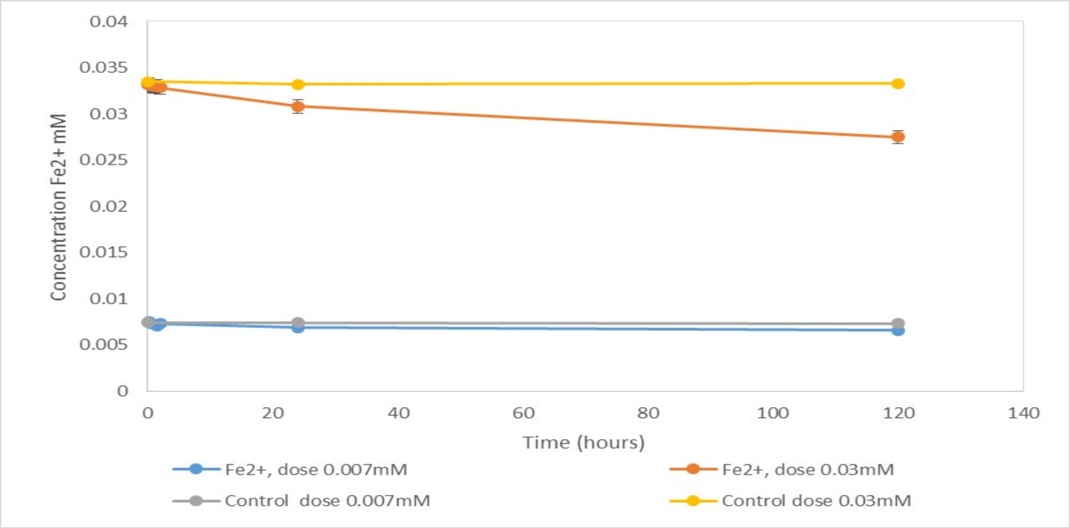

Figure 3.20: Iron concentration for two doses (0.007 and 0.03 mM) in presence of nitrate and their controls.

Figure 3.21 shows the formation of small flocs in the batch reactor with the higher Fe^{2+} dose (0.03 mM) after 5 days. The floc formation is an evidence of the oxidation of Fe^{2+}. On the other hand, the lower dose did not exhibit any change in colour or floc formation. More images can be found in Appendix C.

Figure 3.21: Zoom to floc formation during the reaction of 0.03mM iron and bromate (60ug/L) and nitrate (10mg/L) after 5 days.

3.4.3. INTERACTION EFFECT BETWEEN IRON DOSES AND REACTION TIME AT LOW CONCENTRATION IN PRESENCE OF NITRATE

Factorial analysis shows that there is a highly significant interaction between iron doses and reaction time ($p<0.001$) at different concentrations of bromate and nitrate as it can be seen in Figure 3.22. It can be observed a strong influence of higher dose (0.03 mM) in bromate reduction from 24 hours forward. On contrary, lower dose (0.007 mM) transform few bromate into bromide up to 24 hours. Nitrate concentrations kept constant along the reaction time.

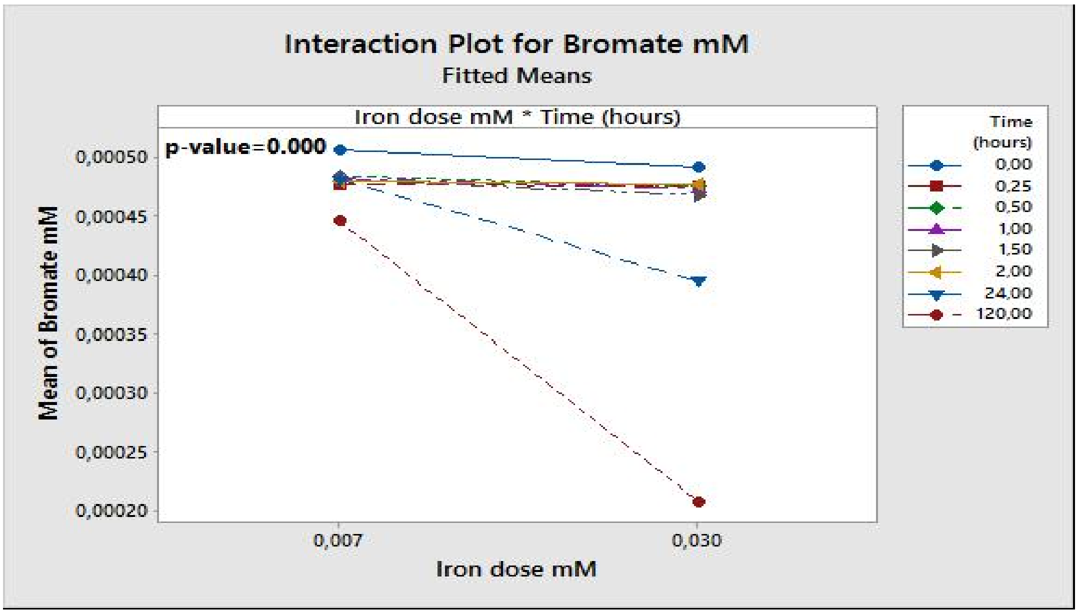

Figure 3.22: 2-way Interaction between iron dose (0.007 and 0.03Mm) and reaction time for bromate reduction in presence of nitrate.

3.5. BROMATE REDUCTION BY LOW IRON (II) CONCENTRATIONS, IN THE ABSENCE OF NITRATE

Bromate reduction in absence of nitrate using similar concentrations of iron (II) found in the dunes was evaluated.

3.5.1. IRON DOSE 0.007 *mM*

Figure 3.23 shows bromate reduction and bromide formation with 0.007 mM iron (II). The reduction of bromate does not show a super steep curve during the first hours as it was shown with high concentrations, however the reduction trend of bromate can be observed. 3% of bromate was reduced during the first 24 hours reaching 7% at the 5th day without reach the equilibrium.

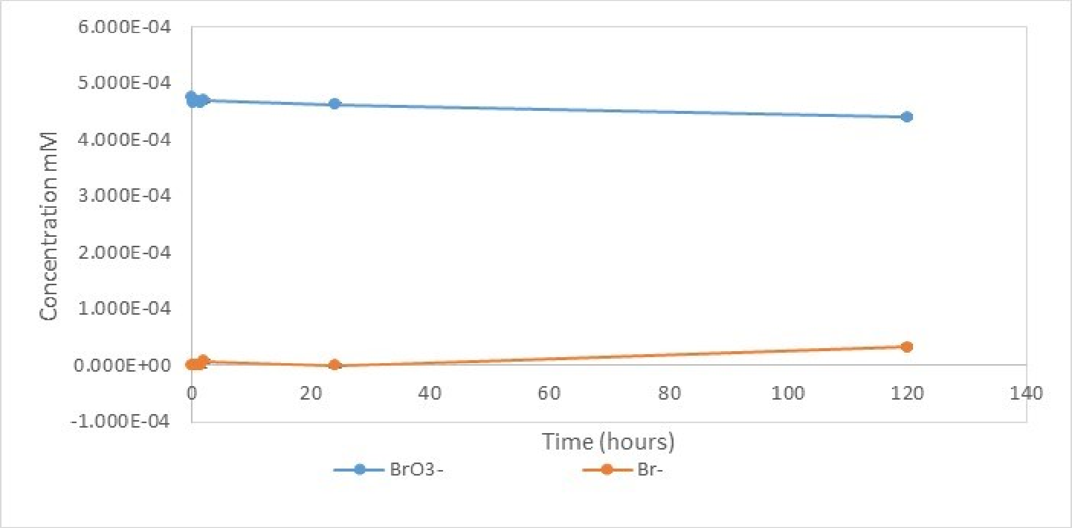

Figure 3.23: Bromate reduction and bromide formation with iron dose 0.007 mM.

3.5.2. IRON DOSE 0.03 mM

Bromate reduction with iron (II) dose of 0.03 mM can be observed in Figure 3.24. There is a fast initial reduction during the first two hours where 7% of bromate was reduced, followed by a slower reduction shown where the curve became less steep. After 5 days, 75% of bromate was reduced.

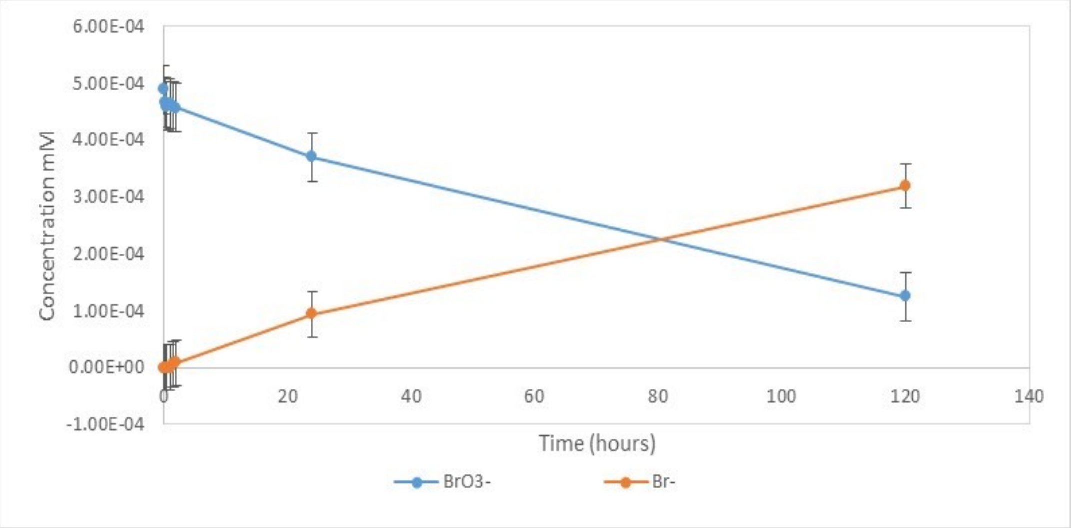

Figure 3.24: Bromate reduction and bromide formation with iron dose 0.03 mM.

Figure 3.25 shows the oxidation of two iron doses over time. It can be seen that the oxidation of iron at higher dose is more notorious than at lower dose. In addition, no iron oxidation was observed in the control bottles.

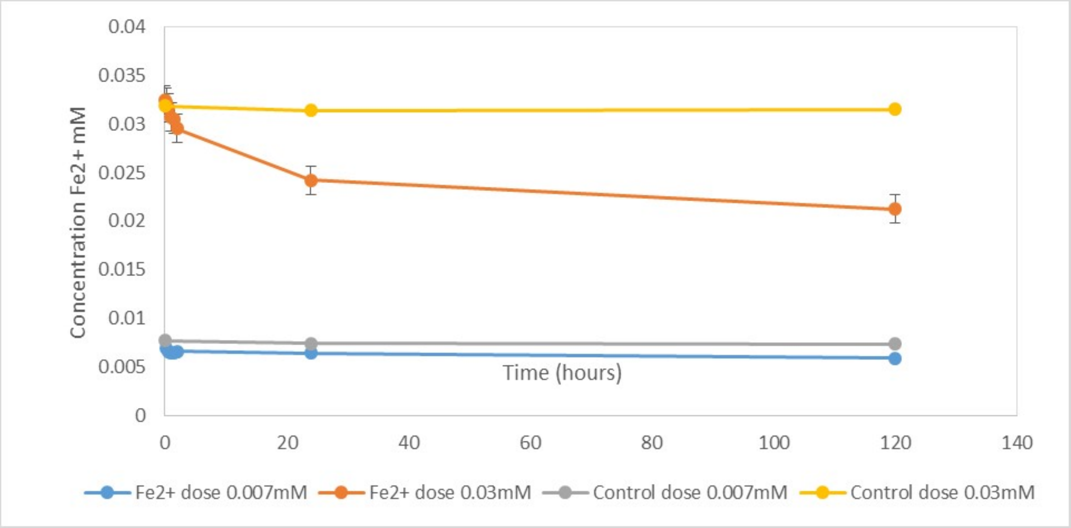

Figure 3.25: Iron oxidation at two different doses.

Moreover, it can be observed from Figure 3.26 that there was no colour change during the experiment, however, the higher dose exhibited floc formation at the bottom of the bottles. More flocs were observed in these experiment than for the same dose with nitrate (Figure 3.21).

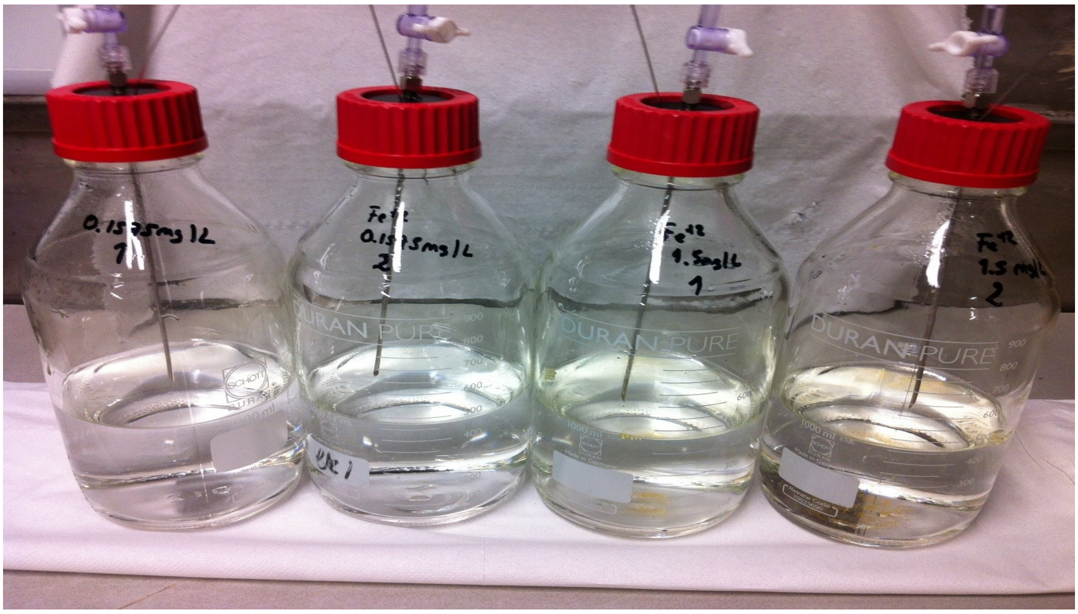

Figure 3.26: Bottles with the two dosages (0.007 and 0.03 mM) of iron and bromate (60 $\mu g/L$) after 5 days.

3.5.3. INTERACTION EFFECT BETWEEN IRON DOSES AND REACTION TIME AT LOW CONCENTRATION

Figure 3.27 shows that the interaction between iron doses and reaction time there is highly significant (p<0.001) according to the factorial analysis. In addition, it can be observed a strong influence of higher dose (0.03 mM) in bromate reduction from the 2^{nd} hour forward, while the lower dose (0.007 mM) transform few bromate into bromide during the 5 days.

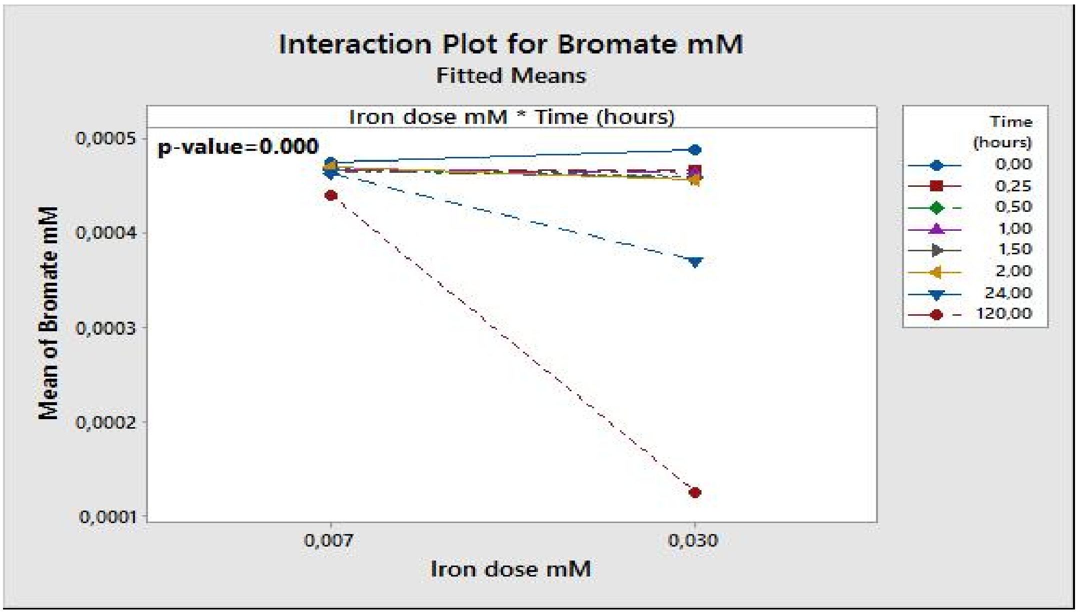

Figure 3.27: 2-way Interaction between iron dose (0.007 and 0.03 mM) and reaction time for bromate reduction.

3.6. COMPARISON OF BROMATE REDUCTION IN PRESENCE AND ABSENCE OF NITRATE

3.6.1. HIGH CONCENTRATION OF BROMATE

The bromate reduction in absence and presence of nitrate in equal concentrations (5 mg/L both) was compared in order to evaluate if there was a significant difference in reduction of bromate.
For 0.27 mM dose, Figure 3.28 shows that there is significant difference during the first 15 min ($p<0.05$) while during the following hours no significant difference was observed.

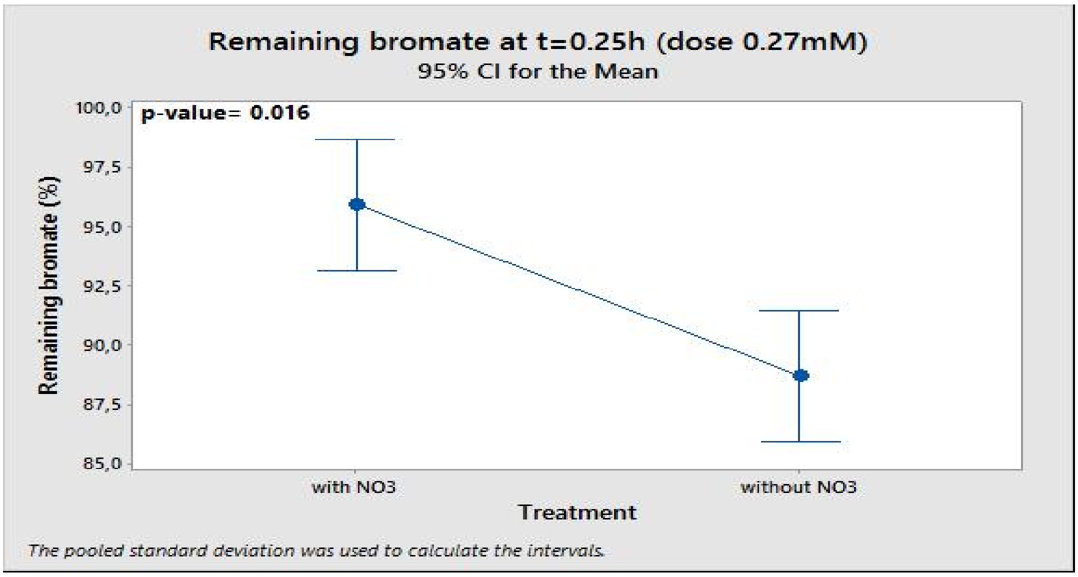

Figure 3.28: Anova for bromate reduction with 0.27 mM iron dose in presence or absence nitrate at time 0.25h.

For the high iron (II) dose of 1 mM, during the first 30 min ($p<0.05$) there was a significant difference in bromate reduction as it can be seen in Figure 3.29 and 3.30. While after 30 min, the difference with absence and presence of nitrate is not significant.

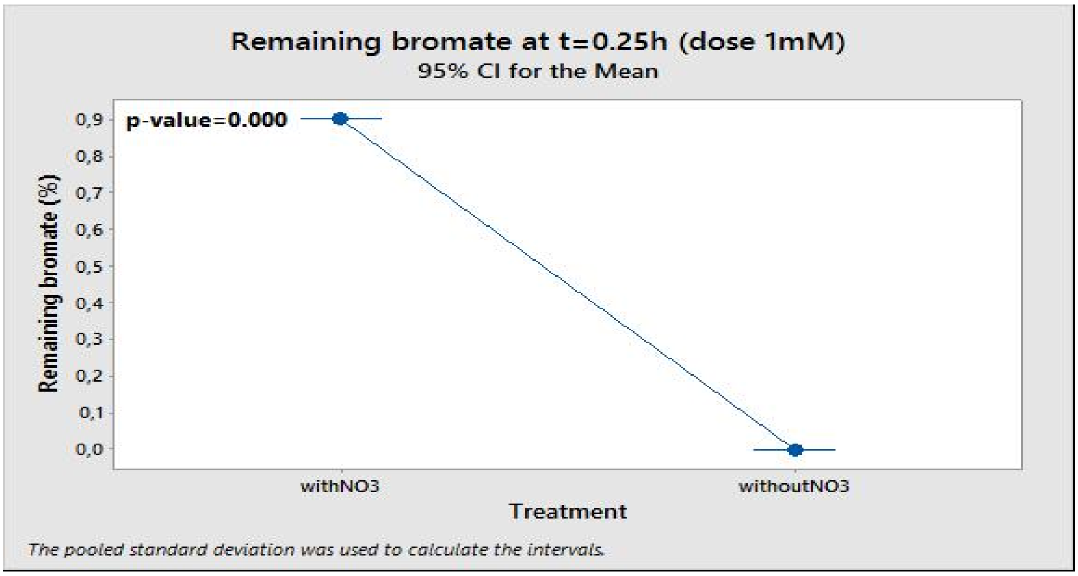

Figure 3.29: Anova for bromate reduction with 1 mM iron dose in presence or absence of nitrate at time 0.25h.

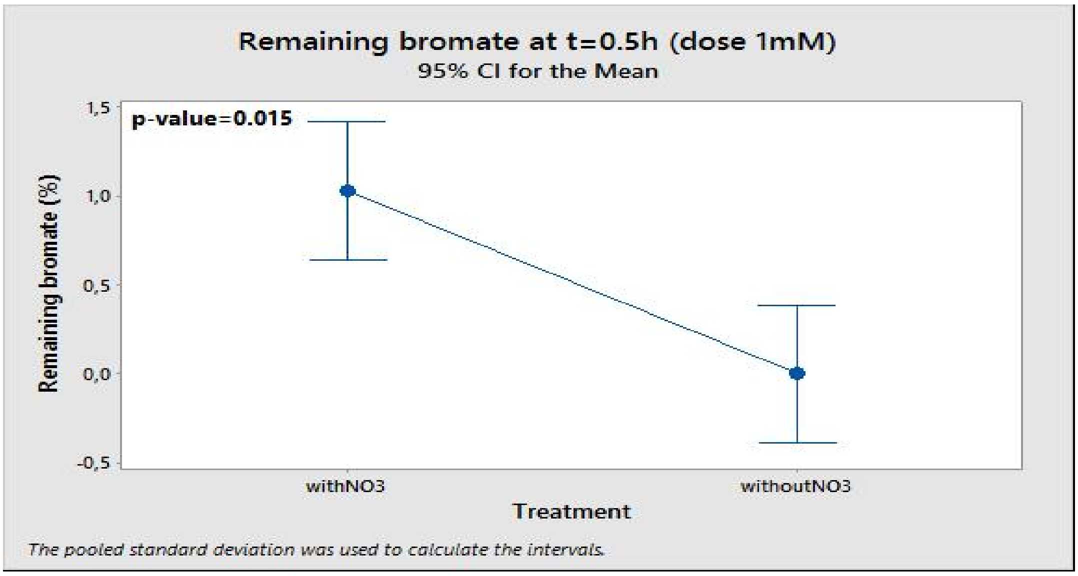

Figure 3.30: Anova for bromate reduction with 1 mM iron dose in presence or absence of nitrate at time 0.5h.

3.6.2. LOW CONCENTRATION OF BROMATE

The reduction of 60 $\mu g/L$ of bromate in absence and presence of nitrate (10 mg/L) was compared to evaluate if there is a significant difference in reduction of bromate. For 0.007 mM dose, Figure 3.31, 3.32 and 3.33 show that there is significant difference at 1 hour (p<0.01), 2 hours (p<0.05) and 120 hours (p<0.01), where the treatment with nitrate indicates more bromate reduction.

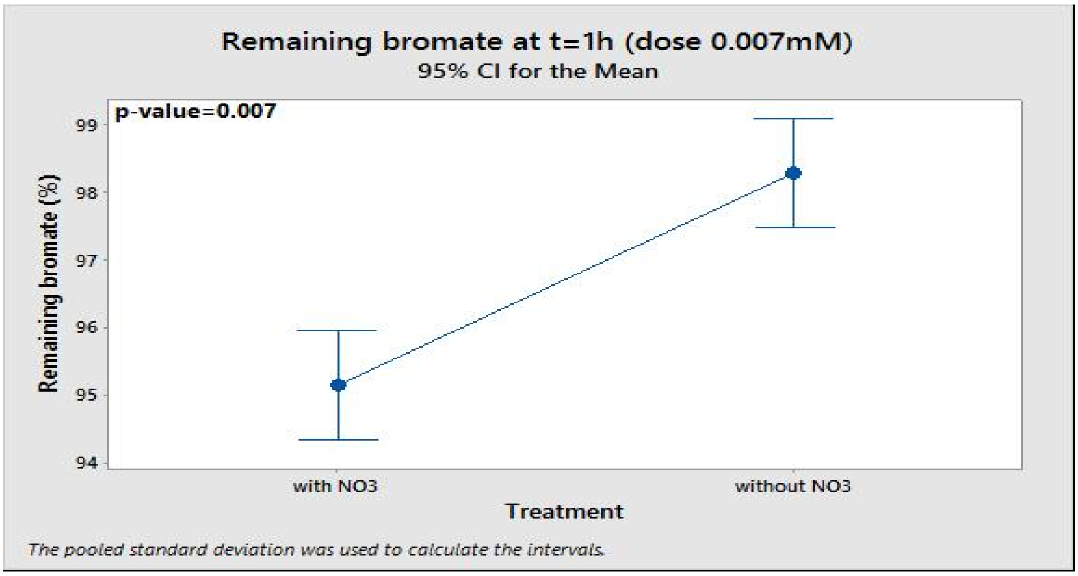

Figure 3.31: Anova for bromate reduction with 0.007 mM iron dose in presence or absence of nitrate at 1h.

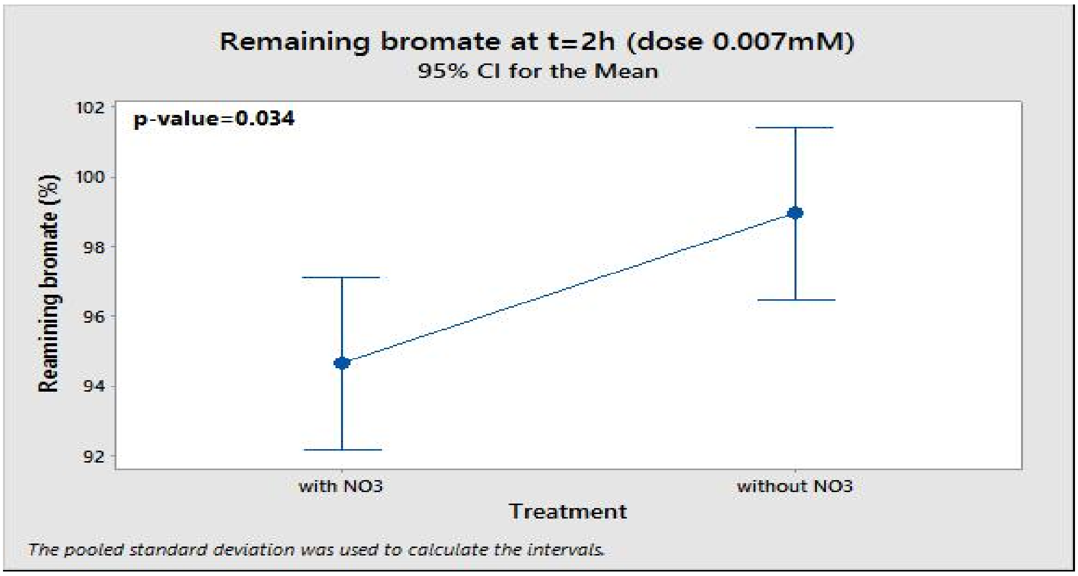

Figure 3.32: Anova for bromate reduction with 0.007 mM iron dose in presence or absence of nitrate at 2h.

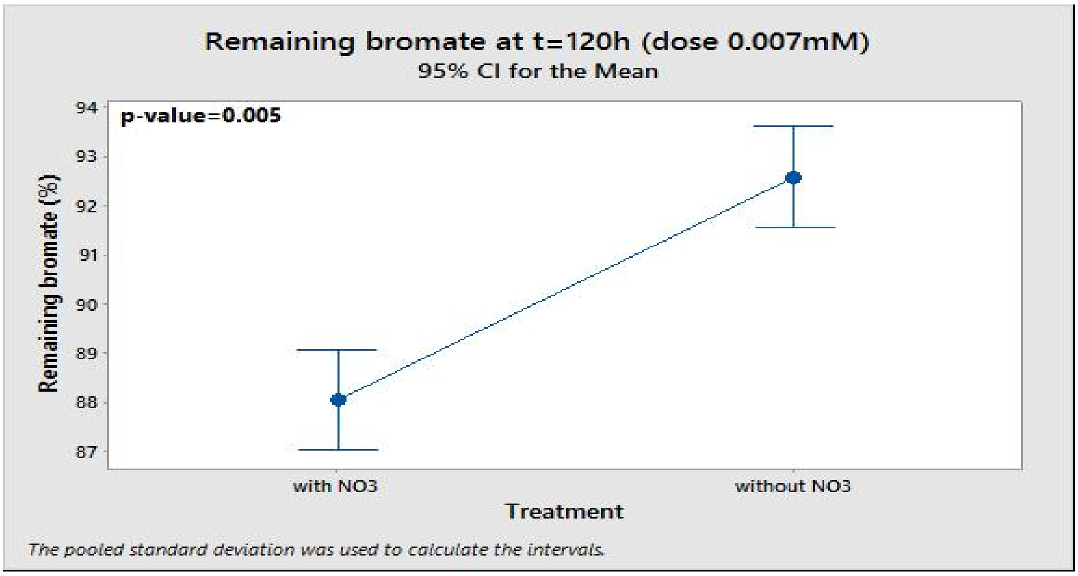

Figure 3.33: Anova for bromate reduction with 0.007 mM iron dose in presence or absence of nitrate at 120h.

At high dose 0.03 mM, the highly significant difference (p<0.01) appears at the 5th day as Figure 3.34 shows.

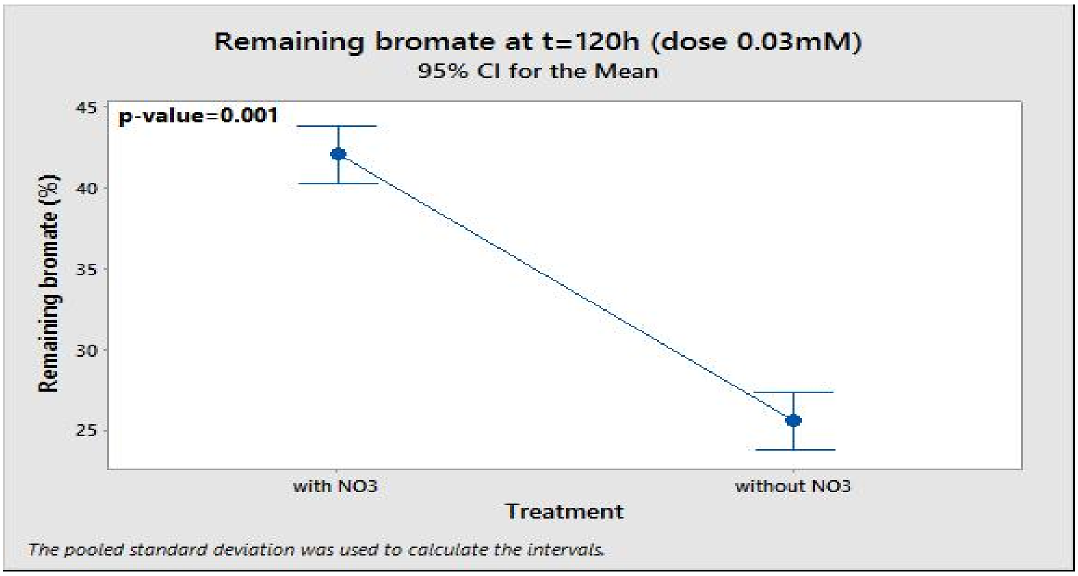

Figure 3.34: Anova for bromate reduction with 0.03mM iron dose in presence or absence of nitrate at 120h.

3.7. ADJUSTING KINETICS FOR LOW BROMATE CONCENTRATION

In the experiments with 5 mg/L of bromate only the results with lower dose of iron (0.27mM) were adjusted to a kinetic model. For the high dose of iron the conversion from bromate to bromide occurred so fast (immediately) that the bromate disappeared, therefore is not possible to model it.

In addition, the data used corresponds to the first hours of reaction for the experiments with 5mg/L of bromate. For the experiments of 60 $\mu g/L$ bromate the data from the 5 days was used.

From equation 1.2 (Siddiqui et al., 1994), the rate for bromate reduction by iron (II) is given by the equation 3.1.

$$\frac{dBrO_3^-}{dt} = -k[BrO_3^-][Fe^{2+}][H^+] \tag{3.1}$$

According to the coefficient of determination, it was found that the bromate reduction obey the first order reaction respect to bromate.

Table 3.1 summarizes the rate constant and coefficient of determination of the first order reaction model for bromate reduction. It can be seen that the reaction rate of bromate reduction at pH 9.5 (0.0021 min^{-1}) is higher than at pH 7.4 (0.0016 min^{-1}).

For bromate reduction in presence of equal nitrate concentration the constant rate is slightly lower (0.0019 min^{-1}) than in absence (0.0021 min^{-1}).

In the case of lower bromate concentration with iron concentration of 0.007 mM in presence of high concentration of nitrate, the rate constant (0.00001 min^{-1}) was higher than in absence of nitrate (0.000009 min^{-1}).

On the contrary in the case of lower bromate concentration with iron concentration of 0.03 mM in presence of high concentration of nitrate the rate constant (0.0001 min-1) is lower than in absence of nitrate (0.0002 min^{-1}).

Table 3.1: First order rate constant and coefficient of determination for the different experiments.

Bromate	Nitrate	Iron dose	pH	Rate constant (min^{-1})	R^2
5 mg/L	0 mg/L	0.27 mM	7.4	0.0016	0.8836
5 mg/L	0 mg/L	0.27 mM	9.5	0.0021	0.8694
5 mg/L	5 mg/L	0.27 mM	9.5	0.0019	0.9378
60 $\mu g/L$	10 mg/L	0.007 mM	9.5	0.00001	0.7582
60 $\mu g/L$	10 mg/L	0.03 mM	9.5	0.0001	0.9973
60 $\mu g/L$	0 mg/L	0.007 mM	9.5	0.000009	0.925
60 $\mu g/L$	0 mg/L	0.03 mM	9.5	0.0002	0.9983

The first order rate presentation for every case can be seen in the Figure 3.35.

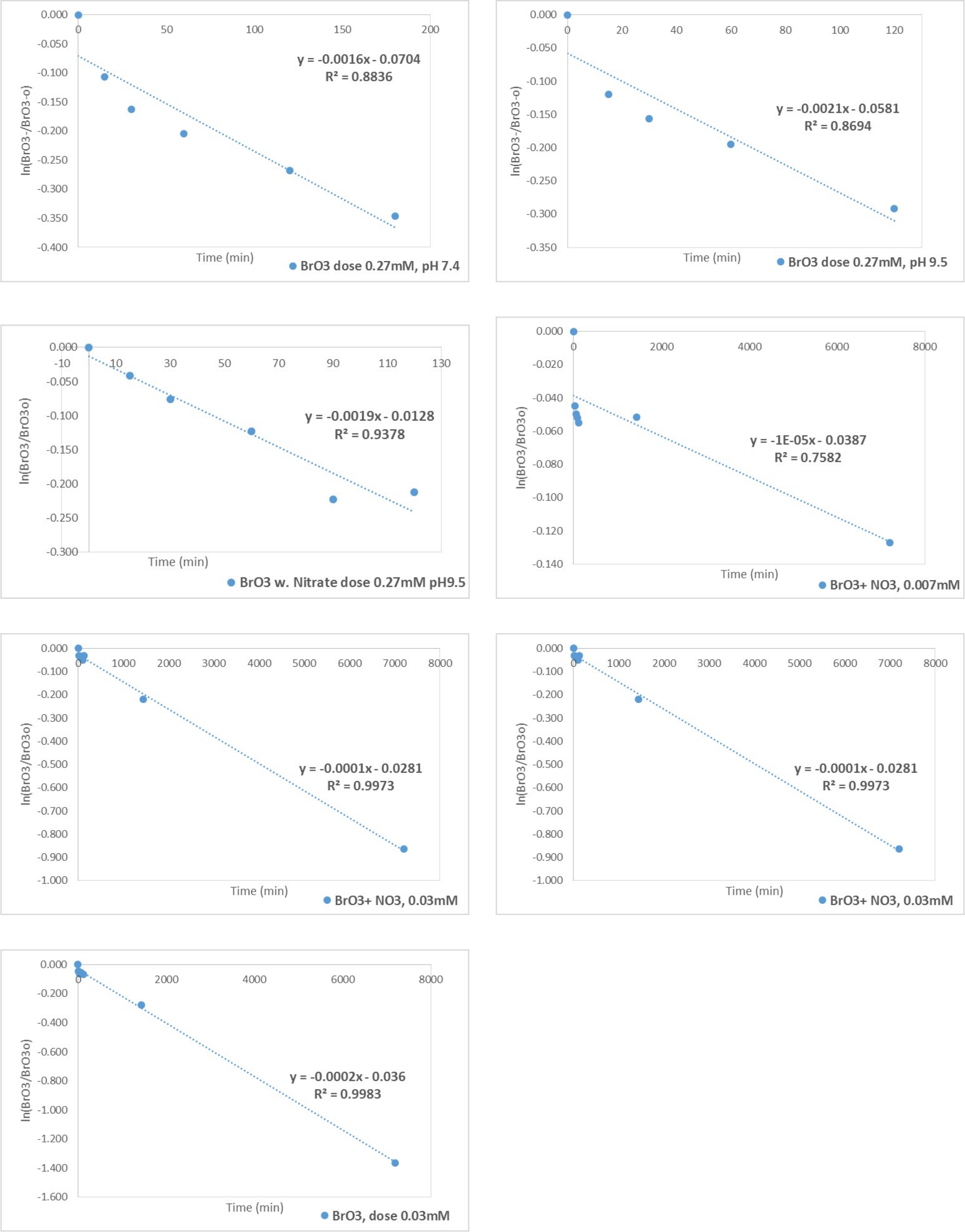

Figure 3.35: First order reaction for two different bromate initial concentrations, three different iron doses. (a) 5 mg/L bromate, dose 0.27 mM at pH 7.4. (b) 5 mg/L bromate, dose 0.27 mM at pH 9.5. (c) 5 mg/L bromate with 5 mg/L nitrate and iron dose 0.27 mM. (d) 60 $\mu g/L$ bromate with 10 mg/L nitrate and iron dose 0.007 mM. (e) 60 $\mu g/L$ bromate with 10 mg/L nitrate and iron dose 0.03 mM. (f) 60 $\mu g/L$ bromate with iron dose 0.007 mM. (g) 60 $\mu g/L$ bromate with iron dose 0.03 mM.

4

Discussion

4.1. Bromate reduction by two iron (II) doses at two different pH

The trend of the bromate reduction and consequently bromide formation is exponentially fast at the beginning (under 2 hours of reaction time) and subsequently decreases until equilibrium is reached. This fact was also observed by other authors who have described the bromate reduction with zero valent iron [33, 34] and with Fe^{2+} [31, 32] in presence of oxygen (aerobic conditions).

The fast bromate reduction at the beginning may be due to the concentration gradient when the Fe^{2+} dose is added into the BrO_3^- solution. Figure 4.1 shows the high concentration of Fe^{2+} with dark orange and then light orange at lower concentrations. Therefore, more Fe^{2+} ions at the beginning are in contact with bromate, reducing it rapidly. Figure 4.1 shows this phenomena.

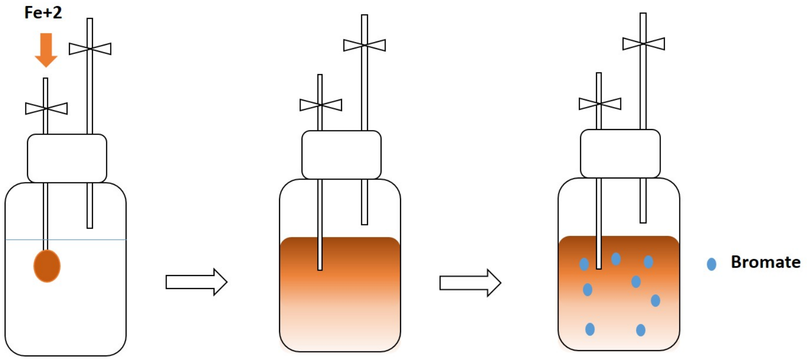

Figure 4.1: Concentration gradient of Fe^{2+} into bottles.

The observed difference of bromide formation between pH 7.4 and 9.5 might be due to the formation of intermediate species during the bromate reduction at pH 7.4 as it has been observed in other studies [32, 37].

According to redox equation 1.2 and 3.1, it is expected that at higher concentration of H^+ (lower pH) and higher iron dose, the reduction of bromate will occur faster [32]. Furthermore the reduction reaction consumed protons which means that it will be catalysed by an acid environment [33]. Nevertheless, Dong et al. (2009) investigated the reduction of bromate with ferrous iron in presence of oxygen at different pH (4.0- 10). Their results showed that bromate reduction was improved at pH below 6.9 or above 8.0. In this study there was not significant difference in bromate reduction at pH 7.4 and 9.5, the difference was in the bromide formation, which occurred faster at pH 9.5.

In addition, at lower pH, Fe^{2+} is more stable. Siddiqui et al. (1994) observed that disappearance of Fe^{2+} was slower at lower pH levels, which might limit the redox reaction.

For the high Fe^{2+} dose of 1 mM, during the first 15 and 30 min all bromate was reduced, which is not the case of the low iron dose which took 5 days to reduce 91% of bromate. This behaviour was expected according to the redox equation 1.2, which shows that higher concentration of Fe^{2+} leads a faster bromate reduction.

Iron oxidation at high concentration even after complete reduction of bromate could be explained in two ways. First due to conversion of residual intermediate species, and second, due to heterogeneous reaction occurring on surface of iron precipitates, where the Fe^{2+} adsorbed on the surface of the precipitates of Fe^{3+} is oxidised [38]. This was also observed in the bromate reduction in presence of equal concentration of nitrate (Figure 3.14).

Siddiqui et al. (1994) investigated the reduction of 50 $\mu g/L\ BrO_3^-$ with DO =7 mg/L, pH =7.5 and an iron dose of 15 mg/L obtaining reduction of 80% after 30 min, while Dong et al. (2009) studied the reduction of 25 $\mu g/L$ BrO_3^- with DO= 2.3mg/L, pH =7.2, T =25°C and an iron dose of 30 mg/L reaching 65% of reduction after 20 min. The doses used in their studies exceeds more than 100 and 450 times the stoichiometry ratio (equation 1.2). In presence of DO, Fe^{2+} needs to be present in excess while in anoxic conditions the Fe^{2+} required by the stoichiometry removed 90% of BrO_3^- within 5 days at pH 7.4 and 9.5, according to the results of this experiment. In this study, experimental ratios of Fe^{2+}/BrO_3^- at both pH were close to the stoichiometric ratio ($Fe^{2+}/BrO_3^- = 6$).

4.2. BROMATE REDUCTION BY HIGH IRON(II) CONCENTRATIONS, IN THE PRESENCE OF NITRATE

Bromate reduction in presence of nitrate took place following a similar trend as in absence of nitrate (first a fast reduction occurs which progressively becomes stable). A similar trend for bromate reduction was described by Siddiqui et al. (1994) and Dong et al. (2009) using Fe^{2+} in the presence of oxygen.

At both iron doses, no variation of nitrate was observed. Therefore, it can be concluded that nitrate does not compete with bromate for iron but hinder its reduction, as bromate reduction during the first 15 min in presence and absence of nitrate is significant different, being faster in absence of nitrate. This may be explained on a molecular level. Based on the Brownian movement. The random movement of the iron particles will lead to their collision with bromate and nitrate molecules of the solution. When there is only bromate in the solution all the iron will collide with bromate, and consequently react with it. In the presence of nitrate the iron particles collide with bromate and nitrate. These two will compete for the collisions, resulting in a lower chance of bromate to collide and react with iron. On the other hand, the nitrate which impacts iron will not be reduced because of the reasons that will be discussed in 4.2.1. In addition, Kirisits & Snoeyink (1999) observed that nitrate hinders the reduction of bromate with biological AC.

The fluctuation of bromate along time using higher iron dose in presence of nitrate (see Figure 3.13) might show apparently backward conversion of intermediate species (i.e.: hypobromite to bromate) [36].

4.2.1. REDUCTION CAPABILITY OF BROMATE AND NITRATE

ATOMIC STRUCTURE

The occurrence of bromate reduction over nitrate reduction might be explained as follows. Even when the oxidation state for both oxo-anions (BrO_3^- and NO_3^-) is $+V$, their atomic structures are different.

The nitrogen atom into nitrate has p-orbital which is half filled (N electron configuration $1s^2 2s^2 2p^3$, where total capacity of orbital p is 6). Therefore, in case of reduction, addition of an electron to this stable structure is not favoured which is reflected by low electron affinity. In addition, nitrate has a smaller atomic radio, making addition of electrons more difficult [33].

On the other hand, electron acceptance is favourable for atoms with larger atomic radio like bromine. Moreover, electronic affinity is higher in elements of group 17 (where bromine belongs), which tend to gain an electron in order to fill valence shell making elements more stable. Also, electron configuration of bromine is $1s^2 2s^2 2p^6 3s^2 3p^6 3d^{10} 4s^2 4p^5$ which shows that 1 electron is needed in orbital p to complete the total capacity. Thus it is easy and energetic convenient to accept 1 electron instead of donate 5 electrons [39].

Furthermore, the bonds between nitrogen and oxygen are stronger than those between bromine and oxygen. The bonds in these molecules are covalent. The strength of covalent bonds is inversely proportional to atomic weights of bonded atoms [33]. Values of bond dissociation energy for $N-O$ and $Br-O$ [40] are given in Table 4.1 among other parameters, where it can be seen the energy needed to break a $N-O$ bond is almost 3 times higher than for $Br-O$. Hence it is more difficult to remove an oxygen atom from nitrate molecule, in other words to add an electron to nitrogen [33].

Nitrate has several resonance structures with double bonds between nitrogen and oxygen which are stronger than a single bond, but even when bromate molecule has 2 double bonds in total, the energy needed is lower than for nitrate. Therefore, according to the atomic structure information nitrate should be more stable than bromate and consequently, the bigger atomic radio and higher electron affinity of bromate might explain the rapid reduction over nitrate [33].

Table 4.1: Information of atomic structure of nitrate and bromate.

Parameter	Nitrate	Bromate
Oxidation state	V	V
Atomic radio	0.75A	1.96A
Electronic configuration	$1s^2 2s^2 2p^3$	$1s^2 2s^2 2p^6 3s^2 3p^6 3d^{10} 4s^2 4p^5$
Electronic affinity	low	high
Bond dissociation energy	$N-O$: 630.57 kJ/mol	$Br-O$: 235.1kJ/mol
Structure	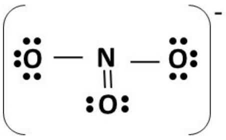	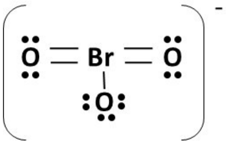

THERMODYNAMICS

As it was described in section 2.3.2, several equations described the nitrate reduction by iron (II). Even though the reaction is thermodynamically feasible, it will not occur spontaneously [41]. For a chemical reaction to happen, the reactants must have a minimum energy. The minimum energy needed to start the reaction, or in other words the barrier that reactants need to overcome is called activation energy [39, 42]. In case of nitrate reduction by iron (II), the activation energy is too high. The activation energy can be reduced using catalysts (enzymes in biological systems) or increasing the temperature. Figure 4.2 shows the reduction of activation energy with the use of enzyme/catalyst. Therefore, the reduction of nitrate will not happen in the absence of catalyst or high temperatures.

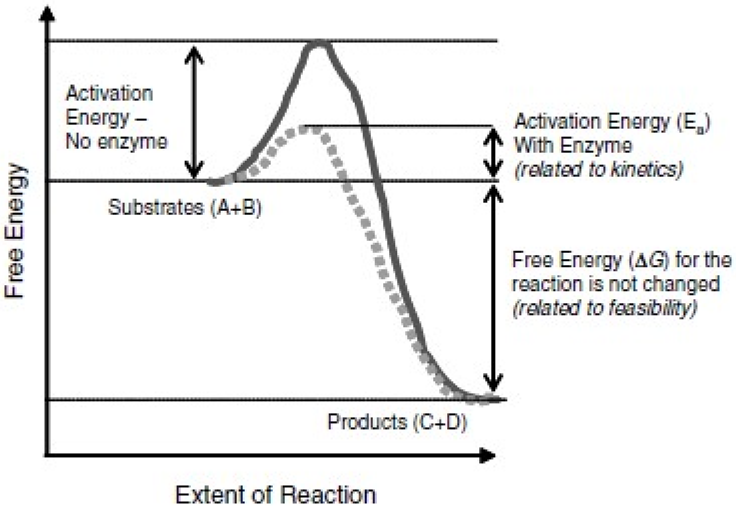

Figure 4.2: Activation energy with and without enzyme/catalyst[42].

In addition, reduction of nitrate by iron without catalyst has been reported unsuccessfully at room temperature [43] or very slow at low temperatures [44]. On the other hand at 75°C, nitrate was reduced by Fe^{2+} with a maximum rate of 16%/hr [45]. The use of catalysts as Cu^{2+}, Ag^{1+}, Cd^{2+}, Ni^{2+} among others has been reported by Ottley et al. (1997).

In relation to the activation energy (AE) of the reaction between bromate and iron (II), this AE should be lower than the AE for the reduction of nitrate with iron (II), as it could be confirmed in the experiments described in sections 3.3 and 3.4, where bromate reduction by iron (II) occurred instead of nitrate reduction.

4.3. REDUCTION OF LOW CONCENTRATION OF BROMATE IN PRESENCE AND ABSENCE OF NITRATE WITH TWO IRON DOSES (SIMILAR TO DUNES)

A peculiar situation happened in the reduction of low bromate concentration in presence of high concentration of nitrate with the low iron dose (0.007 mM). This reaction occurred faster than the bromate reduction with the same iron dose in absence of nitrate. According to results of equal concentrations for bromate and nitrate it was expected that bromate reduction in the absence of nitrate would be faster compared to the reaction in the presence of nitrate. This is also confirmed with the values of the rate constant (k) $1x10^{-5}$ and $9x10^{-6}\ min^{-1}$ in presence and absence of nitrate, respectively. Perhaps the presence of high concentration of nitrate (10 mg/L) could enhance the reduction of low concentration of bromate using low dose of iron (0.007 mM). This does not follow the logic or pattern observed in the previous experiments, and it is not possible to explain with the current knowledge. However, it could not be that absurd, for example the reduction of nitrate by iron (II) under anoxic conditions, proceed more rapidly in the presence of trace quantities of oxygen, where it should be expected that oxygen compete with nitrate for iron [41].

For the high dose of iron (0.03 mM), as it was expected, bromate reduction is higher and faster (according to the rate constant value) in the absence of nitrate than in its presence, reducing 75% and 58% of bromate, respectively. This might be explained by the difference in the atomic structure and activation energy of the redox reaction for bromate and nitrate as it was explained in the section 4.2. In the current study the rate constant obtained in the reduction of 60 $\mu g/L$ bromate with 1.5 mg/L (10 times higher than the stoichiometry) was 0.0002 min^{-1}, while Siddiqui et al. (1994) obtained a higher constant rate of 0.009 min^{-1} to reduce 50 $\mu g/L$ of bromate with 15 mg/L of iron. However, this iron dose was 114 times the stoichiometric amount needed.

The constant rate for 60 $\mu g/L$ and 0.15 mg/L of iron was $9x10^{-6}\ min^{-1}$, and with an iron dose 1.5 mg/L (10 times more), the constant rate increases two orders of magnitude (0.0002 min-1). Therefore, if the iron dose is increased 10 times more (15 mg/L) and assuming a linear and rough estimation the constant rate might increase again in two order of magnitudes, but even if it is only one order of magnitude the results would be higher than the results obtained by Siddiqui et al. (1994) which could remove most of the bromate within 25 min in presence of oxygen.

4.4. BROMATE REDUCTION: WATER TREATMENT TECHNOLOGY OR MANAGED AQUIFER RECHARGE (MAR)?

After the experiments that have been done, there is an unanswered question if this bromate reduction can be applied as a water treatment technology or even suitable in managed aquifer recharge (MAR).

4.4.1. WATER TREATMENT TECHNOLOGY

According to experiments for high concentrations of bromate, it can be demonstrated that bromate reduction by iron (II) would be feasible in a flocculation basin with a residence time of 30 min, with a dose in excess due to oxygen will be present. In order to reduce bromate to its harmless specie bromide. For low concentrations of bromate, it was observed that reduction was slow with the two evaluated doses, however it should be considered that low concentration of iron was the limiting reactant and according to kinetics of the reaction, the more the iron dose the faster the bromate reduction. Therefore a higher dose should be used to increase the rate of the reaction during water treatment. Then bromate will be reduced and the oxidized iron (III) will form flocs and settle as it was observed in the experiments facilitating the iron removal as well.

Therefore, an option for low concentration bromate reduction could be a continuous stirred reactor with residence time of 30 min with anoxic conditions and with an initial pH of 9.5 (before the addition of iron). However due to the decrease of pH, it should be necessary to add NaOH after the residence time to rise the pH close to values for drinking water, which would help not only to increase pH, but also to remove iron in excess, forming hydroxides precipitating and facilitating its removal.

A proposal could be a system like Figure 4.3, where the mixing reactor will be sourced with the influent containing bromate and through another inlet with $FeSO_4$. The effluent will be taken from the top, due to accumulation of iron flocs on the bottom.

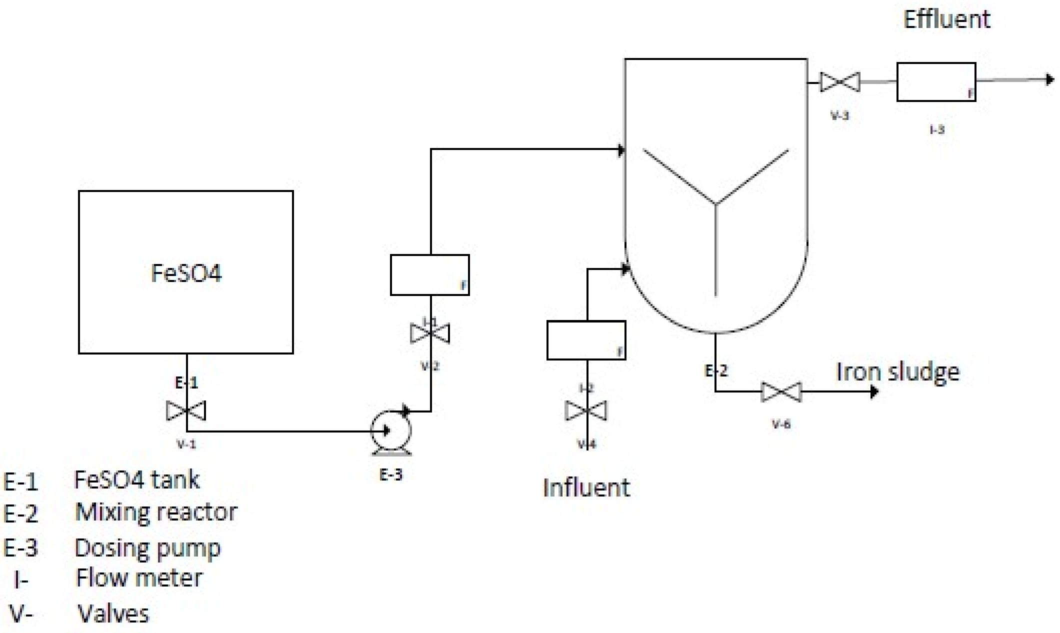

Figure 4.3: Proposal for bromate reduction system.

4.4.2. MAR

On the other hand a slow reaction at low concentrations of iron and bromate may not be a disadvantage at all. Managed Aquifer Recharge (MAR) technologies such as: infiltration ponds are robust process with low cost, due to no chemical addition is needed and its low energy consumption. Initially, MAR was used for the removal of pathogens and natural organic matter (NOM) and turbidity. Nevertheless, recent studies have demonstrated that this process could be a barrier for organic micropollutants [2, 3].

Concentrations of iron used in experiments for low concentration of bromate can be found in dunes from Dunea. In addition, a cross section over two recharge basins near to The Hague can be observed in Figure 4.4 where distribution of nitrate, iron and hydrogen sulphide are spatially distributed indicating the (sub)oxic, anoxic and deep anoxic parts [46].

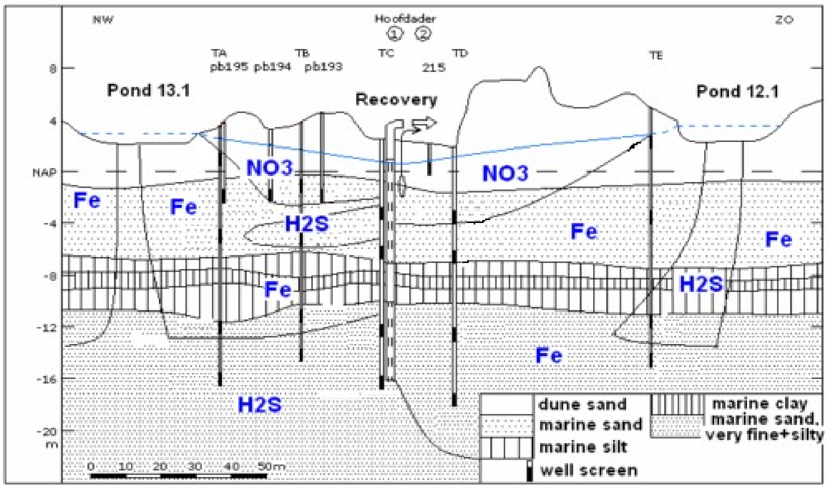

Figure 4.4: Cross section over 2 recharge basins near The Hague [46]

If bromate -containing waters are infiltrated in ponds, the redox environment in dunes would be favoured the reduction of bromate. This redox reaction could happened after the (sub)oxic zone, during the soil passing through the anoxic part of the aquifer and even in the well if there is remaining bromate and iron (II). As it was observed in the experiments at the 5th day with the lower dose 25% of bromate was reduced and with the higher concentration of iron 75% of bromate was reduced and 58% in presence of nitrate concentrations similar to the dunes. Moreover the residence time in dunes is at least 21 days, but on average 120 days [3]. Therefore with this residence time the bromate could be reduced to bromide. It should be noted that the limiting reactant in this equation is iron (II). Figure 4.5 shows how would be bromate reduction and bromide formation and oxidation of iron in dunes during soil passage along the 120 days.

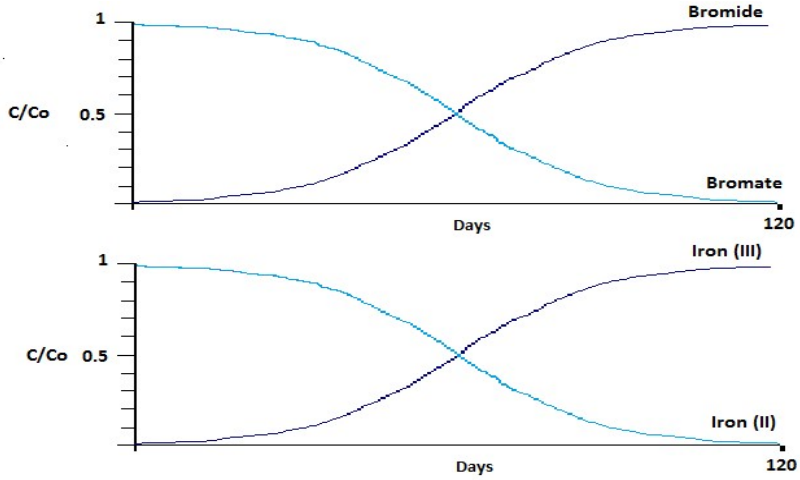

Figure 4.5: Hypothetical behaviour of bromate, bromide and iron during soil passage into dunes.

On the other hand, there might be other components presents in dunes or water which can affect the redox reaction between iron and bromate. From the experiments done in this study, sulphate (as ferrous sulphate) and nitrate did not compete with bromate.

From literature, it is known that in presence of nickel (II), copper (II), silver (I) and cadmium (II) nitrate could be reduced by iron (II), therefore it could be thought that if these metals are present in the dunes, the bromate reduction could be affected. However according to Figure 4.4, nitrate and iron (II) are not in the same part of the dunes, therefore the presence of these metals should not affect the reduction of bromate.

Other important factor is the presence of natural organic matter (NOM). Xie & Shang (2005) studied bromate reduction by zero valent iron in presence of humic acid and quinone (component of NOM) finding that a complexation of humic acid with iron species and its adsorption coated the iron surface and decreased the rate of bromate reduction by iron (0). On the other hand, it was observed that in long term, humic acid regenerates iron (II) and reduce bromate. In presence of only humic acid the simultaneous presence of iron (III) and humic acid increased bromate removal rate [34].

Therefore it is suggested that column experiments will be done simulating the dune passage, and perhaps not only chemical reduction of bromate will occur, but also biological reduction of bromate could be occurred.

5

CONCLUSIONS

1. Iron(II) at higher dosage (1 mM) is capable of rapidly reducing 5 mg/L bromate (30 min) under anoxic condition.

2. The three factors: pH, iron dose and reaction time did not interact each other during bromate reduction, however, the interaction of iron dose and reaction time are highly significant for reduction of bromate in all experiments. In addition, if the independent effect of each factor is evaluated, higher pH has a higher formation of bromide, but no significant difference in bromate reduction is observed, indicating the formation of intermediate species.

3. Bromate at low and high concentrations, in the presence of nitrate was reduced by iron, while nitrate was not reduced, which indicates that Bromate reduction is favoured by iron (II) over nitrate.

4. The increase of iron dose increases the amount of reduced bromate, decreasing the reaction time, therefore making it faster and with no need of large infrastructure to carry on the treatment step during drinking water treatment. The presence of equal concentration of nitrate and bromate, cause a deceleration in bromate reaction only during the first 30 minutes.

5. The presence of nitrate in the reduction of low concentration of bromate has no interference with high iron dose (1.5 mg/L) until the 5th day where reduction of bromate in presence of nitrate reached 58% while in absence reached 75%. On the other hand, the presence of nitrate with low iron dose (0.15 mg/L) seems to accelerate bromate reduction reducing 12% against 7% in absence of nitrate.

6. The reduction of bromate by iron (II) is also a technique that has been studied under oxic conditions with high concentrations of iron (II) to compensate the loss of iron due to its oxidation in presence of oxygen. MAR offers an anoxic environment with iron (II) content, which would favour bromate reduction.

7. The reduction of 60 $\mu g/L$ of bromate during MAR might be feasible with iron concentrations present in dunes. At concentrations of 0.15 and 1.5 mg/L, the 7 and 75% of bromate was reduced after 5 days, respectively. The limiting factors in this redox reaction are reaction time and iron concentration. As a result, with longer reaction time, more bromate will be reduced and taking into account the average residence time in dunes (120 days), time would not be a limiting factor. Therefore, bromate reduction during MAR will depend on iron concentration available in dunes and everything would indicate that bromate might be reduced completely.

8. In order to guarantee the feasibility of bromate reduction during MAR, further experiments should be done (columns with sand from dunes) with a complex matrix, perhaps real water from the dunes, which includes other ions (different from nitrate and sulphate) which could compete with bromate together with NOM, which is present in dunes.

BIBLIOGRAPHY

[1] U. S. E. P. Agency, *Alternative disinfectants and oxidants guidance manual,* Chapter **7**, 1 (1999).

[2] C. Bertelkamp, *Organic Micropollutant Removal during River Bank Filtration*, Ph.D. thesis, TU Delft, Delft University of Technology (2015).

[3] K. Lekkerkerker-Teunissen, *Advanced oxidation and managed aquifer recharge A synergistic hybrid for organic micropollutant removal*, Ph.D. thesis, TU Delft, Delft University of Technology (2012).

[4] O. A. H. Jones, N. Voulvoulis, and J. Lester, *Potential ecological and human health risks associated with the presence of pharmaceutically active compounds in the aquatic environment,* Critical reviews in toxicology **34**, 335 (2004).

[5] R. Andreozzi, V. Caprio, A. Insola, and R. Marotta, *Advanced oxidation processes (aop) for water purification and recovery,* Catalysis today **53**, 51 (1999).

[6] C. Gottschalk, J. A. Libra, and A. Saupe, *Ozonation of water and waste water: A practical guide to understanding ozone and its applications* (John Wiley & Sons, 2009).

[7] K. Lekkerkerker, J. Scheideler, S. Maeng, A. Ried, J. Verberk, A. Knol, G. Amy, and J. Van Dijk, *Advanced oxidation and artificial recharge: a synergistic hybrid system for removal of organic micropollutants,* Water Science and Technology: Water Supply **9**, 643 (2009).

[8] U. Von Gunten, *Ozonation of drinking water: Part ii. disinfection and by-product formation in presence of bromide, iodide or chlorine,* Water Research **37**, 1469 (2003).

[9] W. R. Haag and J. Hoigne, *Ozonation of bromide-containing waters: kinetics of formation of hypobromous acid and bromate,* Environmental Science & Technology **17**, 261 (1983).

[10] F. Edition, *Guidelines for drinking-water quality,* WHO chronicle **38**, 104 (2011).

[11] A. H. Knol, *Peroxone process in drinking water treatment,* Delft University of Technology, Delft. MSc thesis (2012).

[12] R. Song, R. Minear, P. Westerhoff, and G. Amy, *Bromate formation and control during water ozonation,* Environmental technology **17**, 861 (1996).

[13] M. Siddiqui, W. Zhai, G. Amy, and C. Mysore, *Bromate ion removal by activated carbon,* Water Research **30**, 1651 (1996).

[14] S. Li, Q. Yang, Y. Zhong, F. Chen, T. Xie, F. Yao, J. Sun, C. Jiang, X. Li, and G. Zeng, *Adsorptive bromate removal from aqueous solution by commercial strongly basic resin impregnated with hydrated ferric oxide (hfo): Kinetics and equilibrium studies,* Journal of Chemical & Engineering Data **61**, 1305 (2016).

[15] W.-J. Huang and Y.-L. Cheng, *Effect of characteristics of activated carbon on removal of bromate,* Separation and Purification Technology **59**, 101 (2008).

[16] C. J. Johnson and P. C. Singer, *Impact of a magnetic ion exchange resin on ozone demand and bromate formation during drinking water treatment,* Water Research **38**, 3738 (2004).

[17] S. Gyparakis and E. Diamadopoulos, *Formation and reverse osmosis removal of bromate ions during ozonation of groundwater in coastal areas,* Separation Science and Technology **42**, 1465 (2007).

[18] S. Peldszus, S. A. Andrews, R. Souza, F. Smith, I. Douglas, J. Bolton, and P. M. Huck, *Effect of medium-pressure uv irradiation on bromate concentrations in drinking water, a pilot-scale study,* Water Research **38**, 211 (2004).

[19] M. L. Bao, O. Griffini, D. Santianni, K. Barbieri, D. Burrini, and F. Pantani, *Removal of bromate ion from water using granular activated carbon,* Water research **33**, 2959 (1999).

[20] M. J. Kirisits, V. L. Snoeyink, and J. C. Kruithof, *The reduction of bromate by granular activated carbon,* Water Research **34**, 4250 (2000).

[21] L. Wang, J. Zhang, J. Liu, H. He, M. Yang, J. Yu, Z. Ma, and F. Jiang, *Removal of bromate ion using powdered activated carbon,* Journal of Environmental Sciences **22**, 1846 (2010).

[22] S. Hong, S. Deng, X. Yao, B. Wang, Y. Wang, J. Huang, and G. Yu, *Bromate removal from water by polypyrrole tailored activated carbon,* Journal of colloid and interface science **467**, 10 (2016).

[23] J. Restivo, O. Soares, J. Órfão, and M. Pereira, *Bimetallic activated carbon supported catalysts for the hydrogen reduction of bromate in water,* Catalysis Today **249**, 213 (2015).

[24] J.-h. Xu, N.-y. Gao, D.-y. Zhao, W.-x. Zhang, Q.-k. Xu, and A.-h. Xiao, *Efficient reduction of bromate in water by nano-iron hydroxide impregnated granular activated carbon (fe-gac),* Chemical Engineering Journal **275**, 189 (2015).

[25] A. Bhatnagar, Y. Choi, Y. Yoon, Y. Shin, B.-H. Jeon, and J.-W. Kang, *Bromate removal from water by granular ferric hydroxide (gfh),* Journal of hazardous materials **170**, 134 (2009).

[26] H. Zhang, R. Deng, H. Wang, Z. Kong, D. Dai, Z. Jing, W. Jiang, and Y. Hou, *Reduction of bromate from water by zero-valent iron immobilized on functional polypropylene fiber,* Chemical Engineering Journal **292**, 190 (2016).

[27] X. Huang, L. Wang, J. Zhou, and N. Gao, *Photocatalytic decomposition of bromate ion by the uv/p25-graphene processes,* Water research **57**, 1 (2014).

[28] R. Mao, X. Zhao, H. Lan, H. Liu, and J. Qu, *Graphene-modified pd/c cathode and pd/gac particles for enhanced electrocatalytic removal of bromate in a continuous three-dimensional electrochemical reactor,* Water research **77**, 1 (2015).

[29] O. S. Soares, C. M. Freitas, A. M. Fonseca, J. J. Órfão, M. F. Pereira, and I. C. Neves, *Bromate reduction in water promoted by metal catalysts prepared over faujasite zeolite,* Chemical Engineering Journal **291**, 199 (2016).

[30] T. Zhang, P. Hou, Z. Qiang, X. Lu, and Q. Wang, *Reducing bromate formation with h+-form high silica zeolites during ozonation of bromide-containing water: Effectiveness and mechanisms,* Chemosphere **82**, 608 (2011).

[31] Z.-J. Dong, W.-Y. Dong, X.-M. Zhang, X.-H. Yu, Y.-F. Ou, and H. Du, *Removal of bromate by ferrous sulfate reduction in drinking water,* in *2009 3rd International Conference on Bioinformatics and Biomedical Engineering* (IEEE, 2009) pp. 1–4.

[32] M. Siddiqui, G. Amy, K. Ozekin, W. Zhai, and P. Westerhoff, *Alternative strategies for removing bromate,* Journal of the American Water Works Association;(United States) **86** (1994).

[33] P. Westerhoff, *Reduction of nitrate, bromate, and chlorate by zero valent iron (fe 0),* Journal of Environmental Engineering **129**, 10 (2003).

[34] L. Xie and C. Shang, *Role of humic acid and quinone model compounds in bromate reduction by zerovalent iron,* Environmental science & technology **39**, 1092 (2005).

[35] J.-h. Xu, N.-y. Gao, D.-y. Zhao, D.-q. Yin, H. Zhang, Y.-q. Gao, and W. Shi, *Comparative study of nano-iron hydroxide impregnated granular activated carbon (fe–gac) for bromate or perchlorate removal,* Separation and Purification Technology **147**, 9 (2015).

[36] D. Thomas and J. Rohrer, *Determination of chlorite, bromate, bromide, and chlorate in drinking water by ion chromatography with an on-line-generated postcolumn reagent for sub-μg/l bromate analysis,* .

[37] M. J. Kirisits and V. L. Snoeyink, *Reduction of bromate in a bac filter,* American Water Works Association. Journal **91**, 74 (1999).

[38] S. K. Sharma, *Adsorptive iron removal from groundwater* (CRC Press, 2001).

[39] R. Chang, *Chemistry (10th edition)* (McGraw-Hill, 2010).

[40] J. A. Dean, *Lange's handbook of chemistry,* Material and manufacturing process **5**, 687 (1990).

[41] C. Ottley, W. Davison, and W. Edmunds, *Chemical catalysis of nitrate reduction by iron (ii),* Geochimica et Cosmochimica acta **61**, 1819 (1997).

[42] P. J. Alvarez and W. A. Illman, *Bioremediation and natural attenuation: process fundamentals and mathematical models,* Vol. 27 (John Wiley & Sons, 2005).

[43] R. J. Buresh and J. Moraghan, *Chemical reduction of nitrate by ferrous iron,* Journal of Environmental Quality **5**, 320 (1976).

[44] D. Postma, C. Boesen, H. Kristiansen, and F. Larsen, *Nitrate reduction in an unconfined sandy aquifer: water chemistry, reduction processes, and geochemical modeling,* Water Resources Research **27**, 2027 (1991).

[45] H. S. Petersen, *Reduction of nitrate by iron (ii),* Acta chemica Scandinavica. Series A: Physical and inorganic chemistry (1979).

[46] P. Stuyfzand, P. Van Rossum, and I. Mendizabal, *Does arsenic, in groundwaters of the compound rhine-meuse-scheldt-eems delta, menace drinking water supply in the netherlands,* Arsenic in groundwater: a world problem. NNCIAH, Netherlands National Committee of the IAH, Utrecht, The Netherlands , 102 (2008).

[47] V. Gaur and P. Shankar, *Surface modification of activated carbon for the removal of water impurities,* Water Technology Online (2012).

[48] M. Razvigorova, T. Budinova, N. Petrov, and V. Minkova, *Purification of water by activated carbons from apricot stones, lignites and anthracite,* Water Research **32**, 2135 (1998).

[49] S. C. Smith and D. F. Rodrigues, *Carbon-based nanomaterials for removal of chemical and biological contaminants from water: a review of mechanisms and applications,* Carbon **91**, 122 (2015).

[50] C. Xu, J. Shi, W. Zhou, B. Gao, Q. Yue, and X. Wang, *Bromate removal from aqueous solutions by nano crystalline akaganeite (β-feooh)-coated quartz sand (cacqs),* Chemical engineering journal **187**, 63 (2012).

[51] D. G. Evans and R. C. Slade, *Structural aspects of layered double hydroxides,* in *Layered double hydroxides* (Springer, 2006) pp. 1–87.

[52] F. L. Theiss, S. J. Couperthwaite, G. A. Ayoko, and R. L. Frost, *A review of the removal of anions and oxyanions of the halogen elements from aqueous solution by layered double hydroxides,* Journal of colloid and interface science **417**, 356 (2014).

[53] R. Chitrakar, A. Sonoda, Y. Makita, and T. Hirotsu, *Calcined mg–al layered double hydroxides for uptake of trace levels of bromate from aqueous solution,* Industrial & Engineering Chemistry Research **50**, 9280 (2011).

[54] M. J. McAllister, J.-L. Li, D. H. Adamson, H. C. Schniepp, A. A. Abdala, J. Liu, M. Herrera-Alonso, D. L. Milius, R. Car, R. K. Prud'homme, *et al.*, *Single sheet functionalized graphene by oxidation and thermal expansion of graphite,* Chemistry of materials **19**, 4396 (2007).

[55] R. K. Upadhyay, N. Soin, and S. S. Roy, *Role of graphene/metal oxide composites as photocatalysts, adsorbents and disinfectants in water treatment: a review,* RSC Advances **4**, 3823 (2014).

[56] S. Wang, H. Sun, H.-M. Ang, and M. Tadé, *Adsorptive remediation of environmental pollutants using novel graphene-based nanomaterials,* Chemical engineering journal **226**, 336 (2013).

[57] A. K. Mishra and S. Ramaprabhu, *Functionalized graphene sheets for arsenic removal and desalination of sea water,* Desalination **282**, 39 (2011).

[58] Y. Li, P. Zhang, Q. Du, X. Peng, T. Liu, Z. Wang, Y. Xia, W. Zhang, K. Wang, H. Zhu, *et al.*, *Adsorption of fluoride from aqueous solution by graphene,* Journal of colloid and interface science **363**, 348 (2011).

[59] S. Zhang, Y. Shao, J. Liu, I. A. Aksay, and Y. Lin, *Graphene–polypyrrole nanocomposite as a highly efficient and low cost electrically switched ion exchanger for removing clo4–from wastewater,* ACS applied materials & interfaces **3**, 3633 (2011).

[60] S. Vasudevan and J. Lakshmi, *The adsorption of phosphate by graphene from aqueous solution,* Rsc Advances **2**, 5234 (2012).

[61] D. Cohen-Tanugi and J. C. Grossman, *Water desalination across nanoporous graphene,* Nano letters **12**, 3602 (2012).

[62] M. Hu and B. Mi, *Enabling graphene oxide nanosheets as water separation membranes,* Environmental science & technology **47**, 3715 (2013).

[63] H. Chen, Y. Cao, E. Wei, T. Gong, and Q. Xian, *Facile synthesis of graphene nano zero-valent iron composites and their efficient removal of trichloronitromethane from drinking water,* Chemosphere **146**, 32 (2016).

[64] A. Ates and G. Akgül, *Modification of natural zeolite with naoh for removal of manganese in drinking water,* Powder Technology **287**, 285 (2016).

[65] S. Waghmare and T. Arfin, *Fluoride removal from water by calcium materials: a state-of-the-art review‖,* International Journal of Innovative Research in Science, Engineering and Technology **4**, 8090 (2015).

[66] V. Badillo-Almaraz, J. Armando Flores, H. Arriola, F. López, and L. Ruiz-Ramirez, *Elimination of fluoride ions in water for human consumption using hydroxyapatite as an adsorbent,* Journal of radioanalytical and nuclear chemistry **271**, 741 (2007).

[67] S. Gao, R. Sun, Z. Wei, H. Zhao, H. Li, and F. Hu, *Size-dependent defluoridation properties of synthetic hydroxyapatite,* Journal of Fluorine Chemistry **130**, 550 (2009).

[68] M. Jiménez-Reyes and M. Solache-Ríos, *Sorption behavior of fluoride ions from aqueous solutions by hydroxyapatite,* Journal of hazardous materials **180**, 297 (2010).

A

BROMATE REMOVAL TECHNOLOGIES

There are several adsorbent which have been studied for bromate removal such as activated carbon, iron components, double layered and zeolites. On the other hand there are also promising materials which can be used for bromate removal. These materials will be described along this section.

A.1. ACTIVATED CARBON AC

AC is an inert porous material with large specific surface area, able to attract a variety of chemicals/pollutants on its hydrophobic internal surface [47]. Several chemical species have been chemically reduced with granular activated carbon GAC. For instance, nitrate was reduced to nitrite using apricot stone based carbon [48], perchlorate was reduced to chloride in presence of GAC [24]. In fact, since 90s AC has been proven capable of transferring electrons during the reduction reactions and the reduction of bromate to bromide by AC has been studied as well [19].
The bromate that is removed by AC, is first adsorbed, reduced to hypobromite (OBr^-) and finally reduced to bromide (Br^-) on the AC surface as the following reactions show [13]

$$\equiv C + BrO_3^- \rightarrow BrO^- + \equiv CO_2$$
$$\equiv C + 2BrO^- \rightarrow Br^- + \equiv CO_2$$

Where $\equiv C$ is the AC surface and $\equiv CO_2$ represents a surface oxide. These reactions are interfacial reactions involving the interaction of surface bound carbon groups with dissolved bromide species.

Therefore the characteristics of the carbon are important to understand the mechanism of bromate reduction.

A.1.1. AC CHARACTERISTICS

Siddiqui et al. (1996) studied and described the behaviour of different ACs used to remove bromate, trying to find a correlation between their bromate removal capacities and inorganic composition, acid-base groups and other characteristics of AC.

Siddiqui et al. (1996) found that the inorganic composition of carbon is an important factor to inhibit surface reduction of bromate. On the other hand, an inverse trend was observed between the metal content of these ACs and the bromate removal capacities of different ACs. The carbon with the lowest amount of metals as well as iron and sulphur showed the highest bromate removal capacity, implying that these metals act as inhibitors for bromate removal. This can be due to the active surface groups are blocked by these metal oxides or due to oxidation of surface groups by metal groups. The role of carbon surface functional groups present such as sulphide, disulphide and carbonates are fundamental in the AC surface reduction of bromate. The functional groups on the surface may depend on the mineral constituents of AC.

In their study, Siddiqui et al. (1996) classified the surface chemical groups according to the acid-base character finding a strong correlation between these groups and the bromate removal. They found that the AC with a much higher number of basic groups was more effective than other AC for bromate removal, while

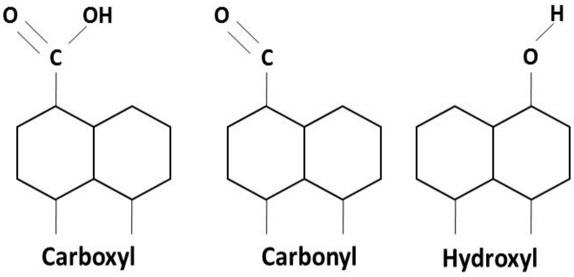

Figure A.1: Functional groups on activated carbon.

the carbon with the highest content of acid groups and carboxyl groups was the least effective. The carboxyl groups correspond to the presence of negatively charged carboxylate anion surface functional group on the AC.

The effects of the surface chemical groups were also previously studied by other authors and compiled by Huang and Cheng (2008). In the previous studies, it was found that carbons with less oxygen in the surface tend to be basic and have an anion exchange capacity due to their positive charge. This can be explained more in detail, oxygen is commonly present in the form of carboxylic acid groups ($-COOH$), phenolic hydroxyl groups ($-OH$) and carbonyl groups ($> C = O$) as Figure A.1 shows. The increase of acidity in the AC is because of the formation of carboxylic acid and phenolic hydroxyl groups. Therefore if the oxygen reduces (which is contained in the functional groups mentioned above) the surface will become basic.

Consequently, basic carbon adsorbs protons, having a positive surface potential and therefore makes the carbon surface more electrostatically attractive to anions. The adsorption of anions decreased as the acidity of the carbon increased, which is attributable to the electrostatic interactions between the anions and the acid groups [15].

The size of the pores is also an important factor. For instance, mesopores provide easier access to large and small fractions of contaminant compounds on the adsorbent surface [49]. Moreover, it was investigated that AC with rich mesopores combined with other parameters like higher zeta potential value, and lower oxygen content could remove bromate more effectively [21]

A.1.2. *pH* EFFECT

The removal of bromate was found to increase when the pH decreased, this is due to the reduction of surface charge of the carbon and the higher reactivity of bromate at low pH. When the pH decreases, protons are adsorbed onto the carbon, then the negatively charged groups decrease and more favourable interaction between carbon and bromate is possible [13, 20]. In most of the investigated AC, the charge at high pH values is negative, which corresponds to the presence of negatively charged carboxylate anionic surface functional groups on the AC. As the pH is lowered, the weakly acidic and basic functional group are protonated resulting in a positive change in zeta potential, until the isoelectric point (or point of zero charge) is reached [13].

A.1.3. PRESENCE OF NOM AND ANIONS

The presence of natural organic matter (NOM) and anions such as bromide, chloride, nitrate and sulphate reduce the bromate adsorption. The adsorption of NOM could block the sites for bromate removal. Regarding the anions, they might occupy the ion exchange sites on the carbon, reducing the access to the sites, in other words, these anions compete for the adsorptive sites on the AC. As a consequence, a low adsorption and a poor bromate removal are expected [19]. The characteristics of the AC such as surface chemistry, type of porous, the pH and presence of competitors need to be considered to achieve a high bromate removal.

A.2. MODIFIED ACTIVATED CARBON

In order to improve the performance of the AC in the removal of pollutants and according to the nature of the target pollutant, the surface of AC can be modified to enhance the affinity for the pollutant, making the surface of the AC accessible for the target pollutant. One method to modify AC is the chemical modification that involves the surface impregnation of AC with metals and their oxides [47].

Some modified activated carbons have been tested to remove BrO_3^- such as bimetallic AC [23], polypyrrole tailored AC [22] and nano iron hydroxide impregnated granular AC (Fe-GAC) [24, 35].

A.2.1. Bimetallic activated carbon

The hydrogen reduction of bromate over supported metallic catalysts has shown to be an alternative for the reduction of bromate, without formation of additional sludge.

Restivo, et al. (2015) investigated the combination of a noble metal (Pd, Pt, Ru, Rh or Ir) with a second metal (Cu, Sn, Ni, Zn or Fe), supported on AC in the removal of bromate. No H_2 chemisorption was noticed. This could be an indication that some interaction exists between the noble metal and the other metal, forming an alloy, or the second metal is covering or hindering the activity of the noble metal and limiting the H2 chemisorption. Despite that, all the combinations showed the conversion of bromate into bromide, without accumulation of secondary products.

The combination of Pd with Cu was the most efficient combination converting completely bromate in less than 10 min of reaction. This combination also presents higher performance than the Pd monometallic catalyst, while the other combinations present similar or lower performances than the Pd monometallic catalyst.

The second metal alone was tested obtaining the following trend: $Cu > Sn > Fe > Zn$. The performances of the second metals tested alone showed that they are less active than the bimetallic catalysts prepared with Pd [23].

A.2.2. Polypyrrole tailored AC

Hong et al. (2016) investigated Polypyrrole (Ppy) deposited into the pores of nut shell-based AC (NAC) to remove bromate. This Ppy-tailored AC (Ppy-NAC) can host positive charges offering sorption capacity for bromate. The maximum adsorption capacity of bromate by Ppy-NAC was 62.5 mg/g according to the adsorption isotherm, 8.3 times higher than NAC [22].

The presence of chloride ions in solution showed that Cl^- exchanged with bromate during the adsorption process. Moreover, bromide was found in solution indicating that some of bromate was reduced to bromide, which is released to the solution and adsorbed on the Ppy-NAC. The mechanisms of bromate removal by the Ppy-NAC includes ion exchange and reduction reaction of bromate on the Ppy-NAC surfaces. Figure A.2 shows the adsorption and reduction of bromate.

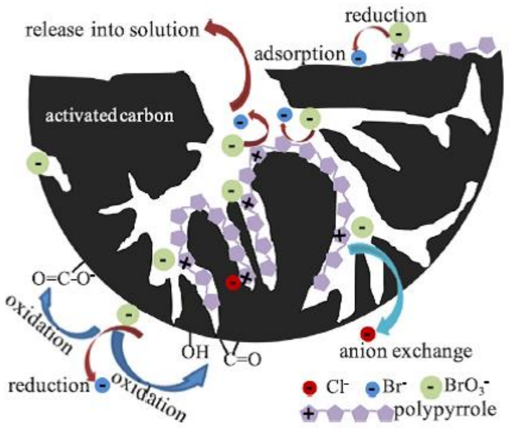

Figure A.2: Diagram of bromate removal by Ppy-NAC [22].

A.2.3. NANO IRON HYDROXIDE IMPREGNATED GAC (Fe-GAC)

Xu et al. (2015) studied the removal of bromate using nanoscale iron hydroxide (FeOOH) particles with SO_4^{2-} attached onto the surface of GAC. Bromate was removed by Fe-GAC firstly by adsorption, then reduced to bromide and removed completely from 0.1 mmol/L (12.8 mg/L) to zero after 50 h.

According to their study, Fe-GAC can work with a broad pH range (2 – 10) with the optimal pH 6 to 8 for bromate reduction. With initial bromate concentrations between 0.05-0.30 $mmol/L$ (6.4-38.4 mg/L) and with iron concentration of Fe-GAC corresponding to 0.6 wt%, 0.9 wt% and 1.2 wt% relative to the GAC mass, the maximum adsorption capacity reached was 0.269 mmol/g (34.4 mg/g) by the Fe-GAC with 1.2 wt%.

At lower bromate concentrations (<0.15 mmol/L (19.2 mg/L)) more than 90% of bromate was removed by chemical reduction, whereas at elevated bromate concentrations, more than 70% of bromate was removed through the reduction mechanism and the remaining fraction (<30%) was adsorbed. Moreover, it was found bromate reduction by Fe–GAC was the main mechanism as can be seen in Figure A.3 [35].

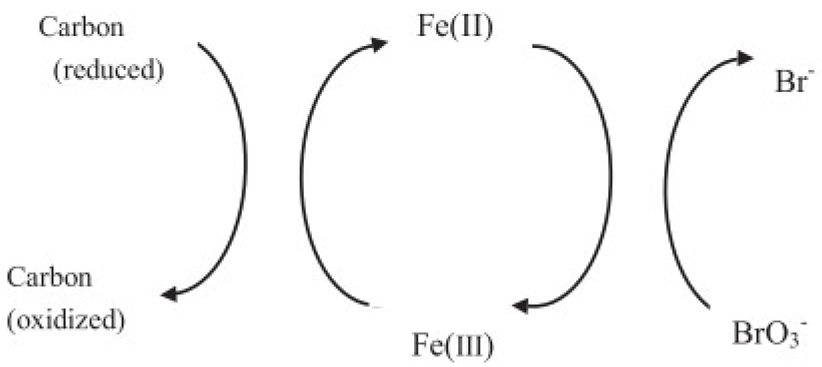

Figure A.3: Bromate removal mechanism in Fe-GAC.

It should be noted that the adsorption process is probably fast while the following reaction is the rate limiting step, which is consistent with the observed slow removal rate of bromate.

Furthermore, the presence of inorganic anions showed inhibiting effects on bromate removal by Fe-GAC with the following order: $PO_43^- > CO_3^{3-} > Cl^- > SO_4^{2-}$.

A.3. IRON

A.3.1. GRANULAR FERRIC HYDROXIDE (GFH)

GFH is a poorly crystallized $\beta - FeOOH$ which includes chloride to support the structure of the adsorbent.

GFH has been used to remove arsenic, fluoride and natural organic matter from water. Bhatnagar et al. (2009) studied the use of GFH for bromate removal. Their study showed that the uptake rate of bromate was rapid at the beginning, adsorbing 75% of bromate in 5 min, following by a slow adsorption reaching the equilibrium within 20 min. The fast uptake indicates that plenty of accessible sites are available for adsorption, however when the concentration increases, saturation of GFH occurred, slowing down the uptake and reaching a plateau indicating that there are no more sites available for adsorption.

Bhatnagar et al. (2009) found that the bromate sorption onto GFH is a two steps process: the first step could be associated with the transport of bromate by surface diffusion and the second step is controlled by pore diffusion. The main mechanism during bromate sorption on GFH was ion-exchange where the bromate ions were exchanged by the chloride ions, as it can be seen below.

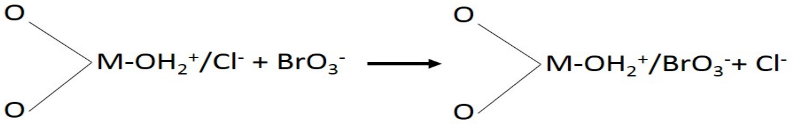

$$\mathrm{O_2{>}M\text{-}OH_2^+/Cl^- + BrO_3^- \longrightarrow O_2{>}M\text{-}OH_2^+/BrO_3^- + Cl^-}$$

The effect of pH was tested with a wide range of different pH (3–12) with an initial bromate concentration of 50 mg/L. High removal efficiency of bromate (95%) was obtained between pH 3–9. A significant decrease was observed in bromate removal rates at pH 10–12, and the optimum bromate removal was observed at pH ranges of 4.0–8.0 [25].

The maximum adsorption potential of GFH for bromate removal was 16.5 mg/g at 25 °C.

The removal of bromate in the presence of competing anions like chloride (Cl^-), fluoride (F^-), nitrate (NO_3^-), carbonate (CO_3^{2-}), sulphate (SO_4^{2-}), and phosphate (PO_4^{3-}) was investigated, showing that there is no big influence on bromate sorption [25].

A.3.2. ZERO VALENT IRON IMMOBILIZED ON FUNCTIONAL POLYPROPYLENE FIBER

Zhang et al. (2016) investigated the use of micro-sized zero-valent iron (mZVI) immobilized in acrylic acid (AA) functionalized polypropylene fiber (PP-g-AA) for bromate removal. mZVI was immobilized firmly on PP-g-AA via complexation and liquid phase reduction, which prevented the aggregation of mZVI and release of Fe ions. The coordination between mZVI with carboxyl groups is shown in Figure A.4. The mZVI presented excellent distribution through the polypropylene fiber due to the carboxyl groups of the acrylic acid and high activity for bromate reduction. The effects of pH on bromate reduction were not high and it was related to the buffering performance of the $-COOH/-COO^-$ groups around the areas where the reduction took place. The inhibitory effects of common anions and humic acid were negligible. The concentration of $Fe^{2+/3+}$ in solution was low (<19.0 $\mu g/L$) and remained constant during the reduction process [26]. Four different contents of iron were evaluating showing that the bromate removal efficiency varied with the content of Fe^0 loaded. The removal efficiency decreased when the Fe^0 content increased as it follows: 16.44 mg/g (92.5%) > 8.44 mg/g (85.4%) > 6.50 mg/g (71.1%) > 33.32 mg/g (69.1%) within 10 min. The mechanism of bromate reduction proposed to include the following two reactions [26]:

$$BrO_3^- + 3Fe + 3H_2O \rightarrow Br^- + 3Fe^{2+} + 6OH^-$$
$$BrO_3^- + 2Fe + 3H_2O \rightarrow Br^- + 2Fe^{3+} + 6OH^-$$

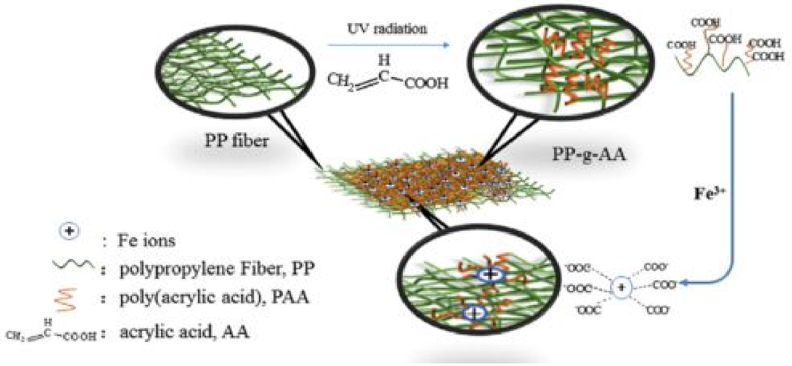

Figure A.4: Fe ions coordination with carboxyl groups on PP fiber

A.3.3. NANO CRYSTALLINE AKAGANEITE ($\beta - FeOOH$)-COATED QUARTZ SAND (CACQS)

Xu et al. (2012) investigated Akaganeite ($\beta - FeOOH$) for bromate removal because of its unique sorption, ion exchange, and catalytic properties. It is synthesized by a simple and readily reproduced method.

The operational conditions were an adsorbent dosage of 20–160 g/L, initial pH between 3–12, contact time 1–240 min, initial bromate concentration of 0.6–10 mg/L and three different temperatures: 15, 25 and 35°C.

The uptake rate of bromate was rapid and the adsorption was almost saturated within 20 min. The optimum adsorbent dose was 100 g/L at a bromate concentration of 200 $\mu g/L$. The adsorption capacities of CACQS for bromate were 47.3, 37.8 and 21.7 $\mu g/g$ at 15, 25 and 35°C, respectively [50].

A.4. Layered double hydroxides (LDH)

LDH are a group of clay minerals which have been used to the remove several anions from water. The basic layer structure of LDHs is based on $Mg(OH)_2$ (brucite), typically associated with small polarizing cations and polarizable anions. The structure of LDH may be derived by substitution of a fraction of the divalent cations in the brucite by trivalent cations, giving a positive charge to the layers, which is balanced by intercalation of anions and water between the layers [51].

The cation ratio M^{2+} : M^{3+} of the LDH adsorbent is an important factor which influenced anion uptake. LDHs can be represented by the general formula:

$$\left[M^{2+}_{1-x}M^{3+}_{x}(OH)_2\right]^{X+}\left[A^{n-}\right]_{x/n} * mH_2O$$

where M^{2+} is a divalent cation, M^{3+} is a trivalent cation, An^{-} is the exchangeable anion (e.g. carbonate, chloride or nitrate) and 0.2 < x < 0.33.

LDH is capable to remove some anions through anion exchange, adsorption and reformation after thermal activation.

Reformation (or memory) effect: Thermal activation of a LDH can be reached by calcination at 300–500 °C and it causes the elimination of water and anions contained in the interlayer resulting in the formation of a mixed metal oxide as Figure A.5 shows. When a thermally activated LDH is exposed to water and anions, spontaneous reformation of a LDH structure may occur and as a consequence the uptake of target anions will take place, improving the anion uptake capacity as it can be seen in Figure A.6.

It should be noted that the presence of competing anions (e.g. carbonate, phosphate and sulphate) had an impact on uptake of the target anion due to the lower affinity of LDHs towards monovalent anions compared to anions with multiple charges.

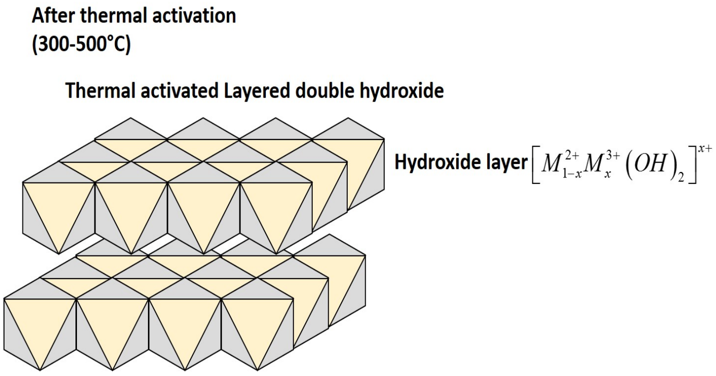

Figure A.5: LDH after thermal activation.

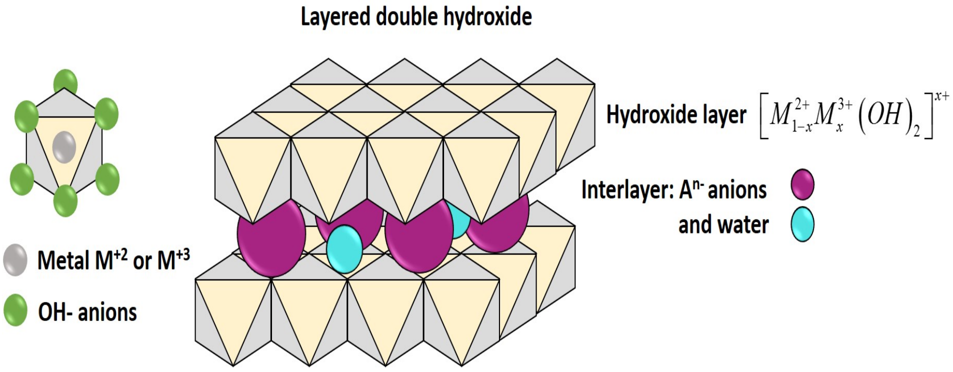

Figure A.6: Removal mechanism of layered double hydroxide.

The temperature for thermal activation is an important factor on anion uptake. The optimum thermal activation temperature is the temperature at which the maximum number of interlayer anions is removed without causing a permanent decomposition of the LDH cation layers. Otherwise, reformation or anion exchange properties will not be exhibited. The optimum thermal activation temperature is usually below 500°C [52].

Chitrakar et al. (2011) tested the removal of trace level of bromate by thermally activated Mg/Al LDHs. Bromate removal was carried out at room temperature using a batch method with an initial concentration between 0.02–0.78 $\mu mol/L$. Thermal activation temperature had a significant impact on bromate removal, which was confirmed with the samples of LDH calcined at 300°C without bromate removal. LDHs thermally activated at 400 and 500°C exhibited much higher bromate removal, than at 300°C, from 0.78 $\mu mol/L$ to less than 0.078 $\mu mol/L$. Even though the initial bromate uptake was fast, equilibrium was reached at 48–72 h and the initial solution pH have little effect on the uptake [53].

A.5. Graphene and graphene oxide Graphene (G) and graphene oxide (GO) are new carbon nanomaterials. Graphene has a large theoretical surface area (2630 m^2/g) [54], which exhibits almost twice the surface area of AC [55], and it could provide a better alternative as an adsorbent. Recently, the interest for graphene in water treatment has increased and it has been tested as photocatalyst, adsorbent and antimicrobial agent removing heavy metals, trichloromethane, bromate and pathogens among others pollutants.

As it could be seen in the functional groups of AC play an important role during the adsorption process. In the case of graphene, this can be functionalized with $-OH$ and $-COOH$ groups via chemical oxidation methods to produce GO. The presence of organic functional groups which can be introduced by surface functionalization can enhance their adsorption capacities.

The negatively charged functional groups provide GO strong acidity and high affinity for basic compounds and cations, making it a good adsorbent for heavy metals. On the contrary, non-functionalized graphene shows hydrophobic surface and presents high adsorption to chemicals being an adsorbent of both cationic and anionic heavy metal ions to some extent [49, 56].

Modification of graphene or graphene oxide with metal oxides or organics can produce various nanocomposites, enhancing adsorption capacity which can be used for anionic metal removal due to functionalization [56].

Regarding the metal anions removal with graphene, synthetized graphene sheets by hydrogen induced exfoliation of graphitic oxide followed by functionalization were used to remove arsenic (As(III) and As(V)) and sodium. The maximum adsorption capacities obtained for arsenate, arsenite and sodium were nearly 142, 139 and 122 mg/g, respectively [57].

A.4.1. ANIONS REMOVAL

Some inorganic anions (F^-, NO_3^-, ClO_4^- and PO_3^{4-}), are also present in water. Due to the negative charge of anions, GO is not effective for the anion adsorption, however, functionalized systems of graphene can be a solution. There are only few investigations that have been reported on their adsorptive removal by graphene and functionalized systems. For example, the adsorption of fluoride by graphene reported that graphene was an excellent adsorbent with an adsorption capacity of 35.6 mg/g at pH = 7.0, 25 °C. Fluoride ions are predominantly adsorbed by the surface-exchange between fluoride ions in solution and hydroxyl ions on the adsorbent, as the reaction below shows [58]:

$$GrapheneOH_2^+(surf) + F^- \rightarrow GrapheneF(surf) + H_2O$$
$$GrapheneOH(surf) + F^- \rightarrow GrapheneF(surf) + OH^-$$

Zhang et al. (2011) reported a 3D nanostructured graphene–polypyrrole (Ppy) nanocomposite for perchlorate (ClO_4^-) removal. The graphene–Ppy nanocomposite exhibited a significantly improved uptake capacity for ClO_4^- compared with Ppy film alone and can be used for ClO_4^- removal through an electrically switched ion exchange [59].

Phosphate adsorption on graphene was reported, obtaining and adsorption capacity of up to 89.37 mg/g at an initial phosphate concentration of 100 mg/L and at a temperature of 20°C [60].

Despite the anions that have been investigated, the removal of bromate using graphene oxide has not been studied, it would be interesting to know the adsorption capabilities of this material for bromate or even bromide removal.

A.4.2. GRAPHENE OXIDE NANOSHEETS AS WATER SEPARATION MEMBRANES

Graphene oxide (GO) nanosheets (oxygenated graphene sheets supporting carboxyl, hydroxyl, and epoxide functional groups) offer a potential for making functional nanocomposite materials with high chemical stability, strong hydrophilicity, and excellent antifouling properties. It should be noted that until now, most of the applications of graphene related to water have focused on adsorption or photocatalysis. The concept of using graphene-based nanomaterials to make membranes for water separation was first evaluated by molecular simulations [61].

In simulations, Cohen-Tanugi and Grossman (2012) indicated that on the contratry with classical RO membranes, where water transport is slow via a solution-diffusion process, nano graphene membranes can allow fast convective water flow across well-defined channels. Nanopores were simulated on the surface of super high strength graphene monolayers letting the water pass through them while rejecting ions or other molecular solutes due to their physical properties such as charge or hydrophobicity.

Furthermore, it was demonstrated that, by controlling pore sizes and functional groups on the nanopores, it is possible to make a monolayer graphene membrane useful for desalination, with a higher water permeability than current RO membranes.

GO nanosheet is a single-atom-thick with lateral dimensions as high as tens of micrometers which makes it highly stacable. Hu and Mi (2013) fabricated a membrane with stacked GO nanosheets. The two-dimensional channels between the stacked GO nanosheets may allow water to pass through while rejecting unwanted solutes, a mechanism similar to that of the pores in traditional membrane structures. Molecular simulations have predicted that water has a very large slip length (i.e., low friction) on graphene surfaces, resulting in an extremely high rate of water flow in graphene nanochannels. In order to fabricate the membrane, GO nanosheets were deposited via a layer-by-layer (LbL) approach on a polydopamine-coated polysulfone support and then cross-linked them by 1,3,5-benzenetricarbonyl trichloride (TMC) GO membrane, using a dead end membrane filtration system [62].

Water flux was tested under a transmembrane pressure of 0.34 MPa. It was observed that water flux of the polydopamine-coated membrane (without any GO layers yet and used as a control) is 1340 ± 40 $l/m2hMPa$, which decreases to 80–276 LMH/MPa after the membrane were coated with 5–50 layers of GO, however, water flux does not decrease when the layers increase.

The separation performance of the GO membrane was examined using NaCl as a representative monovalent salt, Na_2SO_4 as a representative divalent salt, and two organic dyes Methylene blue (MB) and Rodamine-WT where MB is a positively charged cation and R-WT is a negatively charged anion.

The polydopamine-coated membrane had almost no rejection of the salts and less than 10% rejection of the dyes. After GO coating, the rates of rejection of NaCl and Na_2SO_4 increased to 6–19% and 26–46%, respectively, depending on the number of GO layers. In the case of the dyes, the rejection of MB and R-WT were in a range of 46–66% and 93–95%, respectively. The higher rate for R-WT rejection can be explained by two factors: First, the higher molecular weight than MB, cause higher rejection by the size exclusion effect. Second, GO membranes were negatively charged (carboxyl groups) therefore increasing the rejection of negatively charged R-WT instead of positively charged MB [62].

Based on the high R-WT removal (93–95%) obtained by Hu and Mi (2013) due to the rejection of the negative charges of GO membranes and R-WT, it could be interesting to investigate the removal of bromate, which is also negatively charged, using graphene oxide nanosheets membranes.

A.4.3. TiO_2 (P25)-GRAPHENE (PHOTOCALTALYTIC DECOMPOSITION)

Huang et al. (2014) prepared a composite with TiO2 (P25) and graphene that was used as a photocatalyst to reduce bromate to bromide under UV light irradiation.
According to Huang et al. (2014) the photocatalysis shows high efficiency of the bromate removal due to its stable performance at wide pH range and easy combination with UV disinfection. In the photo-reduction of BrO_3^-, TiO_2 was used as catalyst in the conversion of BrO_3^- to Br^-. This reduction process was affected by the electron transport to BrO_3^- on TiO_2. As a result, the TiO_2 was usually coated on the matrix that improved the transport of photo-generated electron [27].

On the other hand, in the composite graphene acts as an acceptor of the photo-generated electrons (e-) from the photo-excited P25 (TiO_2) to increase the charge transportation. Moreover, the large surface of graphene would enhance the adsorption of pollutants onto photocatalysts.

Huang et al. (2014) studied the bromate removal under UV irradiation on different catalysts. The results can be seen in Figure A.7, where BrO_3^- decreased in the solution with increasing reaction time. After 60 min of reaction, the graphene and UV alone provided 0.55 - 0.65 of C/Co indicating that 35-45% of removal efficiency. On the other hand, 0.3 and 0.01 of C/Co were obtained for P25 and P25-GR-1%, respectively, which demonstrated 70% and 99% of BrO_3^- removal efficiency.

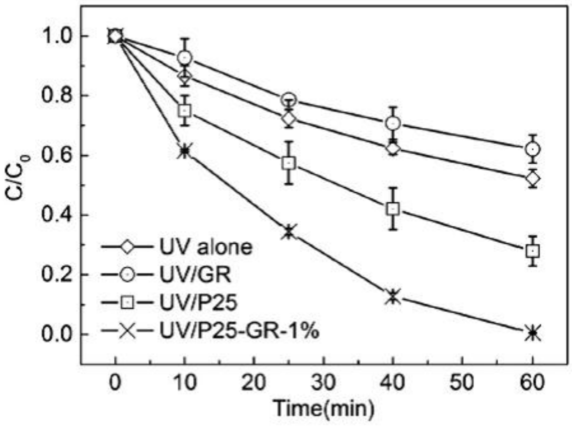

Figure A.7: Photo-reduction of BrO3- by UV/P25, UV/P25-GR-1%, UV/GR and UV alone (Co= 10 mg/L, pH 6.8, catalysts dosage 0.1 g/L)[59].

The mechanism of BrO_3^- reduction is contributed to photo-reducing BrO_3^- to Br^- as the following equation shows:

$$BrO_3^- + 6e^- + H^+ \rightarrow Br^- + H_2O$$

The adsorption of BrO_3^- was limited by the negative surface of the P25-GR composite. This is supported by the removal of BrO_3^- without UV. The study showed that the adsorption of BrO_3^- on P25 and P25-GR without UV provided the C/Co> 0.95 regardless of various pH, indicating that most of BrO_3^- was not removed. This observation suggests that the effect of adsorption plays a minor role in the removal of BrO_3^-. Accordingly, in the case of P25- GR, the BrO_3^- removal is contributed to photo-catalytic reaction rather than the adsorption [27].

A.4.4. GRAPHENE NANO ZERO-VALENT IRON COMPOSITES

Zero-valent iron materials are strong reducing agents which have been extensively applied for removal of a variety of pollutants such as chlorohydrocarbon, nitrobenzenes, chlorinated phenols, heavy metals, and various anions because of its large specific surface area, surface reactivity and relatively low price [63].

One disadvantage is that nano zero-valent iron (nZVI) suffers from strong aggregation and fast oxidation in air, which can reduce the adsorption sites and reactive sites of the particles, resulting in the decrease of the effective contact area between target pollutants and nZVI. To mitigate these problems and improve the stability, nZVI particles had been modified by coating or immobilizing on solid supports materials such as resins, silica, bentonite, diatomite, AC, and multiwalled carbon nanotube to restrain aggregation of nZVI.

Recently, graphene was used as an ideal support material for loading inorganic nanoparticles, inhibiting the aggregation of metal nanoparticles.

The study of Chen et al. (2016) used Graphene/Fe^0 (ZVI) nanocomposites for trichloronitromethane (TCNM). The nanocomposites were prepared via facile carbonization and calcinations of glucose and ferric chloride. The removal of TCNM within 60 min of reaction was of 75.1%, 80.6%, 91.5% and 61.3% at the Fe/C mass ratio of 1:15, 1:10, 1:5 and 1:1 respectively. Therefore, the G-nZVI with Fe/C mass ratio of 1:5 had the best performance in TCNM removal [63].

The TCNM was adsorbed by G-nZVI and reduced by Fe^0. When 100 mg/L TCNM was treated with 60 mg/L G-nZVI, TCNM decreased 60.1%, 88.7% and nearly 100% in 20, 45 and 90 min respectively. The degradation of TCNM is via dichloronitromethane DCNM as a dechlorination intermediate, no other dechlorination intermediates including CNM and nitromethane (NM) were observed during the degradation, which suggests that the reduction of the nitro groups occurred rapidly to form hydrophilic methylamine (MA) which perhaps was the terminal degradation product [63].

The use of graphene ZVI nanocomposites could be a promising material for bromate removal, where the ZVI will reduce bromate to bromide, and graphene will give support stability to iron as Figure A.8 shows.

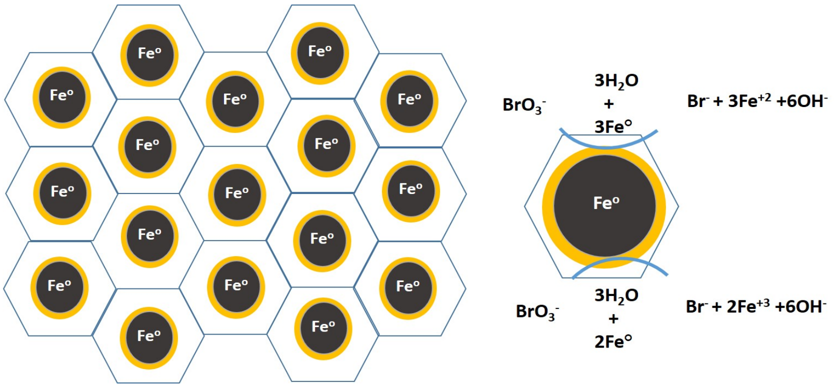

Figure A.8: Proposal of bromate removal mechanism using graphene ZVI nanocomposites.

A.4.5. GRAPHENE-MODIFIED PD/C CATHODE AND PD/GAC (ELECTROCATALYTIC REMOVAL OF BrO_3^-)

Mao et al. (2015) investigated Palladium-reduced graphene oxide modified carbon paper (Pd-rGO/C) cathode and Pd-rGO modified granular AC (Pd-rGO/GAC) particles in continuous three-dimensional electrochemical reactor to remove bromate.

The rGO sheets promoted the electrochemical reduction of BrO_3^-, due to the fact that electron transfer can be enhanced by rGO sheets, the electro-reduction of H_2O to atomic H* on the polarized Pd particles could be significantly accelerated, leading to a faster reaction rate of BrO_3^- with atomic H*, as the equations bellow show.

$$Pd + H_2O + e^- \rightarrow Pd - H* + OH^-$$
$$6Pd - H* + BrO_3^- \rightarrow 6Pd + Br^- + 3H_2O$$

BrO_3^- with an initial concentration of 20 $\mu g/L$ was reduced to be less than 6.6 $\mu g/L$ at a hydraulic retention time of 20 min. Dissolved organic matter inhibited the BrO_3^- reduction. In the experiment with tap water precipitates were generated from Ca^{2+} and Mg^{2+} covering the Pd catalysts, and they were mainly deposited onto the Pd-rGO/C cathode rather than the Pd-rGO/GAC particles [28].

There are not too many literature about the bromate removal with graphene. However, there are studies that report the removal of other pollutants with negative charge. Most of the papers in which graphene was used show this material as the most promising material due to its properties.

Graphene is a new material that should be investigated based on its properties. Even though negative surface charge can be a disadvantage as an adsorbent, graphene sheet can be used to separate bromate through a membrane taking that the negative charge of graphene could reject the bromate ions. On the other hand, as adsorbent graphene might not offer good adsorption capacity. However, it can be used as a composite with iron, combining the high surface area and stability of graphene as a support material and the strong reducing capacity of zero iron to reduce the bromate which might be adsorbed by G-nZVI.

A.5. ZEOLITES

Zeolites are crystalline structures made of aluminium, silicon and oxygen that form a framework with pores and channels which can accommodate cations, water and small molecules. They have been used as adsorbents or catalysts.

The combination of zeolites with metals or surfactants has been used to remove compounds such as manganese [64], bromate and nitrate. H^+-form high silica zeolites have been tested to reduce the formation of bromate during ozonation [30].

In the case of bromate, zeolite has been used as a support material where the main mechanism is the catalytic hydrogenation, where the pollutant is reduced over metal catalysts in presence of a reducing agent, in this case, hydrogen. The use of bimetallic catalysts has been tested to reduce aqueous nitrate to nitrogen, perchlorates, chlorates and halogenated alkanes, alkenes and aromatics.

Soares et al. (2016) tested faujasite zeolite in the sodium form (NaY), with different particle sizes (NaY, 700 nm and nano NaY, 150 nm) impregnated with incorporate copper, palladium, rhodium and thorium [29].

The monometallic catalysts Rh-Y and Th-Y achieved 75% and 85% bromate reduction after 120 min of reaction, respectively. On the other hand, bromate is completely reduced by Pd-Y and Cu-Y after 60 and 120 min of reaction, respectively. The study showed that the incorporation of the promoter metal improves the performance of Pd and Cu catalysts as it was proved with the complete reduction of bromate with PdCu-Y or CuPd-Y bimetallic catalysts after less than 10 min of reaction while with ThCu-Y and RhCu-Y the complete reduction is not achieved at the end of the experiments (120 min). The initial concentration of bromate was 10 mg/L [29].

The removal mechanism involves the dissociative adsorption of hydrogen on the active sites of the catalyst and the reaction with the adsorbed bromate ions, hydrogen also being involved in the reduction of the metal. In addition, bromate can also react directly with hydrogen in solution. For the catalytic reduction, the results confirm that Pd is the best choice of metal due to its higher H_2 adsorption capacity [29].

A.6. HYDROXYAPATITE (HAP)

Hydroxyapatite is a calcium apatite compound $Ca_5(PO_4)_3(OH)$. There is no literature about the use of hydroxyapatite for bromate removal. However, this adsorbent has been used for fluoride removal due to its low cost and affinity for fluoride where an OH from hydroxyapatite $Ca_5(PO_4)_3(OH)$ can be exchanged by fluor forming fluoroapatite $Ca_5(PO_4)_3F$ [65].

Badillo-Almaraz et al. (2007) studied the removal of fluoride using commercial synthetic hydroxyapatite (BIO-RAD®). An adsorption capacity of 100 mmol/100 g (19 mg/g) was obtained at a pH range between 7.0 and 7.5. According to this study, the factors that influence the adsorption is the concentration of hydroxyl ions (pH of the solution) and the concentration of fluoride in the solution. The study of these parameters indicated that the fluoride removal at low concentrations of fluoride in the solution can be explained as an adsorption mechanism, while when the fluoride concentration increase it can be explained as a precipitation phenomenon.

The study did not consider the presence of other ions (only the influence of the OH ions), however, they expounded that there is evidence of the null affinity of hydroxyapatite with the chloride ions [66].

Gao et al. (2009) studied the effect of particle size of synthetic hydroxyapatite on fluoride removal. Three different averaged particle sizes (48.2, 62.8, and 97.9 nm) were investigated in this study. They observed higher adsorption efficiency with smaller particle size. The adsorption capacity of different size HAP was between 0.295 to 0.489 mg/g [67].

The removal efficiency of fluoride increases with an increase in the adsorbent dose (increase of the adsorption sites) and contact time, while it decreases with an increase of initial fluoride concentration and pH of solution [67].

The removal mechanisms are the following: the fluoride ions are first attracted to the HAP surfaces, then the adsorbed fluoride ions are exchanged with the mobile OH^- of the HAP at the nearest surface as the chemical equation below shows:

$$\underset{nano-HAP}{Ca_{10}(PO_4)_6\,(OH)_2} + nF^- = \underset{fluoroapatite}{Ca_{10}(PO_4)_6\,(OH)_{2-n}F_n} + nOH^-$$

Jimenez-Reyes and Solache-Rios (2010) have investigated the fluoride removal using hydroxyapatite as adsorbent. An adsorption capacity of 4.7 mg/g was obtained with a dose of 0.01 g of HAP in 25 ml of solution. A removal of 96% took place by using 0.1 g of HAP and 25 ml of fluoride solution. The maximum adsorption was in pH between 5- 7.3.

In addition, it was found that sulfate, nitrate and chloride ions did not interfere with the fluoride sorption. Desorption occurred when the pH increases suggesting that fluoride ions might be replaced by hydroxyl anions [68].

The defluoridation efficiency of lacunar hydroxyapatite (L-HAP) was investigated by Manzola et al. (2015). The fluoride removal capacity was 18.96 and 8 mg/g at a dose of 0.0174 g and 0.1012 g, respectively. For 0.0527 g amount of L-HAP sorbent with contact time of 72 h, the fluoride removal capacity is 11.63 mg/g for synthetic water and 2.80 for Koundoumawa field water (a real case water), this could be explained by the presence of high concentration of bicarbonate ion.

One alternative for bromate removal could be to use the hydroxyapatite based on the mechanism of fluoride removal where the hydroxyl ions could be replaced by bromate or bromide. However not all the anions will have affinity for hydroxyapatite as is the case which chloride. Based on the results of fluoride removal, it can be interesting to investigate the feasibility of bromate/bromide removal using hydroxyapatite as adsorbent. However, there could be a risk if bromate does not have affinity for hydroxyapatite.

B

CALCULATIONS FOR CHEMICAL SOLUTIONS

The calculations to prepare solutions used in this study are detailed below.

B.1. $FeSO_4$ SOLUTION

B.1.1. $13.125\ mg/L$ ($0.27\ mM$)

To prepare the stock solution for the dose needed to reduce 5 mg/L of BrO_3-, the following calculations were done.

$$\begin{aligned}&5mgBrO_3^- \rightarrow xFe^{2+}\\&128mgBrO_3^- \rightarrow 6*56mgFe^{2+}\\&x = 13.125mgFe^{2+}\end{aligned}$$

To find the concentration of the stock solution.

$$\begin{aligned}&13.125\frac{mg}{L}Fe^{2+}*250mL = C_1*2.5mL\\&1.3125\frac{g}{L}Fe^{2+} = C_1\end{aligned}$$

To determine the amount of $FeSO_4*7H_2O$ to obtain 1.3125 mg/L Fe^{2+} for the stock solution was calculated.

$$\begin{aligned}&56gFe^{2+} \rightarrow 278.01gFeSO_4*7H_2O\\&1.3125gFe^{2+} \rightarrow xFeSO_4*7H_2O\\&x = 6.52gFeSO_4*7H_2O\end{aligned}$$

The stock solution was prepared in 100 mL flask, therefore the amount of $FeSO_4*7H_2O$ in 100 ml was calculated.

$$\frac{6.52g*100mL}{1000mL} = 0.652gFeSO_4*7H_2O$$

Therefore 0.652 g of $FeSO_4*7H_2O$ were needed to prepare the 100 mL stock solution of 1.3 g/L Fe^{2+}.

B.1.2. $52.5\ mg/L$ ($1\ mM$)

To prepare the stock solution for the 52.5 mg/L iron dose, the following calculations were done. The concentration of the stock solution was calculated:

$$\begin{aligned}&52.5\frac{mg}{L}Fe^{2+}*250mL = C_1*2.5mL\\&5.25\frac{g}{L}Fe^{2+} = C_1\end{aligned}$$

The amount of $FeSO_4*7H_2O$ to obtain 5.25g/L Fe^{2+} for the stock solution was calculated.

$$\begin{aligned}&56gFe^{2+} \rightarrow 278.01gFeSO_4*7H_2O\\&5.25gFe^{2+} \rightarrow xFeSO_4*7H_2O\\&x = 26.06gFeSO_4*7H_2O\end{aligned}$$

The stock solution was prepared in 100 mL flask, therefore the amount of $FeSO_4 * 7H_2O$ in 100 ml was calculated.

$$\frac{26.06g * 100mL}{1000mL} = 2.606gFeSO_4 * 7H_2O$$

Therefore 2.6 g of $FeSO_4 * 7H_2O$ were needed to prepare the 100 mL stock solution of 5.25 g/L Fe^{2+}.

B.1.3. $0.15\ mg/L$ $(0.007\ mM)$

To prepare the stock solution for the 0.15 mg/L iron dose, the following calculations were done.

$$\begin{aligned}&0.06mgBrO_3^- \rightarrow xFe^{2+}\\&128mgBrO_3^- \rightarrow 6 * 56mgFe^{2+}\\&x = 0.1575mgFe^{2+}\end{aligned}$$

To find the concentration of the stock solution

$$\begin{aligned}&0.1575\frac{mg}{L}Fe^{2+} * 1000mL = C_1 * 10mL\\&15.75\frac{mg}{L}Fe^{2+} = C_1\end{aligned}$$

To determine the amount of $FeSO_4 * 7H_2O$ to obtain 15.75 mg/L Fe^{2+} for the stock solution was calculated

$$\begin{aligned}&56mgFe^{2+} \rightarrow 278.01mgFeSO_4 * 7H_2O\\&15.75mgFe^{2+} \rightarrow xFeSO_4 * 7H_2O\\&x = 78.19mgFeSO_4 * 7H_2O\end{aligned}$$

The stock solution was prepared in 100 mL flask, therefore the amount of $FeSO_4 * 7H_2O$ in 100 ml was calculated.

$$\frac{0.0782g * 100mL}{1000mL} = 0.00782gFeSO_4 * 7H_2O$$

Therefore 0.0078g of $FeSO_4 * 7H_2O$ were needed to prepare the 100mL stock solution of 15.75 mg/L Fe^{2+}.

B.1.4. $1.5\ mg/L$ $(0.03\ mM)$

To prepare the stock solution for the 1.5 mg/L iron dose the following calculations were done. The concentration of the stock solution was calculated.

$$\begin{aligned}&1.5\frac{mg}{L}Fe^{2+} * 1000mL = C_1 * 10mL\\&150\frac{mg}{L}Fe^{2+} = C_1\end{aligned}$$

The amount of $FeSO_4 * 7H_2O$ to obtain 15.75 mg/L Fe^{2+} for the stock solution was calculated

$$\begin{aligned}&56mgFe^{2+} \rightarrow 278.01mgFeSO_4 * 7H_2O\\&150mgFe^{2+} \rightarrow xFeSO_4 * 7H_2O\\&x = 744.6mgFeSO_4 * 7H_2O\end{aligned}$$

The stock solution was prepared in 100 mL flask, therefore the amount of $FeSO_4 * 7H_2O$ in 100 ml was calculated.

$$\frac{0.745g * 100mL}{1000mL} = 0.0745gFeSO_4 * 7H_2O$$

Therefore 0.0745 g of $FeSO_4 * 7H_2O$ were needed to prepare the 100 mL stock solution of 150 mg/L Fe^{2+}.

B.2. BROMATE SOLUTION

B.2.1. $5\ mg/L$

To prepare a solution with 5 mg/L of BrO_3^- the amount of $NaBrO_3$ needed was calculated.

$$\begin{aligned}&5mgBrO_3 \rightarrow xNaBrO_3\\&128mgBrO_3 \rightarrow 151mgNaBrO_3\\&x = 5.89mgNaBrO_3\end{aligned}$$

Therefore 5.89mg of $NaBrO_3$ were added per litre of solution.

B.2.2. 60 mg/L

To prepare the stock solution for the 60 mg/L of BrO_3^- the following calculations were done.

$$\begin{aligned}&60mgBrO_3 \rightarrow xNaBrO_3\\&128mgBrO_3 \rightarrow 151mgNaBrO_3\\&x = 70.78mgNaBrO_3\end{aligned}$$

The stock solution was prepared in 100 mL flask, therefore the amount of $NaBrO_3$ in 100 ml was calculated.

$$\frac{0.07078g * 100mL}{1000mL} = 0.0071gNaBrO_3$$

Therefore 0.0071g of $NaBrO_3$ were needed to prepare the 100mL stock solution of 60 mg/L BrO_3^-. Then to obtain 60 $\mu g/L$ of BrO_3^-, 1 ml of the 60 mg/L BrO_3^- stock solution was added per 1 L of solution.

B.3. NITRATE

B.3.1. 5 mg/L

To prepare the stock solution for the 5 mg/L of NO_3^- the amount of $NaBrO_3$ was calculated.

$$\begin{aligned}&5mgNO_3 \rightarrow xNaNO_3\\&62mgNO_3 \rightarrow 85mgNaNO_3\\&x = 6.85mgNaNO_3\end{aligned}$$

Therefore 0.0069 g of $NaNO_3$ were added per litre of solution.

B.3.2. 2.8 mg/L

To prepare the stock solution for the 2.84 mg/L of NO_3^- the amount of $NaBrO_3$ was calculated

$$\begin{aligned}&2.84mgNO_3 \rightarrow xNaNO_3\\&62mgNO_3 \rightarrow 85mgNaNO_3\\&x = 3.89mgNaNO_3\end{aligned}$$

Therefore 0.004 g of $NaNO_3$ were added per litre of solution.

B.3.3. 7.8 mg/L

To prepare the stock solution for the 7.83 mg/L of NO_3^- the amount of $NaBrO_3$ was calculated

$$\begin{aligned}&7.83mgNO_3 \rightarrow xNaNO_3\\&62mgNO_3 \rightarrow 85mgNaNO_3\\&x = 10.74mgNaNO_3\end{aligned}$$

Therefore 0.0107 g of $NaNO_3$ were added per litre of solution.

B.4. 2 mM $NaHCO_3$

First, it is necessary to calculate the amount of $NaHCO_3$ in 2 mM.

$$\begin{aligned}&1mol \rightarrow 84gNaHCO_3\\&0.002mol \rightarrow xgNaHCO_3\\&x = 0.168g\end{aligned}$$

Then a stock solution of 100 mL was prepared therefore the amount of $NaHCO_3$ for that volume was calculated.

$$\frac{0.168g * 100mL}{1000mL} = 0.0168gNaHCO_3$$

Therefore 0.017 g of $NaHCO_3$ were weighted to prepare 100 mL of 2 mM $NaHCO_3$.

B.5. COPPER (II) SOLUTION

B.5.1. 1.28 mg/L

To prepare the stock solution for the 1.28mg/L copper dose the following calculations were done. The concentration of the stock solution was calculated as it follows:

$$1.28\frac{mg}{L}Cu^{2+} * 250mL = C_1 * 2.5mL$$
$$0.128\frac{g}{L}Cu^{2+} = C_1$$

First, it is necessary to calculate the amount of $CuSO_4$ to obtain 0.128 g/L of Cu^{2+}

$$0.128gCu^{2+} \rightarrow xCuSO_4$$
$$63.5gCu^{2+} \rightarrow 159.61gCuSO_4$$
$$x = 0.322gCuSO_4$$

Then a stock solution of 100 mL was prepared therefore the amount of $CuSO_4$ for that volume was calculated.

$$\frac{0.322g * 100mL}{1000mL} = 0.0322gCUSO_4$$

Therefore 0.0322 g of $CuSO_4$ were weighted to prepare 100 mL of 0.128 g/L of Cu^{2+}.

C

VISUAL REGISTER OF IRON OXIDATION

The progressive change in colour of the solution due to the oxidation of iron can be observed in the following Figures.

C.1. BROMATE REDUCTION BY TWO IRON (II) DOSES AT TWO DIFFERENT PH

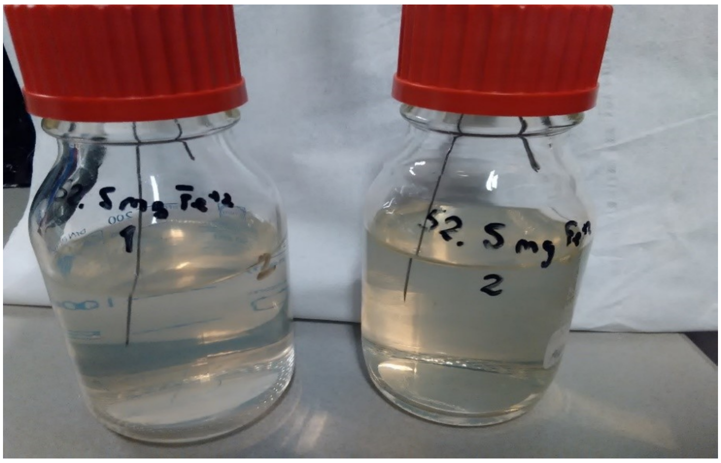

Figure C.1: Coloured solution due to the iron oxidation/bromate reduction with 52.5 mg/L (1 mM) iron dose at 2 hours (pH=7.4).

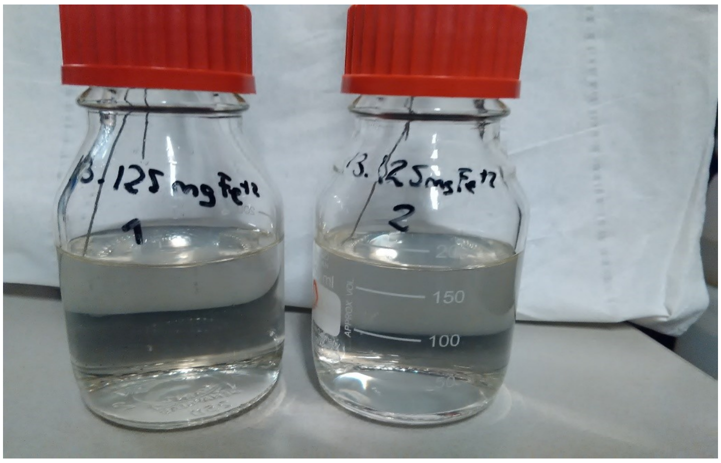

Figure C.2: Coloured solution due to the iron oxidation/bromate reduction with 13 mg/L (0.27 mM) iron dose at 3 hours (pH=7.4).

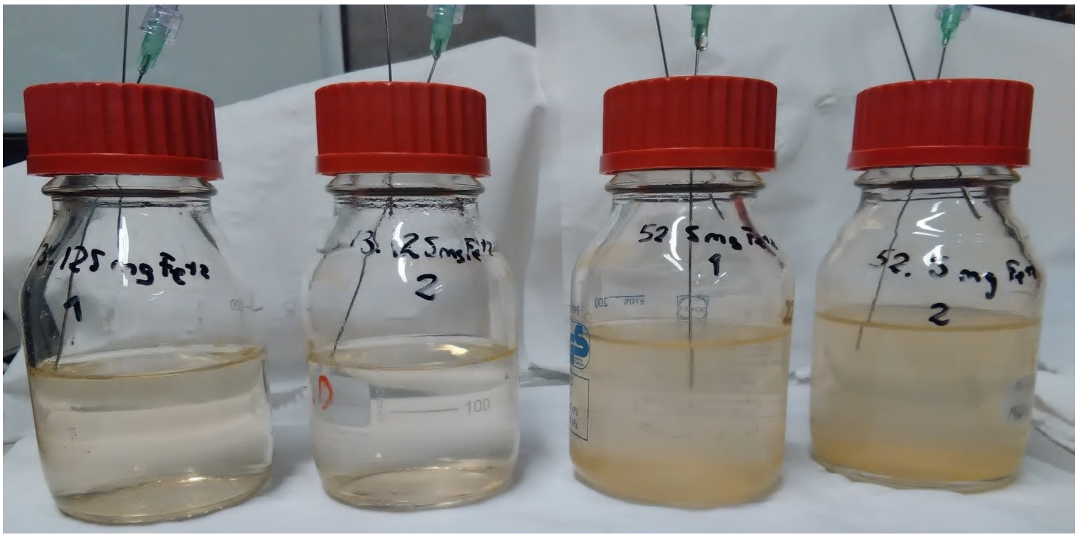

Figure C.3: Coloured solution due to the iron oxidation/bromate reduction at 19 hours (pH =7.4).

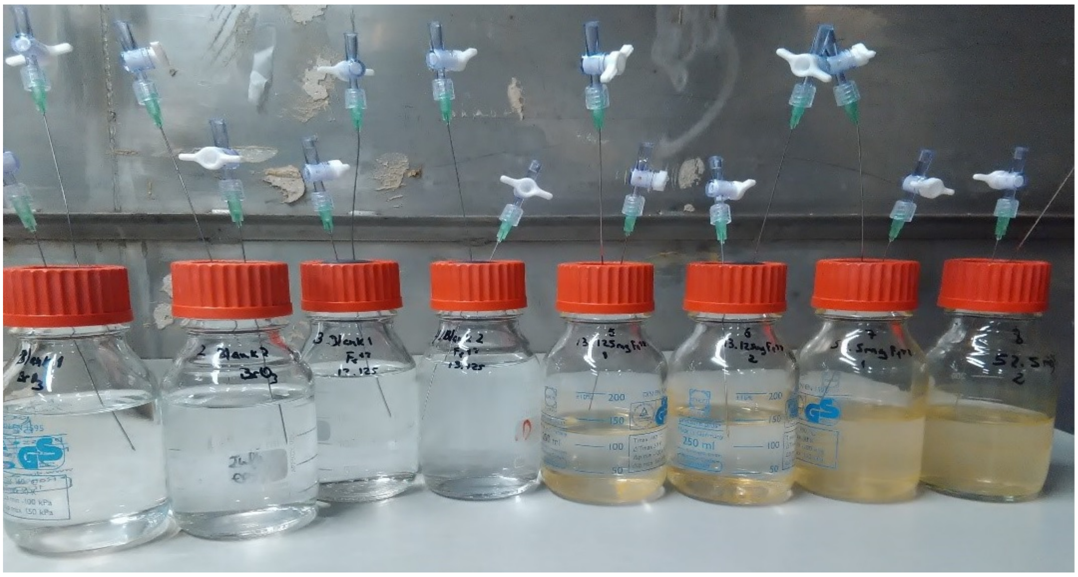

Figure C.4: Difference shade of colours due to iron oxidation at different iron doses at pH 9.5 after 48 hours (the transparent bottles are the controls for iron and bromate)

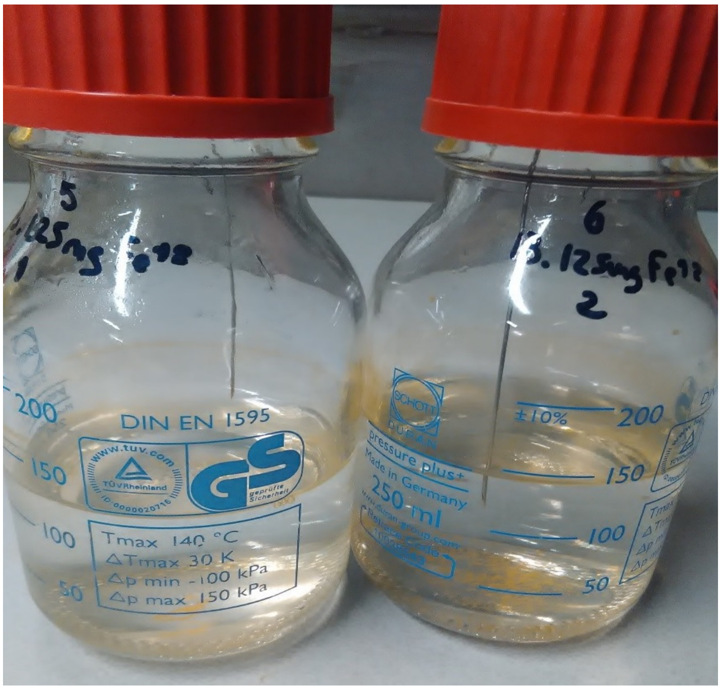

Figure C.5: Floc formation at 48 hours in the dose 13mg/L (0.27 mM) at pH 9.5

C.2. NITRATE REDUCTION BY IRON (II) DOSAGE WITH AND WITHOUT CATALYST

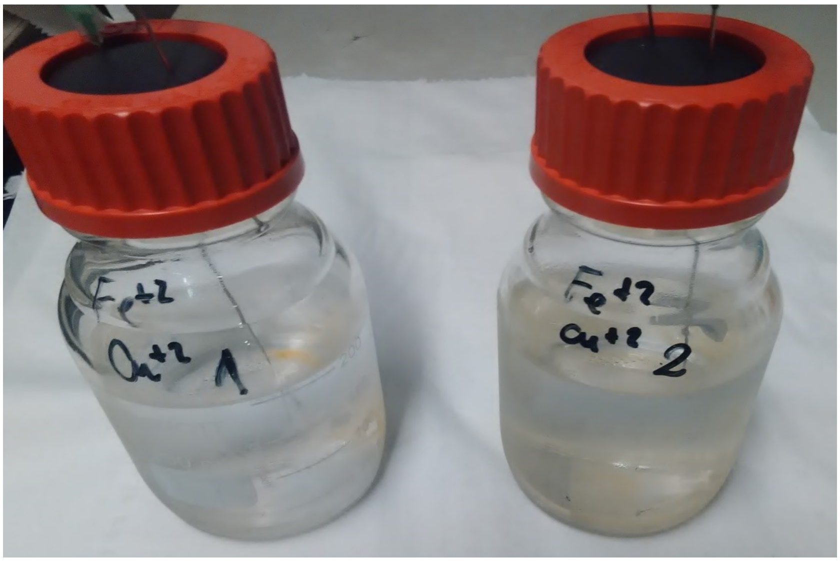

Figure C.6: Bottles with floc formation for the experiment of nitrate reduction in presence of catalyst.

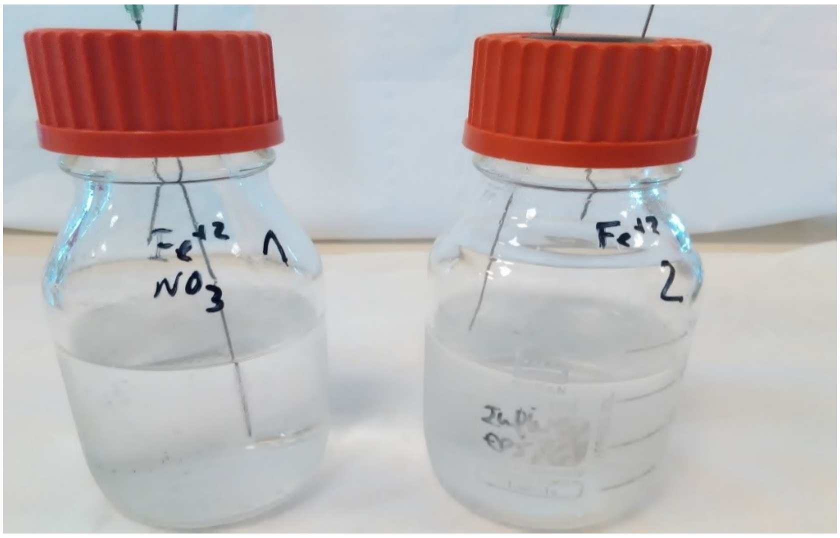

Figure C.7: Bottles without change of colour for the experiment of nitrate reduction in absence of catalyst

C.3. BROMATE REDUCTION BY HIGH IRON (II) CONCENTRATIONS, IN THE PRESENCE OF NITRATE

Figure C.8: Coloured solution due to the iron oxidation/bromate reduction in presence of nitrate at 2 hours.

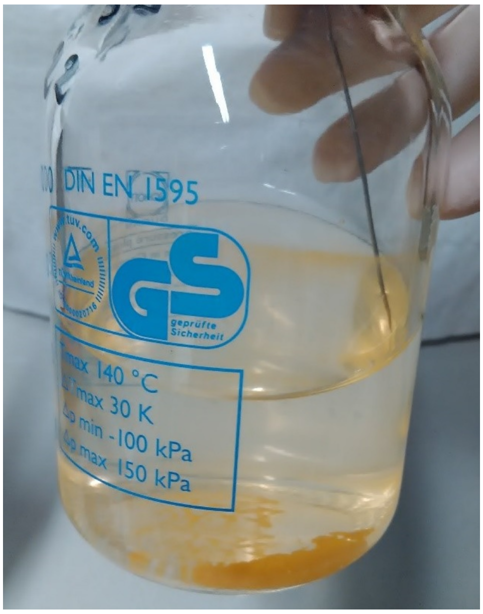

Figure C.9: Floc formation with 1 mM iron dose in presence of nitrate at 72 hours.

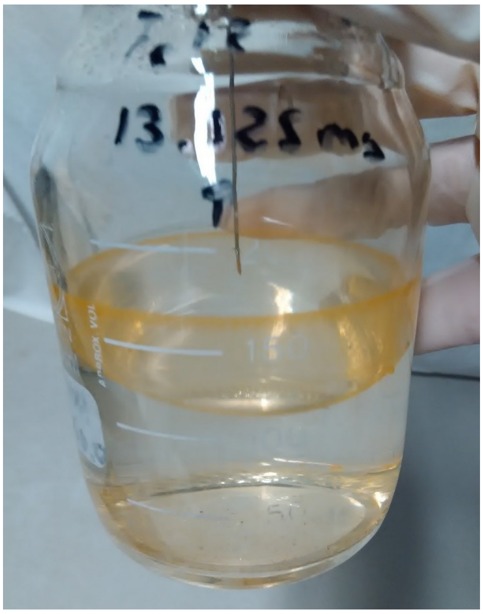

Figure C.10: Floc formation with 0.27 mM iron dose in presence of nitrate at 72 hours.

C.4. BROMATE REDUCTION BY LOW IRON (II) CONCENTRATIONS, IN THE PRESENCE OF NITRATE

Figure C.11: Imperceptible change of colour with the iron dose 0.007 mM during bromate (60 $\mu g/L$) and nitrate (10 mg/L) reduction after 5 days.

Figure C.12: Imperceptible coloration of solution but small floc formation with the 0.03 mM iron dose during the bromate (60 $\mu g/L$) and nitrate (10 mg/L) reduction after 5 days.

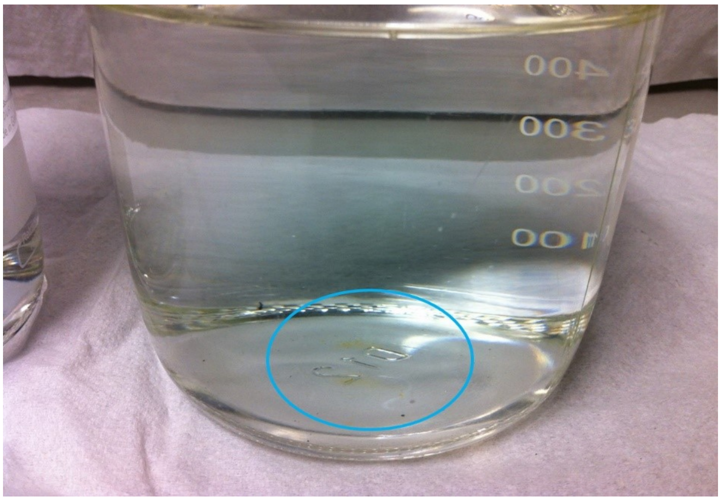

Figure C.13: Zoom to the floc formation with the 0.03 mM iron dose during the bromate (60 $\mu g/L$) and nitrate (10 mg/L) reduction after 5 days.

C.5. BROMATE REDUCTION BY LOW IRON (II) CONCENTRATIONS, IN THE ABSENCE OF NITRATE

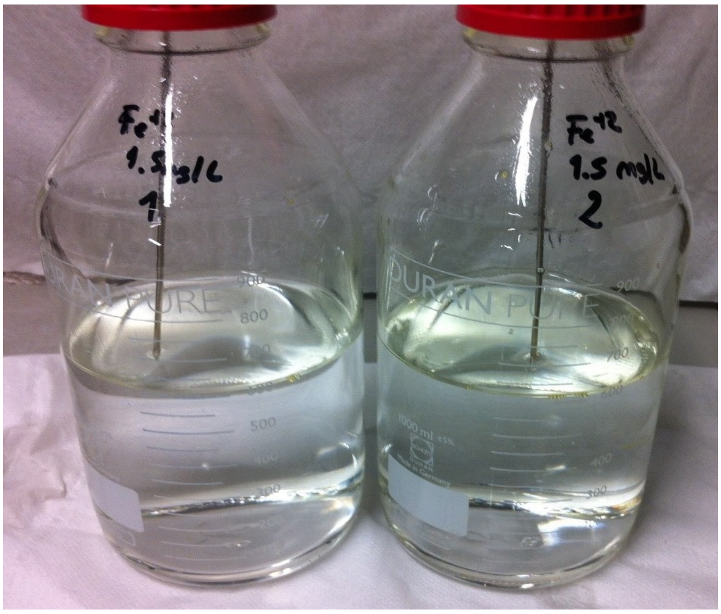

Figure C.14: Bottles with higher dose presents floc formation with 0.03 mM iron dose and bromate (60 $\mu g/L$) after 1 day.

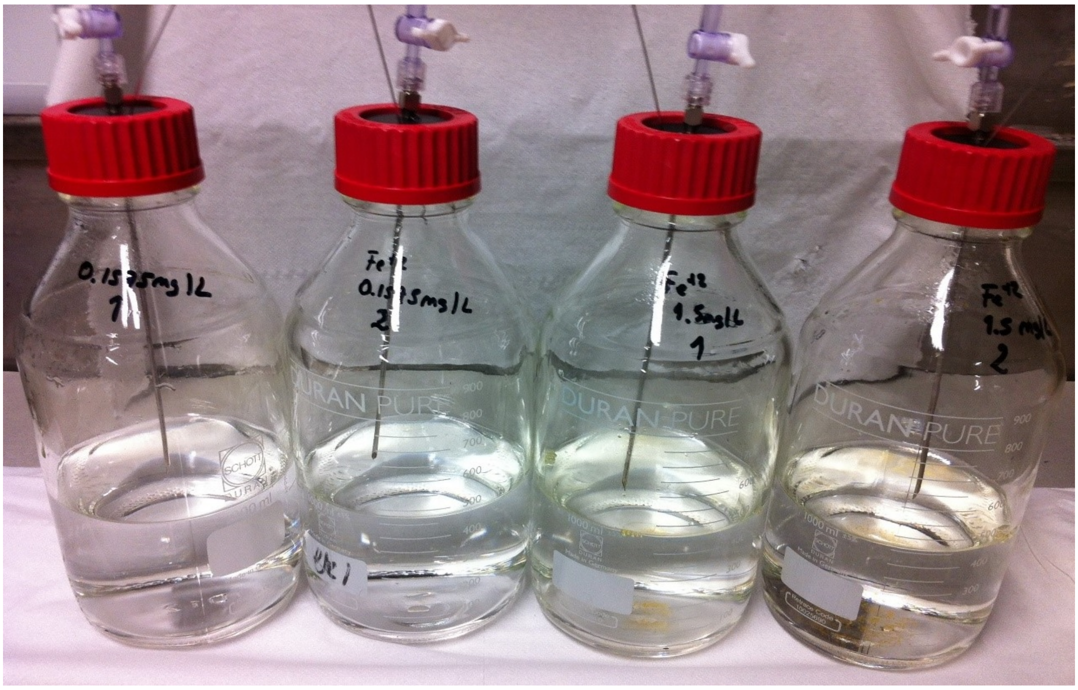

Figure C.15: Bottles with the two iron dosages (0.007 and 0.03 mM) and bromate (60 $\mu g/L$) after 5 days. The higher dose shows the flocs of iron on the bottom of the bottles.

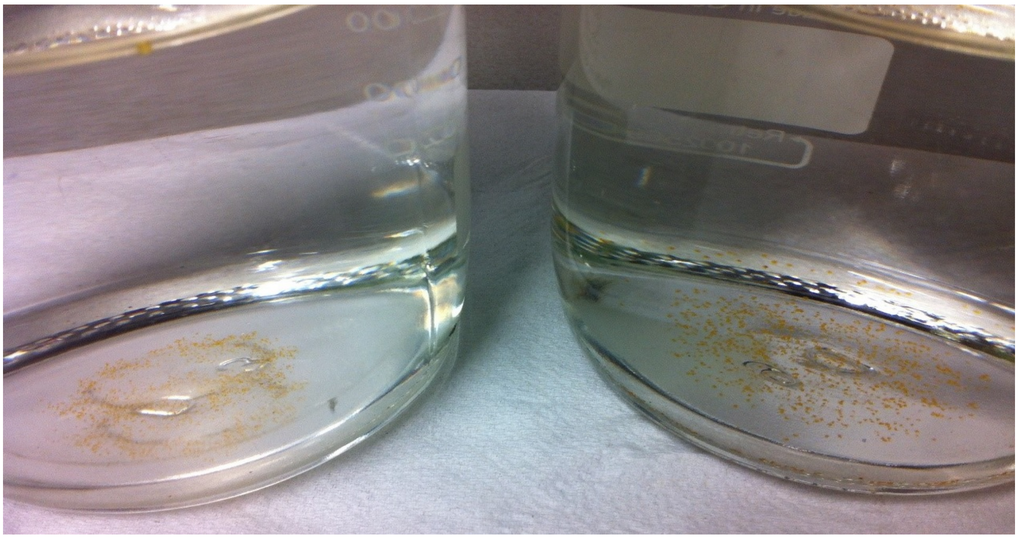

Figure C.16: Zoom of floc formation with the dose 0.03 mM of iron and bromate (60 $\mu g/L$) after 5 days.

D

NITRATE REDUCTION BY IRON (II) AND CATALYST

The reduction of nitrate by iron (II) in presence of catalyst (1.28mg/L Cu^2+) can be observed in the Figure D.1 and D.2. From time 0 to 24 hours, it was analysed with nitrate cuvette test and then by ion chromatography (IC) as it is described in the methodology. From the Figure D.1, it can be seen that into the first 3 hours, the nitrate concentration remained constant. At 17 hours, a decrease in nitrate concentration is observed, increasing again at time 24 to the similar concentration from the beginning. The reduction of nitrate registered at t= 17 hours could be an operational error.

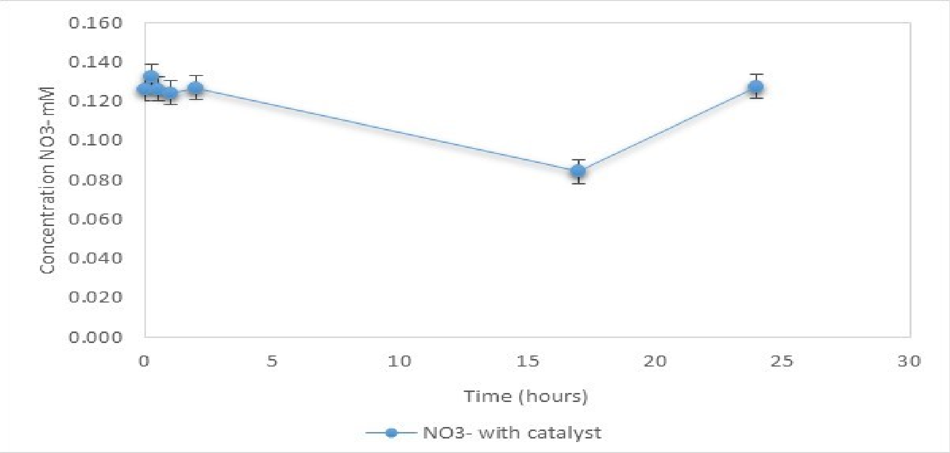

Figure D.1: Nitrate reduction by iron (II) with catalyst measured with cuvette test.

Figure D.2 shows that during the following hours the concentration of nitrate remains without significant variation.

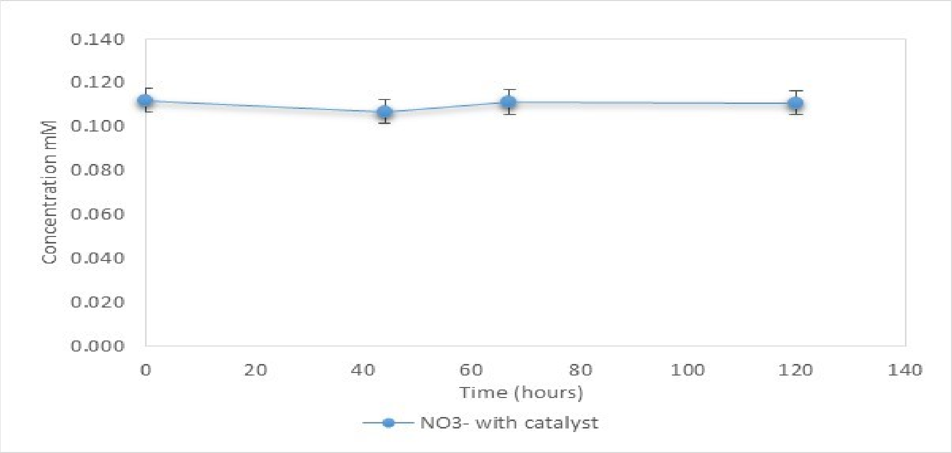

Figure D.2: Nitrate reduction by iron (II) with catalyst measured with IC.

According to Ottley et al. (1997) and Buresh and Morogham (1976) nitrate reduction by iron in presence of Copper was expected, while in its absence was not. The no reduction without catalyst was observed in section 4.2.

On the other hand, for bottles with catalyst at 17 hours, a 33% of reduction is registered, however, there is an uncertainty in this value due to no reduction during the following hours.

It should be noted that the nitrate concentration contained in the acidified iron (II) stock solution and which was added into the bottles, was not taken into account for the calculations of the dosages of iron and cooper. According to the stoichiometric relation $Fe2+/NO_3^-/Cu^{2+}$= 8/ 1/ 2.5, more iron and copper was needed for the reduction of the new initial nitrate concentration (increased from 5 to 7.16 mg/L after the dose addition giving a ratio of $Fe2+/NO_3^- \approx 5$).

Therefore, it could be possible that not enough copper and iron was available to reduce nitrate. On the other hand, Ottley et al. (1997) registered the chemical catalyst of nitrate reduction by iron using copper (II) at 20°C and with an excess of iron (Fe^{2+}/NO_3^-= 10) while this study was conducted at 12°C and with a lower ratio. Perhaps the temperature could be a conditional factor, especially knowing that the activation energy and consequent nitrate reduction can be reduced increasing the temperature as it was observed by Petersen (1979).

Despite the fluctuation of iron along the time as it can be seen in the Figure D.3, there was observed the formation of orange flocs in the bottles with catalyst and no change of colour in the bottles without catalyst as it can be seen in the Appendix C. The flocs formation might be due to contamination with oxygen (it was the first experiment), iron oxidation and consequently small nitrate reduction or the reduction from Cu (II) to copper mineral in solid phase which cannot be neglected according to [41].

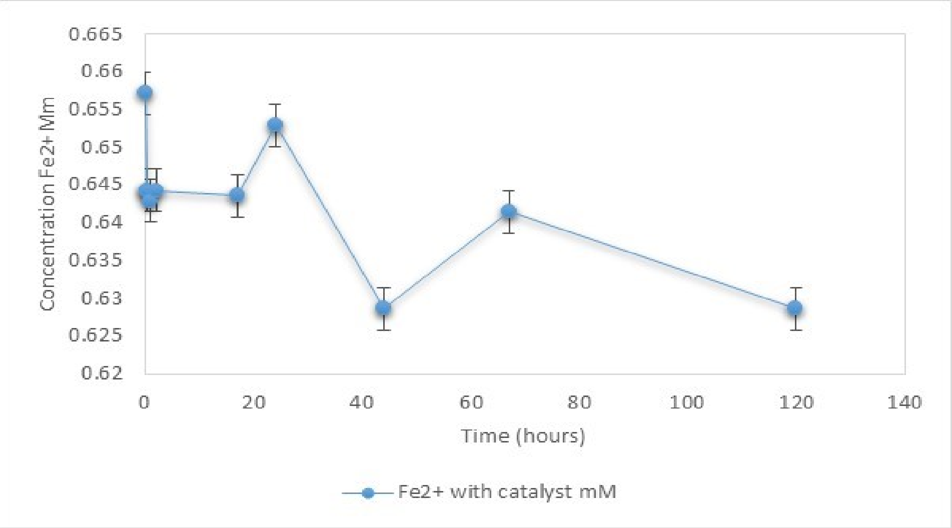

Figure D.3: Iron oxidation during nitrate reduction